

INTERNAL MEMO

To: Claire Bowen, INSERT c.c. Convenor, PGR Contact
From: Jane Collins, REGIS 21 June, 2007
Subject Bar on Access Application - Miss Betty Petrillo, 0232793

Notification has been received that the above student has successfully completed his/her programme of study. A Bar on Access has been approved by Cardiff University for the following student, which although is regarded as operative as soon as the work is submitted, the period approved shall be calculated from the date on which the candidate is formally notified by the University that s/he has qualified for a degree:

Name: Miss Betty Petrillo, 00232793
Thesis Title: Design and Synthesis of Artificial Receptors for Phosphorylated Amino Acid.
Degree: PhD
Duration of Bar on Access 1-year
Notification Date: 21/03/2007
Expiry Date: 21/03/2008

Jane Collins
Executive Officer
Swyddog Gweithredol
Postgraduate Admissions and Student Records
Derbyn Ôl-raddedigion a Chofnodion Myfyrwyr
Email: postgraduate@cf.ac.uk
Tel: 029 20870436

**DESIGN AND SYNTHESIS OF ARTIFICIAL
RECEPTORS FOR PHOSPHORYLATED
AMINO ACIDS**

A Thesis submitted to the University of Wales in accordance with the
requirements for the degree of

**DOCTOR OF PHILOSOPHY
BY EXAMINATION AND THESIS**

By

Betty Petrillo

Molecular Recognition Research Unit (MRRU)
Drug Delivery Department
The Welsh School of Pharmacy
Cardiff University



September 2006

Supervisor: Dr. Christopher John Allender

UMI Number: U584080

All rights reserved

INFORMATION TO ALL USERS

The quality of this reproduction is dependent upon the quality of the copy submitted.

In the unlikely event that the author did not send a complete manuscript and there are missing pages, these will be noted. Also, if material had to be removed, a note will indicate the deletion.



UMI U584080

Published by ProQuest LLC 2013. Copyright in the Dissertation held by the Author.
Microform Edition © ProQuest LLC.

All rights reserved. This work is protected against
unauthorized copying under Title 17, United States Code.



ProQuest LLC
789 East Eisenhower Parkway
P.O. Box 1346
Ann Arbor, MI 48106-1346

To my loved Family and my dear friend Laura

Acknowledgements

First of all I would like to express my warmest gratitude to Dr. Chris Allender, my supervisor, for his lovely support and help.

I would like to thank GE healthcare for funding my project and Dr. Val Millar and Dr. Najeeb Said for their support.

A very special thank to Dr Andrea Brancale to give me sage advice and to help me in finding the strength to go on with my studies.

Thank to Ron Edwards for his technical support and to Colin Jones and Paul Sutton for always having a smile in the morning.

I would like also to thank my specials friends Laura, Marco ('king' of the NMR) and Alessandro for being so helpful and encouraging whenever I needed them. Without them, this would not have been possible.

Special thanks to all the friends of my group, Chris Jeans, Anna, Chris Jones, Pete, Sophie, Ollie, Jimmy and Darren for the wonderful atmosphere in the laboratory and their efforts in trying to improve my English.

Thank you to the coffee crew, Chris T., Elinor, Rebecca, Zoe, Stuart, Wing, Siti for illustrating me the Welsh culture and helping me to make my life in Cardiff.

I would also like to thank Abdel "London", Tina and Mikhaela for being invaluable friends and for giving me the strength I needed.

A special thank to Sion for his patience in trying to understand my 'italian-english' and for helping me till the last days of my study.

Finally, thanks to all the chemistry group, especially Antonella and Giovanna for introducing me to the 'chemistry world' and some friends, members of the department, Maria Chiara, Maria, Lorella, Stephane, Felice, Micaela, Costantino, Plinio and Malina for their support.

Thanks to Carlos to make me believe that it is never too late to make your dreams become true.

Abstract

The research detailed in this thesis describes the development of a high-throughput molecularly imprinted polymer (MIP) receptor that binds to phosphorylated serine residues. This new receptor would need to be biologically compatible (i.e. binds in aqueous media) and have a high degree of specificity and affinity for the phosphorylated residue compared to the non-phosphorylated amino acid. Importantly, the artificial receptor should not rely on neighbouring amino acid residues for its binding affinity or specificity.

Different molecular imprinting approaches were investigated to imprint the template molecule, Boc-phospho-L-serine methyl ester. The most successful approach was found by using an amidine group in stoichiometric monomer-template interactions.

To determine the binding affinity and specificity of the MIP, an equilibrium evaluation was used. Batch analyses for the template specie and a range of cross-reactants were performed in aqueous systems and the enantioselectivity was evaluated using the D-enantiomer of the template molecule. Furthermore, the selectivity of the MIP was investigated with a series of peptides containing phosphorylated serine.

The results of these studies provide evidence of selective binding sites in the MIP for Boc-phospho-L-serine methyl ester. The thesis concludes by discussing some applications of the MIP in life sciences, e.g. as an alternative to antibody assays.

TABLE OF CONTENTS

<u>CHAPTER ONE: INTRODUCTION</u>		1
1.1	PROTEIN PHOSPHORYLATION	2
1.1.1	PROTEIN KINASES: NATURE AND MECHANISM OF ACTION	5
1.1.2	PROTEIN PHOSPHATASES : STRUCTURE AND FUNCTION	9
1.1.3	DETECTION OF PROTEIN PHOSPHORYLATION	10
1.1.3.1	RADIOLABELLING	10
1.1.3.2	FLUORESCENCE LABELLING	11
1.1.3.3	ANTIBODIES	13
1.2	MOLECULARLY IMPRINTING POLYMER	14
1.2.1	INTRODUCTION	14
1.2.2	BRIEF OF HISTORY	15
1.2.3	MOLECULAR IMPRINTING METHODOLOGIES	15
1.2.3.1	COVALENT APPROACH	15
1.2.3.2	NON- COVALENT APPROACH	18
1.2.3.3	SEMI- COVCALENT AND SACRIFICIAL SPACER APPROACH	20
1.2.3.4	PROS AND COS OF THE THREE IMPRINTING APPROACHES	22
1.2.4	STOICHIOMETRIC APPROACH	24
1.2.5	POLYMER MATRIX	24
1.2.5.1	TEMPLATE MOLECULE	25
1.2.5.2	FUNCTIONAL MONOMER	26
1.2.5.3	CROSSLINKING AGENT	28
1.2.5.4	POROGENS	30
1.2.5.5	INITIATION METHODS	31
1.2.6	CONSIDERATION IN THE DESIGN OF NON-COVALENT IMPRINTING SYSTEM	32
1.2.6.1	NON-COVALENT TYPE OF INTERACTIONS	33
1.2.6.2	THERMODYNAMIC CONSIDERATIONS	35
1.2.7	APPLICATIONS OF MOLECULAR IMPRINTING	36

1.2.7.1	CHROMATOGRAPHY	37
1.2.7.2	CATALYSIS AND ARTIFICIAL ENZYMES	38
1.2.7.3	BIOSENSOR	38
1.2.7.4	PSEUDOIMMUNO ASSAY	39
1.3	CONCLUSION	41
	BIBLIOGRAPHY	42
	<u>CHAPTER TWO: AIMS AND OBJECTIVES</u>	55
2.1	AIM	56
2.2	OBJECTIVES	56
	<u>CHAPTER THREE: DESIGN AND SYNTHESIS OF THE TEMPLATE AND THE FUNCTIONAL MONOMER</u>	57
3.1	MIP DESIGN	58
3.1.1	IMPRINTING OF PHOSPHATES OR PHOSPHONATES	58
3.1.2	DESIGN OF THE TARGET MOLECULE	62
3.1.3	RATIONAL BEHIND THE CHOICE OF THE AMIDINE AS THE FUNCTIONAL MONOMER	64
3.1.3.1	BIOLOGICAL AND SYNTHETIC RECEPTORS	64
3.1.3.2	APPLICATIONS OF AMIDINE-BASED MOLECULARLY IMPRINTED POLYMERS	64
3.1.4	CONCLUSION	65
3.2	SYNTHESIS OF THE TEMPLATE MOLECULE	66
3.2.1	INTRODUCTION	66
3.2.2	PHOSPHORYLATION METHODS	66
3.2.2.1	ARBUZOV REACTION	66
3.2.2.2	PHOSPHORYLATION USING NMI AS BASE	69
3.2.2.3	PHOSPHORYLATION USING A GRIGNARD REAGENT	70
3.2.2.4	PHOSPHORYLATION USING TRIETHYLAMINE	

AS BASE	70
3.2.2.5 DEPROTECTION OF DIETHYLPHOSPHO- BOC-L-SERINE METHYL ESTER BY TRIMETHYLSILYL BROMIDE	71
3.2.2.6 SYNTHESIS OF BOC-PHOSPHO-L-SERINE METHYL ESTER BY USING <i>N,N'</i> -DIISOPROPYL-BIS-(4-CHLOROBENZYL)- PHOSPHORAMIDATE	72
3.2.3 HYDROGENATION METHODS	75
3.2.4 PURIFICATION OF BOC-PHOSPHO-L-SERINE METHYL ESTER	77
3.2.5 BOC-PHOSPHO-D-SERINE METHYL ESTER	82
3.2.5.1 SYNTHESIS OF THE D-ENANTIOMER	82
3.3 SYNTHESIS OF THE <i>N,N'</i>-DIETHYL-4-VINYL BENZAMIDINE	84
3.4 CONCLUSIONS	88
BIBLIOGRAPHY	89
<u>CHAPTER FOUR: VIRTUAL ANALYSIS</u>	91
4.1 MOLECULAR MECHANIC-THEORY	92
4.1.2 SYSTEMATIC CONFORMATIONAL SEARCH	94
4.1.3 MONTE CARLO METHODS OR RANDOM SEARCH	95
4.1.4 STOCHASTIC CONFORMATIONAL SEARCH	96
4.2 CONFORMATIONAL STUDY OF AMIDINE ISOMERS	98
4.2.1 INTRODUCTION	98
4.2.2 METHODS	99
4.2.3 RESULTS AND DISCUSSION	99
4.2.4 CONCLUSION	103
4.3 MOLECULAR DYNAMICS	104
4.3.1 INTRODUCTION	104

4.3.2	PRINCIPLES	104
4.3.3	METHOD	105
4.3.4	RESULTS	105
4.4	NMR SPECTROSCOPY	107
4.4.1	INTRODUCTION	107
4.4.2	METHODS	107
4.4.3	RESULTS AND DISCUSSION	
4.4.3.1	NMR OF AMIDINE AT DIFFERENT TEMPERATURES	108
4.4.3.2	NMR STUDIES OF THE AMIDINE IN PRESENCE OF DIFFERENT COUNTER IONS AND SOLVENTS	110
4.4.4	CONCLUSIONS	113
4.5	FURTHER DISCUSSION	113
	BIBLIOGRAPHY	114
	<u>CHAPTER FIVE: PREPARATION AND CHARACTERISATION OF BOC-PHOSPHO-L-SERINE METHYL ESTER MOLECULARLY IMPRINTED POLYMER</u>	115
5.1	INTRODUCTION	116
5.1.1	POLYMER AND POLYMERISATION	116
5.1.2	FREE RADICAL POLYMERISATION	118
5.1.3	DESIGN OF A BOC-PHOSPHO-SERINE METHYL ESTER MOLECULARLY IMPRINTED POLYMER	121
5.1.4	CHARACTERISATION OF PARTICLE SIZE BY LASER DIFFRACTION	123
5.1.4.1	PRINCIPLES	123
5.2	MATERIALS AND METHODS	126
5.2.1	PREPARATION OF PHOSPHO SERINE IMPRINTED	

	POLYMERS	126
5.2.2	SEDIMENTATION	127
5.2.3	CENTRIFUGATION	127
5.2.4	LASER DIFFRACTION	127
5.2.5	TEMPLATE REMOVAL	128
5.2.6	DETECTION LIMIT OF BOC-P-SERINE METHYL ESTER	128
5.3	RESULTS AND DISCUSSION	129
5.3.1	CENTRIFUGATION	129
5.3.2	POLYMER PREPARED WITH PROTOCOL 1	130
5.3.3	POLYMER PREPARED WITH PROTOCOL 2	131
5.3.4	DETECTION LIMIT FOR BOC-PHOSPHO-L-SERINE METHYL ESTER	132
5.3.5	WASHING STEP	132
5.4	CONCLUSION	132
	BIBLIOGRAPHY	133
	<u>CHAPTER SIX: OPTIMISATION OF EXPERIMENTAL CONDITIONS FOR THE EQUILIBRIUM EVALUATION OF THE IMPRINTING EFFECT</u>	134
6.1	INTRODUCTION	135
6.1.2	BATCH ANALYSIS	135
6.1.3	ANALYSIS OF BOC-PHOSPHO-L-SERINE METHYL ESTER	137
6.2	MATERIALS AND METHODS	140
6.2.1	pKa CALCULATIONS	140
6.2.2	BATCH REBINDING	141
6.2.3	HPLC ANALYSIS	141
6.3	RESULTS AND DISCUSSION	142

6.3.1	INTRODUCTION	142
6.3.2	PROTONATION STATE OF THE PHOSPHORYL GROUP OF THE SERINE AT DIFFERENT pH VALUES	142
6.3.3	PROTONATION STATE OF THE AMIDINE AT DIFFERENT pH VALUES	145
6.3.4	BATCH REBINDING: PARAMETERS AFFECTING HOST-GUEST INTERACTIONS	146
	6.3.4.1 SOLVENT EFFECT	146
	6.3.4.2 pH – MODIFIED SYSTEMS	148
	6.3.4.3 COMPETITOR ION TYPE EFFECT	153
	6.3.4.4 CONCENTRATION EFFECT	156
6.4	CONCLUSION	160
	BIBLIOGRAPHY	161
	<u>CHAPTER SEVEN: CONFIRMATION OF AN IMPRINTING EFFECT</u>	162
7.1	INTRODUCTION	163
7.2	MATERIALS AND METHODS	166
	7.2.1 REAGENTS	166
	7.2.2 BATCH REBINDING	166
	7.2.3 HPLC ANALYSIS	166
7.3	RESULTS AND DISCUSSION	167
	7.3.1. HPLC PERFORMANCE	167
	7.3.2 CROSS-REACTIVITY STUDIES	168
	7.3.2.1 BATCH RESULTS	168
	7.3.3 ENANTIOMERIC EFFECT	170
	7.3.3.1 BATCH RESULTS	170
7.4	CONCLUSION	171

BIBLIOGRAPHY	172
<u>CHAPTER EIGHT: STUDY OF THE IMPRINTING EFFECT FOR PHOSPHO-SERINE CONTAINING PEPTIDES</u>	173
8.1 INTRODUCTION	174
8.2 MATERIALS AND METHODS	177
8.2.1 REAGENTS	177
8.2.2 BINDING STUDIES-PEPTIDE PAIR A	177
8.2.3 BINDING STUDIES - PEPTIDE PAIR B	177
8.2.4 FLUORESCENCE DETERMINATION FOR PEPTIDE PAIR A AND B	179
8.3 RESULTS AND DISCUSSION	179
8.3.1 BINDING STUDIES	179
8.3.1.1 PEPTIDE PAIR A	179
8.3.1.2 PEPTIDE PAIR B	183
8.4 CONCLUSIONS	185
<u>CHAPTER NINE: GENERAL DISCUSSION AND FUTURE OUTLOOK</u>	186
9.1 DISCUSSION	187
9.2 FUTURE OUTLOOK	189
BIBLIOGRAPHY	192
<u>APPENDIX I</u>	193
EXPERIMENTAL PROCEDURES	

LIST OF FIGURES

	<i>Page</i>
Figure 1.1 Protein phosphorylation process. A protein kinase moves a phosphate group from ATP to the protein. A protein phosphatase removes the phosphate and the protein reverts to its original state.	3
Figure 1.2 The chemical structures of the phosphoamino acids known to be formed biologically.	6
Figure 1.3 Dissociative vs. associative transition states for phosphoryl transfer.	8
Figure 1.4 Schematic representation of the molecular imprinting technique: a) and b) pre-polymerisation complex between template and functional monomer(s); c) polymer formation; d) template extraction which leaves binding sites complementary to the original template.	16
Figure 1.5 The first example of covalent imprinting.	18
Figure 1.6 Non-covalent molecular imprinting of 9-ethyladenine.	19
Figure 1.7 Semi-covalent approach for the imprinting of <i>p</i> -aminophenylalanine ethyl ester.	21
Figure 1.8 First example of sacrificial spacer.	22
Figure 1.9 Example of target molecule (L-hystidinyL-L-cysteine-amide) containing a variety of functional elements.	26
Figure 1.10 Representation of functional monomers for non covalent molecular imprinting.	27
Figure 1.11 Selection of common cross-linkers used in molecular imprinting protocols.	29
Figure 1.12 Chemical structures of selected chemical initiators.	32

Figure 1.13	Scheme of biosensor device.	39
Figure 1.14	The number of articles published from 1931-2003.	41
Figure 3.1	Chemical warfare nerve agents Sarin (1) and Soman (2)	59
Figure 3.2	The molecular structures of the degradation products of nerve agents.	59
Figure 3.3	Structures of triphenyl (9) and diphenyl (10) phosphates.	60
Figure 3.4	Chemical structures of the urea-based functional monomer (14) and the templates: phosphorus ester triphenyl phosphate (12), phosphorus ester diethylphenyl phosphate (13) and triphenyl phosphine oxide (11).	61
Figure 3.5	Boc-phospho-L-serine methyl ester chosen as target molecule.	63
Figure 3.6	Chemical structure of <i>N,N</i> -diisopropyl-bis-(4-chloro)-benzyl phosphoramidate.	73
Figure 3.7	Structure of the monobenzyl Boc-phospho-L-methyl ester.	76
Figure 3.8	¹ H-NMR of Boc-phospho-L-serine methyl ester after hydrogenation.	77
Figure 3.9	¹ H-NMR of Boc-phospho-serine methyl ester after preparative HPLC.	78
Figure 3.10	¹ H-NMR spectrum in D ₂ O of Boc-serine methyl ester before treatment with ion exchange resin.	79
Figure 3.11	¹ H-NMR spectrum in D ₂ O of Boc-phospho-L-serine methyl ester after treatment with ion exchange resin.	79
Figure 3.12	Retention time at 4.80 of Boc-phospho-L-serine methyl ester observed in the LC.	80

Figure 3.13	Mass spectrometry of Boc-phospho-L-serine methyl ester. Peak at 298 inherent to the template and at 597 and 896 inherent to the dimers.	81
Figure 3.14	Structure of Boc-phospho-D-serine methyl ester.	82
Figure 3.15	¹ H-NMR of N,O-diethyl-4-vinyl-benzamidate and ethyl 4-vinylbenzoate.	86
Figure 3.16	¹ H-NMR of N,O-diethyl-4-vinyl-benzamidate (35).	87
Figure 4.1	Molecular mechanic force fields include (i) stretching energy; (ii) bending energy; (iii) torsion energy; (iv) non bonded energy, which accounts for repulsion, van der Waals attraction and electrostatic interactions.	93
Figure 4.2	Plot of molecular conformations vs potential energy.	96
Figure 4.3	Isomers of <i>N,N'</i> -diethyl-4-vinyl benzamidine.	98
Figure 4.4	Generated conformations and conformation energies.	100
Figure 4.5	Conformation energy and molecular structure of (E,E)- <i>N,N'</i> -diethyl-4-vinyl benzamidine and Boc-phospho-L-serine methyl ester complex.	101
Figure 4.6	Conformation energy and molecular structure of (E,Z)- <i>N,N'</i> -diethyl-4-vinyl benzamidine and Boc-phospho-L-serine methyl ester complex	102
Figure 4.7	Potential energies of (E,E) and (E,Z) isomers of the amidine in absence of template and the preferential conformation (E,E) which bound the phosphate group of the Boc-L-serine methyl ester.	103
Figure 4.8	Binding energies for <i>N,N'</i> -diethyl-4-vinyl benzamidine-Boc-phospho-L-serine methyl ester.	106

Figure 4.9	Predicted chemical shifts for the <i>N</i> -ethyl groups of the E,E and E,Z isomers.	108
Figure 4.10	¹ H-NMR of <i>N,N'</i> -diethyl-4-vinyl benzamidine in CDCl ₃ .	109
Figure 4.11	¹ H-NMR of <i>N,N'</i> -diethyl-4-vinyl benzamidine in CDCl ₃ at different temperatures. Signals at ~1.19 ppm and at ~ 3.30 ppm are inherent to the CH ₃ and CH ₂ of the two <i>N</i> -ethyl groups .	109
Figure 4.12	¹ H-NMR Amidinium chloride in DMSO.	110
Figure 4.13	¹ H-NMR of amidine in DMSO.	111
Figure 4.14	¹ H-NMR of monomer-template complex in DMSO.	111
Figure 4.15	¹ H-NMR of template-monomer complex in D ₂ O.	112
Figure 5.1	Addition-condensation system.	117
Figure 5.2	Initiation step.	119
Figure 5.3	Propagation step.	120
Figure 5.4	Termination step.	120
Figure 5.5	Scheme of MIP preparation.	123
Figure 5.6	Fourier optics configuration used by the Mastersizer 2000.	125
Figure 5.7	Particle size distribution for polymer prepared with protocol 1.	130
Figure 5.8	Particle size distribution for polymer prepared with protocol 2.	131
Figure 6.1	Batch analysis process.	136

Figure 6.2	Molecular structure of the ion pair reagent tetrabutylammonium chloride used to combine the Boc-phospho-L-serine methyl ester.	139
Figure 6.3	Binding for Boc-phospho-L-serine methyl ester imprinted in polar and apolar solvents (n=5 ± SD).	147
Figure 6.4	Binding for aqueous Boc-phospho-L-serine methyl ester at different pHs; pH=2.9 (0.001% trifluoroacetic acid); pH= 4 (0.01% Acetic acid); pH= 7 (0.01% trizma base HCl buffer 15 mM); pH= 8.2 (NaOH 2N)*; pH= 9.5 (0.01% borate); pH= 11 (NaOH 2N) *; (n=5 ±SD).	149
Figure 6.5	Binding for aqueous Boc-phospho-L-serine methyl ester at: (a) pH= 2 in HCl 2N and TFA 0.01%; (b) pH= 7 in 0.01% tris HCl 2N and ammonium acetate 1%; (c) pH= 8.2 in NaOH 2N solution and 0.3% di-sodium orthophosphate; (n=5 ± SD).	154
Figure 6.6	Binding for aqueous Boc-phospho-L-serine methyl ester at: (a) different concentration of trifluoacetic acid (TFA); (b) different concentration of ammonium acetate (AA); (c) different concentration of di-sodium orthophosphate; (n=5 ± SD).	157
Figure 7.1	Molecular structure of adenosine 5'-triphosphate (ATP)	164
Figure 7.2	Molecular structure of uridine 5'-triphosphate (UTP)	164
Figure 7.3	Molecular structure of Boc-phospho-D-serine methyl ester	165
Figure 7.4	Standard curve obtained from plotting a series of ATP and UTP standards (H ₂ O/ 0.001 %TFA) against peak area analysed using HPLC. Five standards were used ranging from 10 to 100µM.	167
Figure 7.5	Comparison of binding data between the template and the cross-reactants in an aqueous solution of 0.001 TFA; (n=5 ± SD).	169

Figure 7.6	Binding for L/D templates in H ₂ O/ TFA 0.01% and H ₂ O/ TFA0.001%; (n=5 ± SD).	170
Figure 8.1	Molecular structure of acridone-SRRRRW-OH containing a fluorescent label, a serine, four arginines and a tryptophan and acridone-pSRRRRW-OH containing a fluorescent label, a phospho serine, four arginines and a tryptophan.	175
Figure 8.2	Molecular structure of GSG consisting of a fluorescent label, a glycine, a serine and a glycine and GpSG consisting of a fluorescent label, a glycine, a serine and a glycine.	176
Figure 8.3	Binding for non-phospho (NP) and phospho (P) peptide pair A in 0.01% Acetic acid/ H ₂ O (pH4).	179
Figure 8.4	Binding for peptide pair A in (a) aqueous 1% orthophosphate and (b) in aqueous 10% orthophosphate.	181
Figure 8.5	Binding for Acridone-SRRRRW-OH (NP peptide) and Acridone-pSRRRRW-OH (P peptide) in a buffer solution of ammonium acetate 10 mM.	182
Figure 8.6	Binding of the non phosphorylated peptide B for NIP in different aqueous systems of varying pHs.	183
Figure 8.7	Binding of peptide pair B using (a) MeOH/H ₂ O (8:2) and (b) MeOH/H ₂ O (8:2) + 0.001% TFA (pH= 2.3) .	184
Figure 8.8	Binding of peptide pair B using MeOH/H ₂ O (4:6) + 0.001% TFA to achieve a pH= 2.3.	185
Figure 9.1	Principle of IMAP assay.	190

LIST OF TABLES

	<i>Page</i>
Table 1.1	Diseases caused by mutations in particular protein kinases and phosphatases. 4
Table 1.2	Assay techniques for high-throughput screening of kinases. 12
Table 1.3	Example of the most common non covalent interactions and approximate bond energies 33
Table 3.1	Synthetic variations and phosphorus shifts (δ ^{31}P NMR data) for Arbuzov Reaction. 68
Table 5.1	Differences between step- and chain growth polymerisation. 118
Table 5.2	Centrifugation conditions 129
Table 5.3	Sedimentation and centrifugation process 130
Table 6.1	Ionisation state of the phosphorylated/acid group at different pH values. 145
Table 6.2	Ionisation state of the amidine/basic group at different pH values. 146
Table 6.3	Distribution coefficients (DC) and imprinting factors for MIP/NIP measured after 24 hours incubation with 100 μM Boc-phospho-L-serine methyl ester 149
Table 6.4	Distribution constants and imprinting factors for MIP/NIP measured after 24 hours incubation with 100 μM Boc-phospho-L-serine methyl ester in different solutions 155
Table 6.5	Distribution constants and imprinting factors of six MIPs measured after 24 hours incubation with 100 μM Boc-phospho-L-serine methyl ester 158
Table 7.1	Distribution coefficients and imprinting factors for the cross-reactants (ATP/UTP) and Boc-phospho-L-serine methyl ester in an aqueous solution of 0.001% TFA. 168

Table 7.2	Binding data for L and D enantiomers of Boc-phospho-serine methyl ester.	171
Table 8.1	Aqueous systems used for the batch analyses of peptide pair B. (*NaOH 2N and HCl 2N were added dropwise to water to reach the desired pHs).	178
Table 8.2	MeOH/H ₂ O systems used for the batch analyses of peptide pair B.	178

LIST OF SCHEMES

	<i>Page</i>
Scheme 3.1 Arbuzov Reaction of the phosphorylation of Boc-L-serine methyl ester. <u>Reagent and conditions</u> : (i) CH ₂ Cl ₂ , 0°C, 5 min.; (ii) 25°C, 30 min.; (iii) Pyridine, CH ₂ Cl ₂ , 4 hrs	67
Scheme 3.2 Attempted phosphorylations. <u>Reagents and conditions</u> : (i) Iodine, pyridine, dichloromethane, 25°C, 4 hrs; (ii) Iodine, pyridine, dichloromethane, 0°C, 4 hrs; (iii) Iodine, pyridine, dichloromethane, 0°, 4 hrs, 4 eq. phosphite; (iv) Iodine, pyridine, dichloromethane, 24 hrs.	68
Scheme 3.3 Attempted synthesis using NMI as base.	69
Scheme 3.4 Phosphorylation method by using the Grignard reagent	70
Scheme 3.5 Alternative synthesis for serine phosphorylation.	71
Scheme 3.6 Deprotection of diethyl phospho-boc-serine methyl ester	72
Scheme 3.7 Preparation of the phosphoramidate by three step reactions	73
Scheme 3.8 Synthesis of the intermediate N-Boc-O-phospho-4-chloro-(dibenzyl)-L-serine methyl ester (29), made by addition of phosphoramidate (27) to the Boc-L-serine methyl ester in the appropriate conditions.	74
Scheme 3.9 Final step of the synthesis of Boc-phospho-L-serine methyl ester (29).	75
Scheme 3.10 Boc-D-serine esterification and phosphorylation. <u>Reagents and conditions</u> : (i) <i>N,N'</i> -diisopropyl-bis-(4-chloro)-benzylphosphoramidate, 1H-tetrazole/MeCN; (ii) meta-chloroperbenzoic acid (MCPBA); (iii) Pd 10%, H ₂ O/ <i>t</i> -BuOH.	83
Scheme 3.11 Amidine synthesis.	85

ABBREVIATIONS

ATP	adenosine triphosphate
AIBN	azobisisobutyronitriles
BAZO	1,1'-azobis cyclohexane-carbonitrile
Boc	t-butyloxycarbonyl
C _b	bound concentration of a substrate
C _f	free concentration of a substrate
CHCl ₃	chloroform
CH ₂ Cl ₂	dichloromethane
C _T	total concentration of a substrate
DC	distribution coefficients
DMF	dimethylformamide
DMSO	dimethylsulfoxide
DVB	divinylbenzene
EGDMA	ethyleneglycol dimethacrylate
FP	fluorescence polarisation
FRET	fluorescence resonance energy transfer
HPLC	high-performance liquid chromatography
MAA	methacrylic acid
MCPBA	meta-chloroperbenzoic acid
MeCN	acetonitrile
MeOH	methanol
MIP	molecularly imprinting polymer
MOE	Molecular Operating Environment

MS	mass spectrometry
NIP	non-imprinted polymer
NMI	N-methylimidazole
NMR	Nuclear Magnetic Resonance
PETRA	pentaerythritol
TBA-Cl	tetrabutylammonium chloride
TFA	trifluoroacetic acid
TFMAA	trifluoromethacrylic acid
TLC	thin-layer chromatography
TRIM	trimethylolpropane trimethacrylate
UTP	uridine 5'-triphosphate
UV	ultraviolet
VDW	van der Waals

Chapter 1

Introduction

1.1 PROTEIN PHOSPHORYLATION

Protein phosphorylation is one of the most important and universal mechanisms of protein regulation in eukaryotic organisms, which affects nearly every aspect of cell life¹. During the 1970s, although many scientists concluded that protein phosphorylation-dephosphorylation was an exclusive feature of higher organisms, Garnak and Reeves² reported that the catalytic activity of isocitrate dehydrogenase (IDH) from *Escherichia coli* was regulated by phosphorylation on serine residues³. This evidence subsequently led to the discovery of a number of protein kinases/phosphatases in prokaryotic organisms establishing the existence and the importance of regulatory protein phosphorylation in bacteria³.

Protein phosphorylation and dephosphorylation, catalysed by protein kinase and protein phosphatase enzymes (Figure 1.1), has emerged as a prominent mechanism for the regulation of a range of molecular processes including metabolism, growth, differentiation, motility, membrane transport, learning and memory⁴⁻⁶. When phosphorylated by the appropriate protein kinase, a regulatory protein or enzyme is activated, inhibited, or “marked” for targeting by other regulatory factors⁷⁻¹⁰. The simplicity, flexibility and reversibility of this post-translational process, coupled with the ready availability of adenosine triphosphate (ATP) as a phosphoryl donor, is why it has been evolved to regulate so many biological processes.

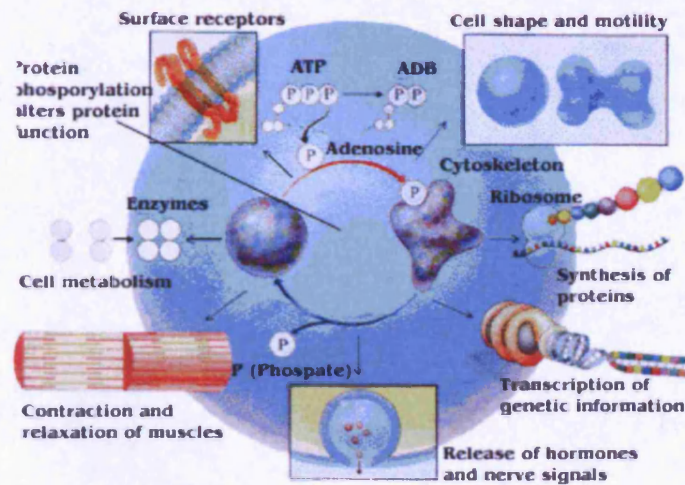


Figure 1.1: Protein phosphorylation process. A protein kinase moves a phosphate group from ATP to the protein. A protein phosphatase removes the phosphate and the protein reverts to its original state, (Adapted from ref.11).

As many as one third of the proteins formed by phosphorylation involves the formation of phosphoserine, which accounts for ~ 90% of all cellular phosphorylation, whereas ~ 10% of the phosphorylation occurs on threonine residues and only ~ 0.1% on tyrosine residues¹².

Therefore, it is not surprising that abnormal protein phosphorylation is a cause or consequence of many pathological conditions, such as cancer¹³, diabetes¹⁴, heart disease¹⁵, hypertension¹⁶, stroke¹⁷ and that kinases and phosphatases have become a major target for drug design¹⁸. A number of diseases that result from mutations in particular protein kinases and phosphatases are listed in Table 1.1.

Table 1.1: Diseases caused by mutations in particular protein kinases and phosphatases, (Adapted from ref.9).

Disease	Kinase/Phosphatase
Myotonic muscular dystrophy	Myotonin protein kinase
Papillary renal cancer	Met receptor kinase
Chronic myelogenous leukaemia	Abelson tyrosine kinase
Li-Fraumeni syndrome	Chk2 kinase
Williams syndrome	Lym kinase-1
Wolcott-Rallison syndrome	eIF2A-kinase 3
X-Linked myotubular myopathy	MTM1 Tyr phosphatase

To ensure signalling fidelity, kinases must be sufficiently specific and act only on a defined subset of cellular targets. Understanding the basis for this substrate specificity is essential for identifying the role of an individual protein kinase in a particular process¹⁹. In recent years, several small, cell-permeant inhibitors of protein kinases have been developed that exhibit a relatively high degree of specificity for a particular protein kinase and these have been useful in identifying the physiological substrates and cellular functions of these enzymes²⁰. They include Cyclosporin, the immuno-suppressant drug that inhibits a protein phosphatase and permits the widespread use of organ transplantation²¹, and its successor, Rapamicin, which inhibits a protein kinase²². The availability of more cell-permeant protein kinase inhibitors would be extremely useful in helping to delineate the physiological roles of these enzymes. A number of other compounds have been reported to inhibit particular serine/threonine protein kinases specifically, and are being used extensively in cell-based assays

to evoke physiological roles for these enzymes. However, the specificity of many of these compounds has not been rigorously tested ²⁰.

1.1.1 PROTEIN KINASES: NATURE AND MECHANISM OF ACTION

Protein kinases are major players in the phosphorylation cascades central to intracellular signalling²³. They catalyze protein phosphorylation, whereas their counteracting enzymes, protein phosphatases, catalyze protein dephosphorylation¹⁹. Reversible protein phosphorylation is a critical facet of cellular signalling networks and it has been established that these two enzyme superfamilies represent attractive therapeutic targets for a range of diseases, including leukemias, solid tumors, cardiovascular diseases and immune/inflammatory disorders²⁴.

Protein kinases catalyze phosphoryl transfer by serving as a template for the two substrates ATP and peptide/protein/tyrosine and inducing phosphoryl movement from nucleotide to a side chain hydroxyl¹⁹.

The typical acceptors for eukaryotic phosphorylation are the hydroxyamino acids serine (Ser), threonine (Thr) and tyrosine (Tyr), while prokaryotes favour the use of histidine (His) and the carboxyamino acids [aspartic acid (Asp) and glutamic acid (Glu)] as phospho-acceptors. Lysine (Lys), arginine (Arg) and cysteine (Cys) have also been identified as phosphate acceptors in both prokaryotes and eukaryotes²³. Figure 1.2 shows the structure of the phosphoamino acids known to be synthesised biologically.

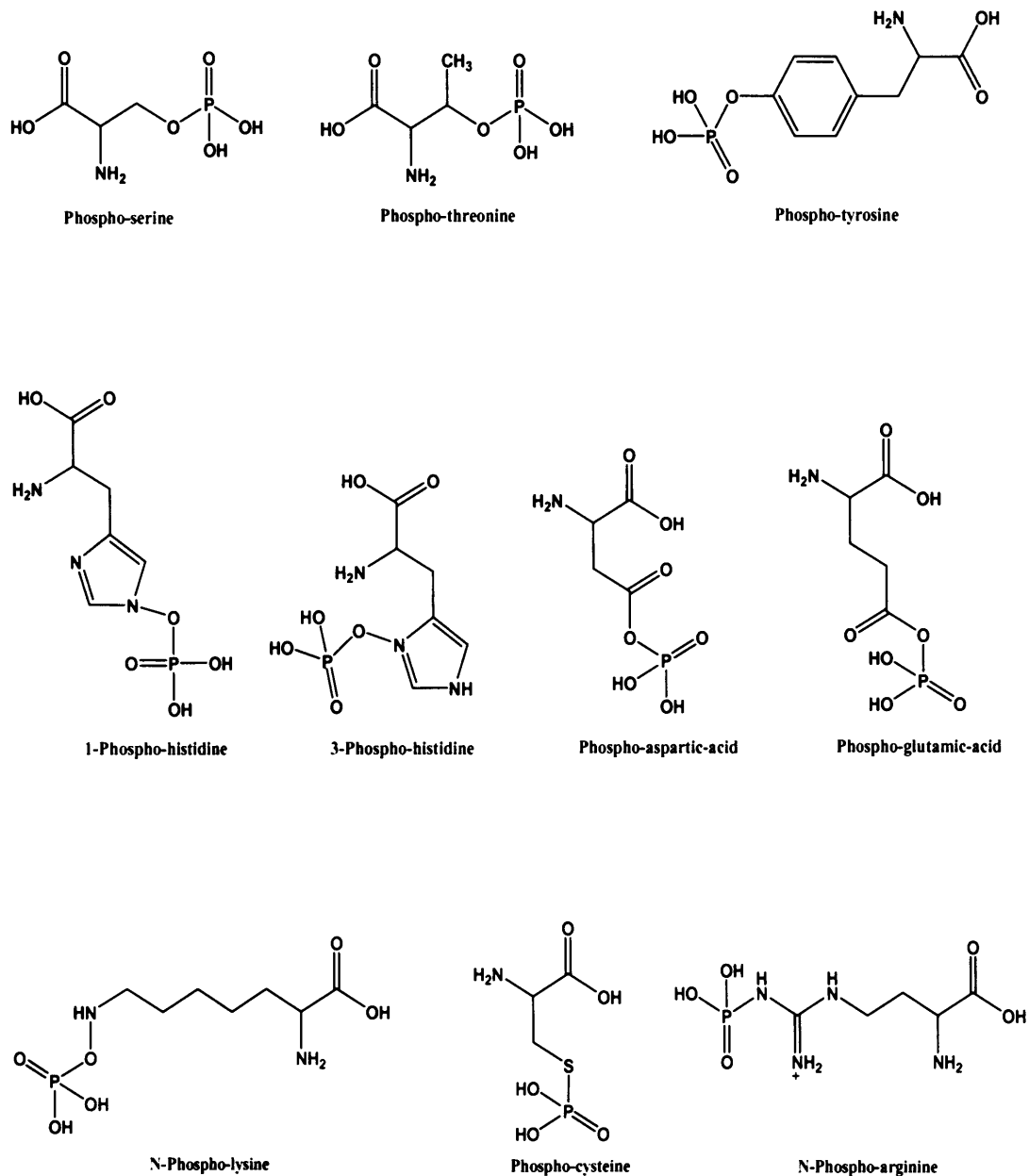


Figure 1.2: The chemical structures of the phosphoamino acids known to be formed biologically.

The majority of the protein kinases fall into two large classes based on their ability to phosphorylate either serine/threonine or tyrosine side-chains. Protein kinases that phosphorylate serine or threonine are termed serine protein kinases [SPKs] and those that phosphorylate tyrosine are called tyrosine protein kinases [TPKs]²⁵. There is a third

class of kinases that can phosphorylate both serine and tyrosine side chains^{26,27}. This group, termed dual-specific protein kinases, is small in number and is not well characterized from a mechanistic standpoint²⁵. Protein kinases poorly phosphorylate free amino acids and rely on local residues for high affinity. In general they phosphorylate peptide regions based on the residues immediately flanking the site of phosphorylation²⁵.

The other phosphoamino acids, such as phospho-His [His(P)], phospho-Cys [Cys(P)] and phospho-Asp have been shown to be the phosphorylated reaction intermediates in several enzymes and are unstable under the conditions of standard protein purification procedures²³. Although there is an emerging awareness of critical roles of His (P) and Cys (P) in regulation, analytical techniques are limited, as detection is generally based on radiolabelling and an enzymatic approach, which is limited by the available enzymes²³.

Protein kinases follow a ternary complex kinetic mechanism in which direct transfer of the phosphoryl group from ATP to protein substrate occurs. They require an essential divalent metal ion, usually Mg^{2+} , to facilitate the phosphoryl transfer reaction and assist in ATP binding. While the phosphoryl transfer mechanism is chemically simple, the phosphorylation of protein substrates in the active site of a protein kinase is complex and involves structural changes²⁵. The mechanism of phosphoryl groups transfer from donors to acceptors in solution reactions has been studied extensively and, in principle, it may in the extreme, utilize two different transition states, either associative or dissociative¹⁹ (Figure 1.3). In an associative transition state, analogous to a tetrahedral intermediate in organic acyl transfer reactions, a bond is formed between the attacking oxygen and the reactive phosphorus atom, while the bond to the departing adenosine diphosphate (ADP) would not yet have been significantly broken (Figure 1.3). A dissociative transition state, analogous to an SN_1 reaction in organic substitution

reactions, is one in which the importance of the nucleophilicity of the attacking hydroxyl is diminished and departure of the leaving group (ADP) is well advanced (Figure 1.3). Of course, these putative structures reflect extreme cases and it is possible for a given phosphoryl transition state to incorporate aspects of both. In general, it has been proposed that protein kinases are likely to utilize a dissociative transition state²⁷.

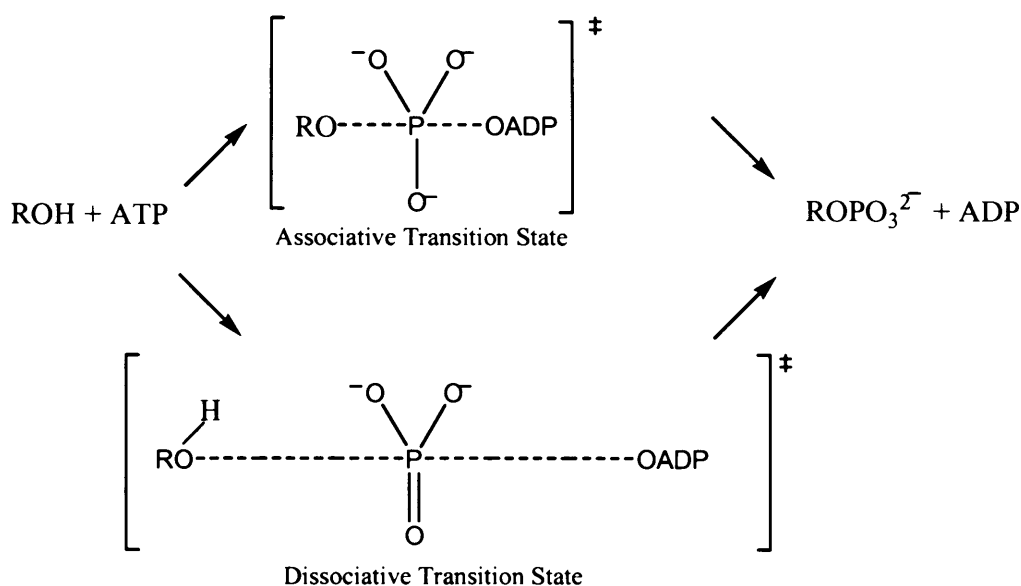


Figure 1.3: Dissociative vs. associative transition states for phosphoryl transfer, (Adapted from ref.28).

One of the most important features of protein kinases is their substrate specificity, which to a large extent is determined by the primary sequence around the phosphorylation site of their targeting proteins. To understand the regulatory mechanisms at the cellular level, it is necessary to identify the specific amino acid residues that are phosphorylated¹². Because all kinases use ATP as a phosphate source, an analysis of phosphorylated proteins inside the cell does not reveal which kinases are responsible for the placement of which phosphate groups. If a single kinase could be activated at a particular time without activating other kinases, it would be possible to identify its downstream targets;

however, known biological stimuli activate multiple kinases at once²⁹. Many of these kinases also have overlapping substrate specificities, further complicating the issue²⁹. As a result, great efforts have been made to identify the potential kinase substrates, including combinatorial synthesis of peptide libraries with radioisotope-based or antibody-based detection^{30,31}.

1.1.2 PROTEIN PHOSPHATASES : STRUCTURE AND FUNCTION

In the field of protein phosphorylation, kinases played the dominant role and phosphatases were considered to be the passive partners reversing the effects of kinases³². Indeed, the kinases must act first and presumably evolved earlier; however, the function of phosphatases is far from being inferior³³. The steady state level of phosphorylation of a given protein can be modulated either by kinase or by the phosphatases, making the two types of enzyme equally important in cellular regulation³⁴. Serine/threonine-specific protein phosphatases can be divided into four main families. Type 1 phosphatases (PP1) dephosphorylate the β -subunit of phosphorylase kinase specifically, whereas type 2 phosphatases dephosphorylate preferentially the α -subunit of phosphorylase kinase. The type 2 phosphatases comprise three enzymes (PP2A, PP2B, and PP2C) that can be distinguished by their requirement for cations. PP2A, like PP1, does not have an absolute requirement for divalent cations, whereas PP2B and PP2C are Ca^{2+} /calmodulin- and Mg^{2+} -dependent, respectively^{35, 36}.

Tyr-specific phosphatases (PTP) were discovered later but had a faster development. They all contain an essential cysteine and arginine residue in the active site that forms a covalent intermediate with the phospho substrate³⁷.

1.1.3 DETECTION OF PROTEIN PHOSPHORYLATION

Detection of protein phosphorylation requires analysis at two levels: firstly, to determine if a protein is a phosphoprotein and secondly, to identify the amino acids on which phosphorylation occurs.

A number of techniques are used in phosphorylation studies to detect phosphoproteins, such as the *in vivo* or *in vitro* incorporation of ^{32}P , the use of specific antibodies which recognise Ser(P), Thr(P) or Tyr(P) as part of the epitope, enzymatic or chemical removal of phosphate, and analysis using chromatographic methods [high-performance liquid chromatography (HPLC), thin-layer chromatography (TLC)], electrophoresis, or mass spectrometry (MS). A combination of these techniques is often employed to achieve the best results²³.

1.1.3.1 RADIOLABELLING

The classical approach for the detection of phosphorylation is the incorporation of radiolabelled phosphate into phosphoproteins^{5,23}. *In vivo*, protein labelling involves the incubation of intact organisms, cells or tissues with [^{32}P]phosphate or [γ - ^{32}P]ATP in permeabilised cells. The next step involves the purification of the phosphorylated proteins without their further modification by cellular proteases, protein kinases, phosphatases, or protease/phosphatase inhibitors³⁸. *In vitro*, protein labelling involves incubation of a cell-free system containing a divalent cation (Mg^{2+} or Mn^{2+}), with a protein kinase [or cell fraction containing a protein kinase(s)] and [γ - ^{32}P]ATP as the substrate that serves as the phosphate donor for most protein phosphorylation reactions³⁸.

Radiolabelling methods are very sensitive, and provide excellent resolution, although the *in vivo* method is limited to organisms or cells where the radio label can be incorporated during cell growth²³. The major disadvantages are: (1) in order to obtain high specific labelling,

relatively large amounts of ^{32}P *in vivo* or high specific activity of [γ - ^{32}P]ATP *in vitro* are required; (2) the difference in metabolic phosphorylation/dephosphorylation rates results in a different proportion of ^{32}P incorporation into Ser, Thr and Tyr residues which depends also upon the labelling time. Therefore, caution must be made in drawing conclusions about the ratios of phosphorylated Ser, Thr and Tyr and indeed other kinds of protein phosphorylation; (3) constitutively phosphorylated proteins with a slow phosphate turnover rate may not be detected in short *in vivo* labelling studies^{23,5}.

1.1.3.2 FLUORESCENCE LABELLING

Another general approach for detecting protein bound phosphate groups is to derivatise them with a molecular label such as a fluorophore. Several fluorescent probes have been developed recently, such as environment-sensitive fluorophores adjacent to the phosphorylated residue^{39,40}, placement of fluorescence resonance energy transfer (FRET) partners flanking a sequence that undergoes a conformational change upon phosphorylation⁴¹ and signalling via metal chelation⁴² between the newly introduced phosphate and an external⁴³ or internal⁴⁴ chelator. These probes are elegantly designed⁴⁵, but their affinity and sensitivity (i) may be affected by the amino acid sequence of the target phosphopeptide, (ii) may involve non-versatile design strategies, or (iii) may require technically challenging microfluidic setups³⁹. Therefore, there is considerable scope for the continued development of novel chemical approaches^{46,47} for assaying protein kinase activity and some new approaches are summarized⁴⁸ in Table 1.2.

Table 1.2: Assay techniques for high-throughput screening of kinases, (Adapted from ref.49).

Technique	Principle	Pros and cos
Fluorescence polarization (FP) assay	Depolarization of polarized light is dependent on molecule size, with small molecules depolarizing light faster. Fluorophore-labeled tracer peptides are used to give a signal after binding to antiphospho-antibodies during the detection step.	+ nonradioactive, low enzyme need, high miniaturization potential, bead free - signal-decrease assay, tracer and antibody needed, peptide size limited
IMAP assay	Special form of fluorescence-polarization assay. Fluorophore-labeled peptides have to be used as substrates and phosphorylation is monitored through mass increase by binding of detection beads coated with trivalent metal ions.	+ nonradioactive - peptide size limited to 5 kDa, so protein substrates cannot be used, 20-30% peptide turnover is required for a good signal
Caliper assay	Electrophoretic separation of substrate and phosphopeptides in microfluidic devices. Reactions may be performed on-chip or off-chip.	+ nonradioactive, high accuracy due to measurement of substrate consumption and product formation, highly miniaturized on-chip format -20-30% peptide turnover required for a good signal, limited throughput
Electroluminescence assay⁵⁰	Signal is generated in an electrochemical reaction that depends on recruitment of ruthenium complexes to electrodes.	+ nonradioactive -availability of specific antibodies, relatively high cost
IQ (Pierce)⁵¹ assay	Phosphorylation of peptides allows binding of a proprietary quencher, thereby reducing fluorescence.	+ nonradioactive -signal-decrease assay, compound interference
Kinase-Gio (Promega)	ATP consumption in a kinase reaction is monitored through luciferase activity.	+ nonradioactive - signal-decrease assay, off-target hits due to the coupled enzyme format, so need for additional selectivity testing
PKlight (Cambre)⁵² assay	ATP consumption by the kinase is measured. Remaining ATP is detected by bioluminescence.	+ nonradioactive - signal-decrease assay, off-target hits due to the coupled enzyme format, so need for additional selectivity testing

1.1.3.3 ANTIBODIES

One potentially attractive non-radioactive assay is to use phospho-specific antibodies that recognize the product of the kinase reaction, which have the advantages of simplicity and radiometric signal processing not requiring the use of radioisotopes or other specialised reagents²⁰. The simplest approach is to use phospho-specific antibodies that recognise peptides containing either a phosphoserine, phosphothreonine or phosphotyrosine residue. This method can be extremely sensitive since antibodies can detect as little as a few femtomol (fmol) of phosphorylated epitopes⁵³. In addition, due to the highly specific nature of antibody-antigen recognition, cross-reactivity of one phosphoamino acid antibody (e.g., anti-phosphotyrosine) to other phospho amino acids or non-phosphorylated amino acids has been shown to be minimal³⁰. Indeed, such antibodies have been used successfully for the assay of protein tyrosine kinases^{53,54}. The potential specificity of such antibodies generated against specific phosphorylation epitopes makes site-specific phosphorylation analysis feasible, providing the relevant antibodies can be prepared²⁹. However, the development of equivalent assays for serine/threonine-specific protein kinases or phosphatases has not been possible since sufficiently good antibodies, for phospho-serine or phospho-threonine containing peptides, are not available. It is therefore necessary to develop separate phospho-specific antibodies for each phosphorylated substrate²⁰. This is a key point since it means that at the present time, it is not possible to use an antibody assay to observe peptide phosphorylation (at serine or threonine) without prior knowledge of the peptide target. This is a particularly relevant problem when trying to elucidate enzyme-substrate relationships and an alternative molecular recognition approach, that would target phosphoserine and phosphothreonine independently of peptide amino acid composition, would be of great value.

1.2 MOLECULARLY IMPRINTING POLYMER

1.2.1 INTRODUCTION

The developing technique of molecularly imprinted polymer (MIP) provides an alternative strategy to antibodies for targeting both specific and non specific serine/threonine phosphorylation events.

Biological recognition agents such as antibodies and enzymes have been widely employed as the specific-affinity sensing agents in analytical biochemistry, biosensors, diagnostic kits, and other applications^{55,56}. The specificity of these molecules has referred on both protein sequence and conformation⁵⁷. Antibody-assays are very efficient and sensitive but they present a number of potential drawbacks mainly related to antibodies fragility and instability. Therefore, this study aimed to use MIPs as antibody substitutes, in order to generate a general assay that could detect a wide variety of protein kinases and that could possibly resolve the high specificity of the antibodies. As antibody and receptor binding mimics, MIPs have been prepared that recognise target molecules with high affinity and specificity⁵⁸⁻⁶³. A significant benefit when compared to antibodies is that they tend to be physically and chemically robust which means that they can be used in harsher conditions (organic solvents, pH extremes, high pressures and elevated temperatures) than normally associated with the use of antibodies⁶⁴.

1.2.2 BRIEF OF HISTORY

Molecular imprinting, as we know it today, started in 1972 but the concept itself has a long history. Around 1930, the Soviet chemist M.V. Polyakov reported the post-polymerisation selective adsorption of different additives in silica particles, for chromatography application, prepared using a novel synthetic procedure⁶⁵. However, the concept of template-mediated assembly dates back to the 1940s when Linus

Pauling proposed that antibody formation took place in the presence of an antigen which served as a template for antibody formation⁶⁶. Although this theory was later proven to be incorrect, it represented the first example of “bio-imprinting” and inspired the work of his student, Frank Dickey⁶⁷. The methodology used by Dickey was very similar to that of Polyakov with the difference that Polyakov introduced the template (additives) during the drying process, while Dickey introduced the template (dye compound) prior to polymerisation⁶⁸. The results were striking where the resultant polymer showed a number of selective recognition sites for the original template. Thus, Dickey started, without intention, the era of molecularly imprinted polymer technology, which was then challenged by other groups⁶⁹⁻⁷¹.

Since those early days, the methodology of molecular imprinting has evolved along two routes, depending on the kind of relationship between the template molecule and the functional monomer(s)⁷². The general principles of molecular imprinting involve the binding of a target molecule to an appropriate monomer through covalent or non covalent interactions. This complex then is polymerized in presence of a cross-linking monomer in order to rigidly fix the spatial arrangement of the functional monomers. Upon removal of the template species, cavities in the matrix are revealed whose size and functionality are complementary to that of the template (Figure 1.4).

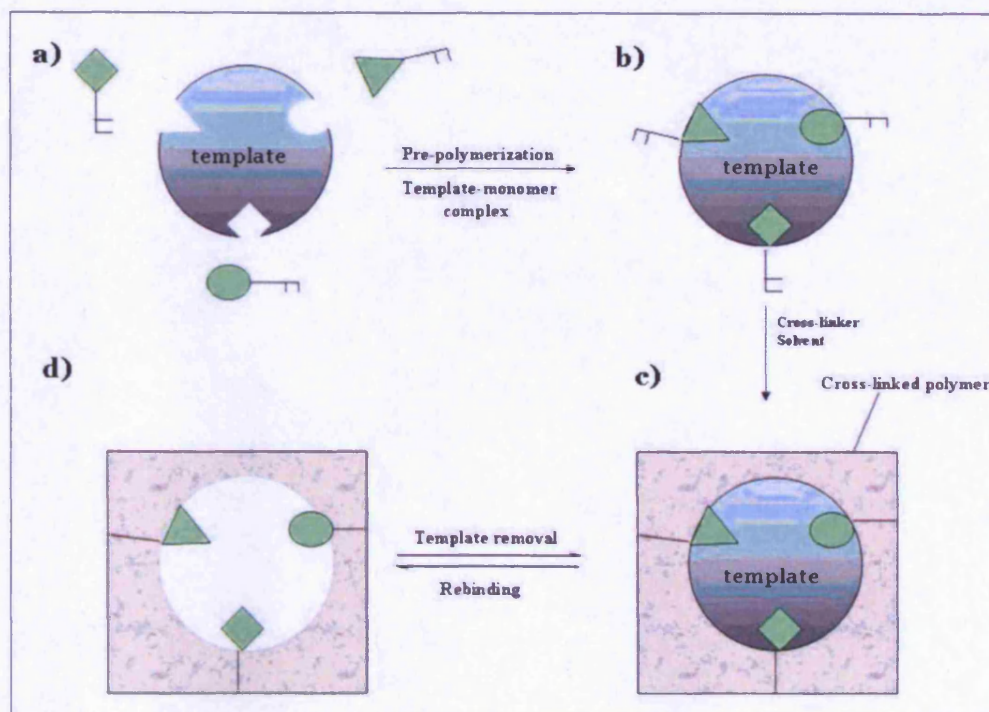


Figure 1.4: Schematic representation of the molecular imprinting technique: a) and b) pre-polymerisation complex between template and functional monomer(s); c) polymer formation; d) template extraction which leaves binding sites complementary to the original template.

Non-covalent imprinting, due to its versatility and practical simplicity over the covalent method, has been widely adopted today. Its use is involved in a number of applications which include membrane separations⁷³, selective sorption⁷⁴, capillary electrophoresis⁷⁵ and various types of sensors⁷⁶.

For further information, the reader is referred to the following review articles^{72,77-81}.

1.2.3 MOLECULAR IMPRINTING METHODOLOGIES

Molecular imprinting approaches can be classified in three ways depending on the type of interaction between the template guest and the host functional monomer(s): a) covalent bonding; b) non covalent bonding; c) semi covalent and sacrificial spacer approach.

1.2.3.1 COVALENT APPROACH

Covalent imprinting is characterised by the use of templates which are covalently bound to one or more polymerizable groups. After polymerisation, the template is cleaved and the functionality left in the binding site is capable of binding the target molecule by re-establishment of the covalent bond⁸¹.

The boronate ester approach was undoubtedly the most successful of the reversible covalent methods⁸². The method was first developed by Gunter Wulff at the University of Bonn, where he synthesised the boronate di-ester of phenyl- α -D-mannopyranoside by using two molecules of 4-vinylphenylboronic acid⁸². The boronate sugar was then co-polymerised with large amounts of cross-linking agent such as ethylene dimethacrylate in the presence of an inert solvent. The template molecules were then extracted from the polymer networks by mild hydrolysis with, for example, aqueous methanol, leaving a polymer cavity containing boronic acid residues in the exact spatial arrangement necessary to rebind the template (Figure 1.5).

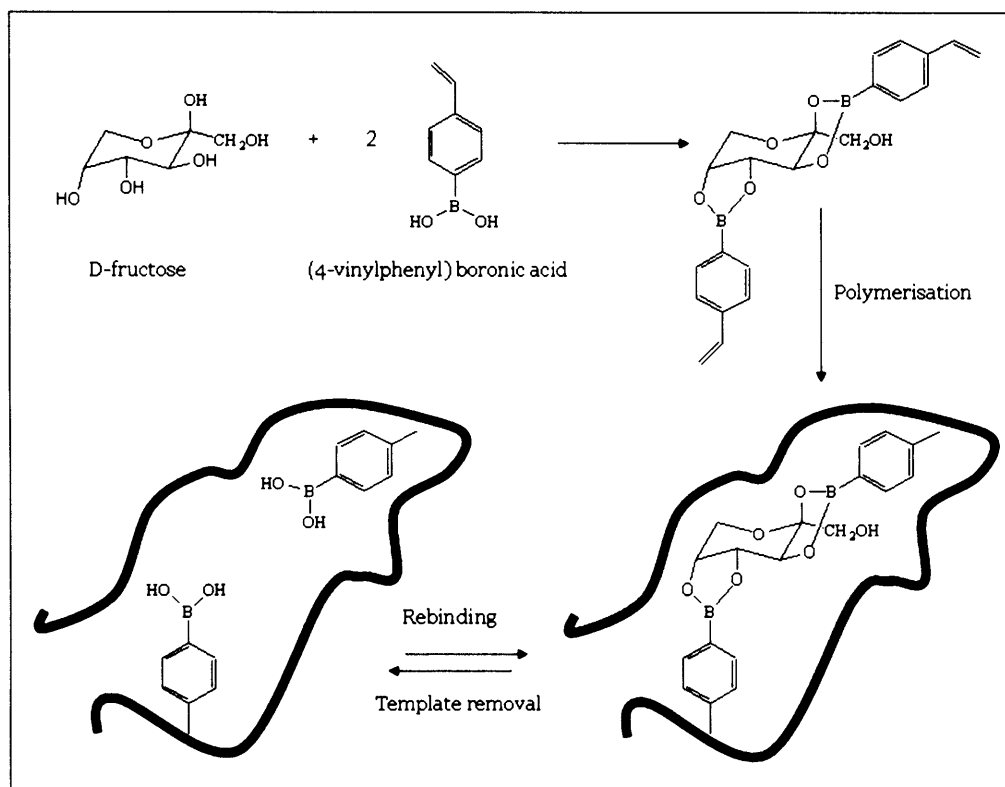


Figure 1.5: The first example of covalent imprinting, by the group of Wulff⁸².

This work was the first in a series of papers making use of reversible covalent interactions as the basis for recognition⁸³.

The advantage of covalent imprinting is that functional groups are only associated with the template site; however, only a limited number of compounds (alcohol (diols)⁸⁴⁻⁸⁸, aldehydes^{89,90}, ketones⁹¹⁻⁹⁴, amines^{95,96} and carboxylic acids⁹⁷⁻¹⁰⁰) can be imprinted using this approach.

1.2.3.2 NON-COVALENT APPROACH

Non-covalent imprinting approach, popularised by the Klaus Mosbach group¹⁰¹ at the University of Lund in Sweden in the 1980s, has been applied to a much wider range of template molecules including steroids¹⁰², β -blockers¹⁰³, peptides¹⁰⁴ and theophylline¹⁰⁵. This method relies on self-assembling functional monomers around the template in the polymerisation mixture and, because no covalent bonds are formed

between the template and polymer, template removal involves simply washing the polymer repeatedly with a suitable solvent. Specific rebinding relies on reformation of the non-covalent interactions that were responsible for stabilisation of the pre-polymerisation complex⁷⁷ (Figure 1.6).

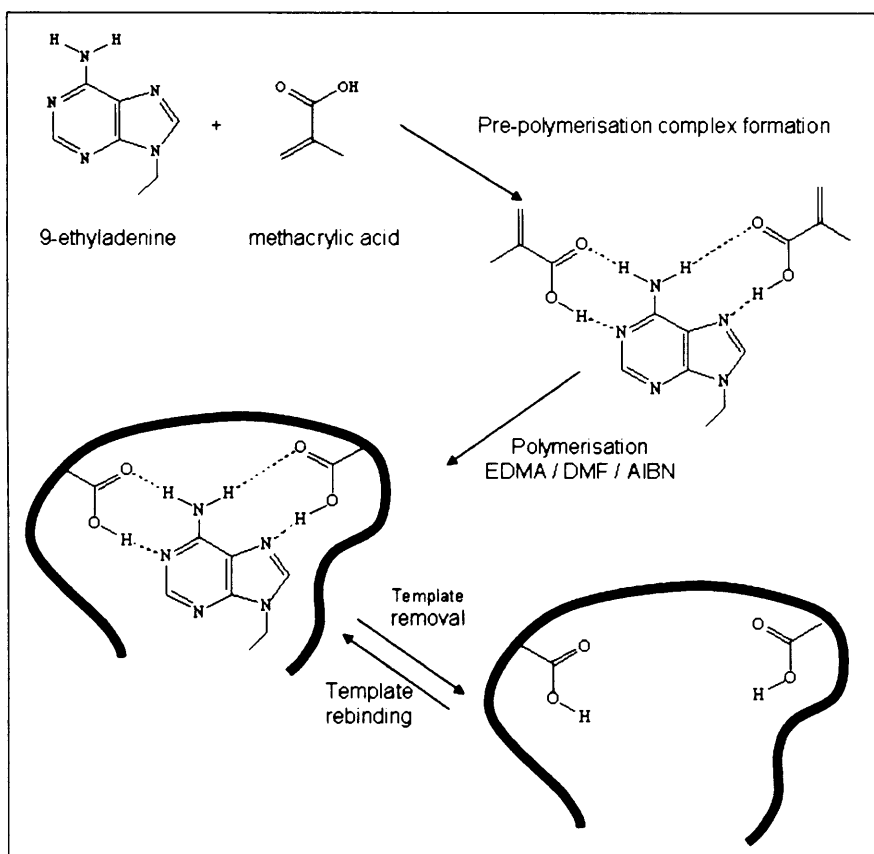


Figure 1.6: Non-covalent molecular imprinting of 9-ethyladenine reported by Shea *et al.*¹⁰⁶.

This is the predominant method currently used because it offers much more flexibility in terms of the functionalities on a template that can be targeted⁸⁰.

1.2.3.3 SEMI- COVALENT AND SACRIFICIAL SPACER APPROACH

Semi-covalent imprinting attempts to combine the advantages of both approaches, where covalent template structure is used in the polymerisation step and rebinding is entirely non-covalent in nature⁸⁰. Two variations in the semi-covalent approach can be distinguished⁸¹: (i) the template and the monomer are connected directly by an ester or amide linkage or (ii) the template and the monomer are connected using a spacer group.

The first semi-covalent approach was reported by Sellergren and Andersson⁸⁶ for the imprinting of *p*-aminophenylalanine ethyl ester. A structural analogue was used which possesses two polymerisable groups attached *via* ester linkages. After hydrolysis the carboxylic acid groups left in the polymer binding site interacts with the amino acid through a mixture of hydrogen bonding and electrostatic interactions (Figure 1.7).

However, this apparently simple process presents some drawbacks: template hydrolysis is often not straightforward and the steric requirements of an acid and an alcohol in hydrogen-bonding contact are rather different from the corresponding ester, which can sometimes compromise the imprinting⁸⁰.

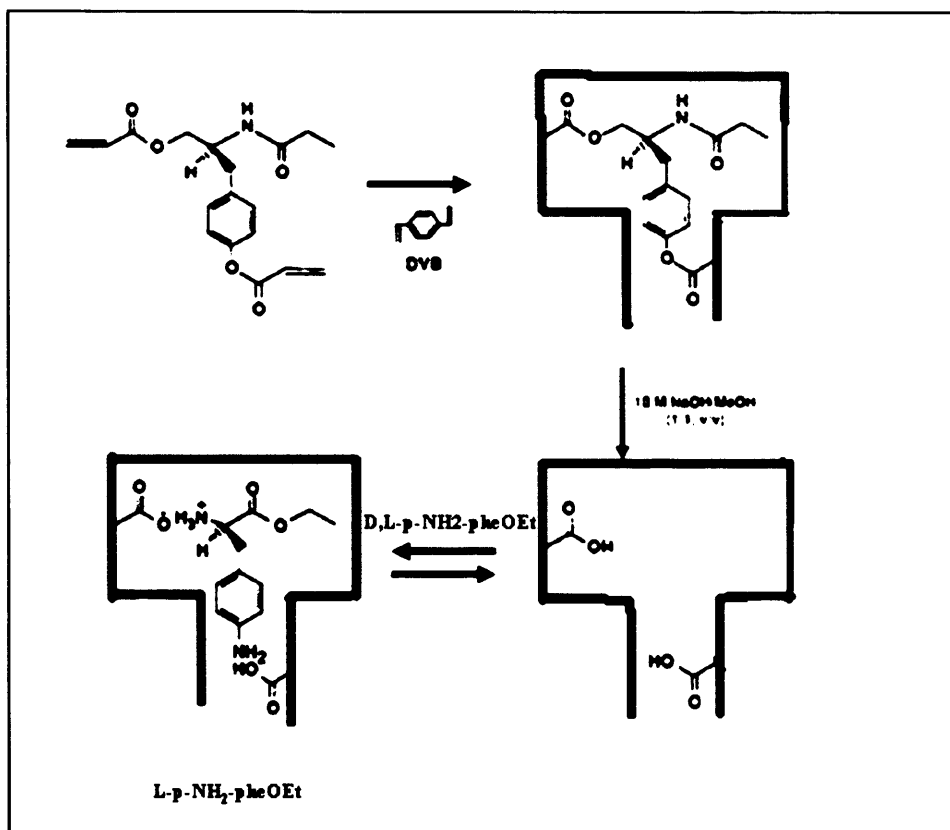


Figure 1.7: Semi-covalent approach for the imprinting of *p*-aminophenylalanine ethyl ester, (Adapted from ref.86).

In order to overcome some limitations of the semi-covalent technique, Whitcombe *et al.*^{107,87} introduced a sacrificial spacer between the template and the functional monomer, which was subsequently removed with the template. In the first example the template, cholesterol, was attached *via* a carbonyl spacer to 4-vinylphenol carbonate to produce cholesteryl 4-vinylphenyl carbonate as the template monomer. After polymerisation the cholesterol was cleaved from the polymer by base hydrolysis leaving a phenolic hydroxyl group in the binding site capable of interacting with cholesterol through hydrogen bond formation. The carbonyl spacer group was lost as CO₂ leaving sufficient room between functional groups to establish hydrogen bonding¹⁰⁷ (Figure 1.8).

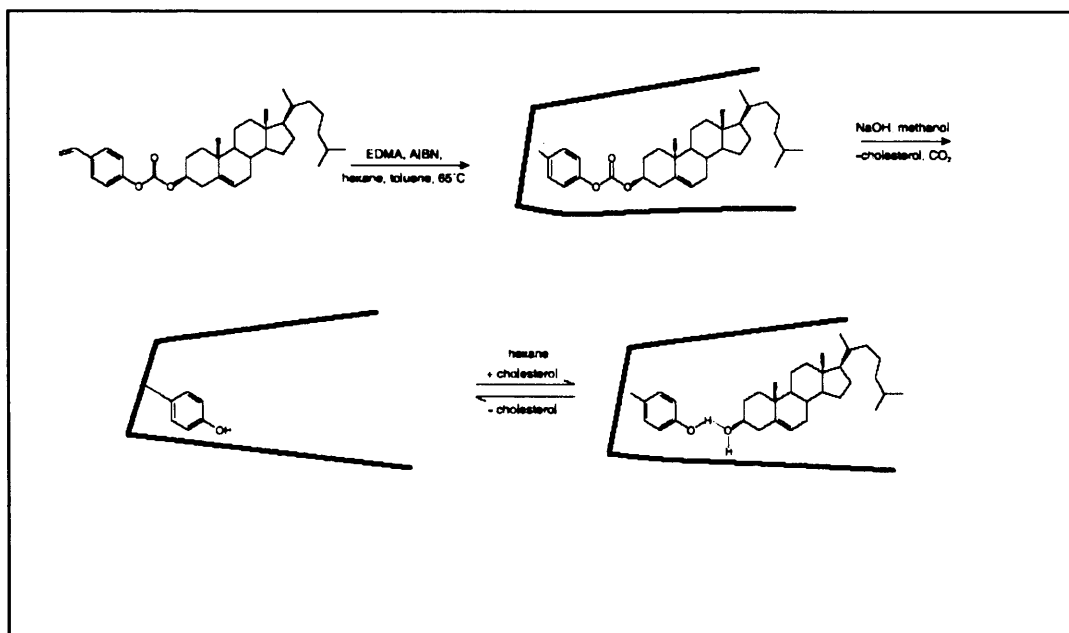


Figure 1.8: First example of sacrificial spacer described by Whitcombe et al.¹⁰⁷

It has been shown that MIPs for cholesterol made in this way perform better than non-covalent imprinted polymers when used as stationary phase in HPLC¹⁰⁸.

A number of hydroxyl group^{109,110} containing molecules have been imprinted using this method and the use of a carbonyl spacer in the form of the carbamate group, in order to introduce even amine groups^{111,112} into the binding sites, has also been reported.

1.2.3.4 PROS AND COS OF THE THREE IMPRINTING APPROACHES

An advantage of the covalent approaches is the stoichiometric nature of the covalent pre-polymerisation step which means that all functional groups in the resultant imprinted polymers are only found in sites associated with template. This may help to lower non-specific analyte-polymer interactions⁸⁰. Further advantages of the semi-covalent approach is its compatibility with a wider range of polymerisation

conditions, allowing them to be used for the imprinting of emulsion¹¹³ and dendrimers¹¹⁴, and the fact that entrapped template remains covalently bound to the polymer avoiding the problem of leaching under normal condition of use¹¹⁵. However, the covalent approach presents a fundamental drawback since the re-binding step can be very slow due to the necessary formation of a covalent bond between template and MIP¹¹⁶.

In contrast, due to its simplicity and broad applicability to a range of template structures, the non-covalent approach has established itself as the main methodology. In the non-covalent approach, components are simply mixed together and left to interact resulting in a mixture of different solution adducts which are in dynamic equilibrium⁸⁰. The other great strength of the approach is the range of chemical functionalities that can be targeted. These include ion-pairs, hydrogen bonding groups and aromatic systems⁸⁰. However, the non-covalent approach has three distinct drawbacks. The first is the heterogeneity of the binding site population that is formed. This occurs due to the complex and varied array of pre-polymerisation complexes that form in solution and also their transient nature due to the relative weakness of the interactions that hold them together. The second problem is the widespread distribution of the functional monomer around the polymer network, outside receptor cavities, giving rise to low affinity non-specific binding of the analyte to the polymer. The third problem is the low yield of functional high-affinity receptor sites relative to the amount of template present in the pre-polymerisation mixture^{80,116}.

These problems have driven research toward specifically designed high affinity monomers to be utilized in stoichiometric molecular imprinting approaches (section 1.2.4).

1.2.4 STOICHIOMETRIC APPROACH

In order to optimise the non-covalent approach, a different type of imprinting called ‘stoichiometric noncovalent interaction’¹¹⁷ has been developed. In principle, stoichiometric imprinting is non-covalent molecular imprinting using selected high affinity monomers. Such monomers have been designed to form multiple hydrogen bonds with the template and binding constants (K_a) in the range 10^3 - 10^7 M^{-1} have been reported. Crucially this makes them behave like a covalent bond¹¹⁸. Therefore, this method combines the high yields and fast rebinding kinetics usually observed with the non-covalent approach with the precise location of functional groups and the high accessibility of the free cavities for molecular recognition, typical of covalent imprinting¹¹⁹. The classical example of the stoichiometric interaction in non-covalent imprinting is the interaction of polymerisable amidines with carboxylic acids, phosphates and phosphonates as introduced by Wulff¹²⁰.

1.2.5 POLYMER MATRIX

The structure of the matrix is crucial in the imprinting process and a number of key properties are desirable. The polymer should possess¹²¹:

- i. High rigidity, to preserve the shape of their cavities after removing the template.
- ii. Flexibility, necessary to allow fast binding and release of the substances within the cavities.
- iii. The accessibility of as many cavities as possible. This depends on the flexibility of the polymer chain, on the inner surface area of the polymer and on the pore size distribution within the macroporous polymer¹²¹.
- iv. Mechanical stability, for application in situations where the polymer would be under pressure e.g. HPLC.
- v. Thermal stability for use in applications where elevated temperatures might be desirable in order to improve kinetics¹²¹.

Therefore, in order to improve the quality and quantity of recognition sites, a number of factors have to be considered when designing the polymer. These include molecular composition, the method of polymerisation and required polymer format. These variables all have some influence on the key steps of pre-polymerisation complex formation and its entrapment into the solid state¹¹⁶.

1.2.5.1 TEMPLATE MOLECULE

In all molecular imprinting processes the template is of central importance since it directs the organisation of the functional groups contained within the functional monomers¹²². In general, small and highly functional templates produce more specific polymers¹²³, although other factors such as solubility⁷² and rigidity¹²⁴ are also important. Rigid templates with limited conformational fluidity can lead to more homogenous binding site populations¹²⁵. Furthermore, if the template possesses more than one functional group capable of interacting with the monomer, this can increase binding site heterogeneity¹²⁶ (Figure 1.9).

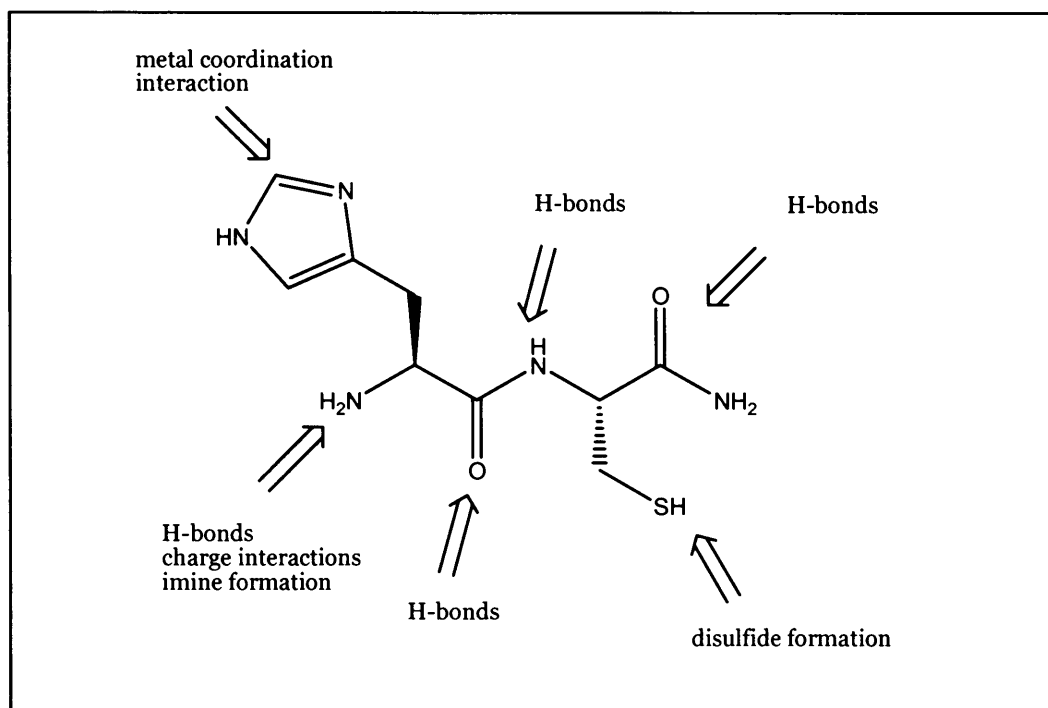


Figure 1.9: Example of target molecule (L-histidyl-L-cysteine-amide) containing a variety of functional elements, (Adapted from ref.127).

A large number of small molecules have been successfully imprinted¹²⁸, while the imprinting of larger templates is still a challenge due to their solvent incompatibility, slow mass transfer and conformational flexibility. However, a number of adapted protocols have been reported for proteins¹²⁹ and even cells¹³⁰.

1.2.5.2 FUNCTIONAL MONOMER

The functional monomer is responsible for specific interactions between the template and the polymeric matrix. Therefore, the choice of monomer and its stoichiometry with template and crosslinker will determine the pre-arrangement and type of interaction created. In the non-covalent imprinting approach, the most widely used functional monomer is methacrylic acid (MAA) due to its hydrogen bond donor and acceptor characteristics⁸⁰. MAA also benefits from the bulk of the methyl group, which probably restricts rotation and conformational

flexibility, compared with acrylic acid, and also provides additional van der Waals interactions, which help to define the general shape-selective elements of the receptor sites⁸⁰. Thus, a large number of MIPs, expressing high binding affinity and selectivity to various target analytes, have been successfully reported based on this approach^{131,132}. However, MAA is not the only monomer that has been used to prepare MIPs and a range of other polymerisable species has been identified based on their template complementarity.

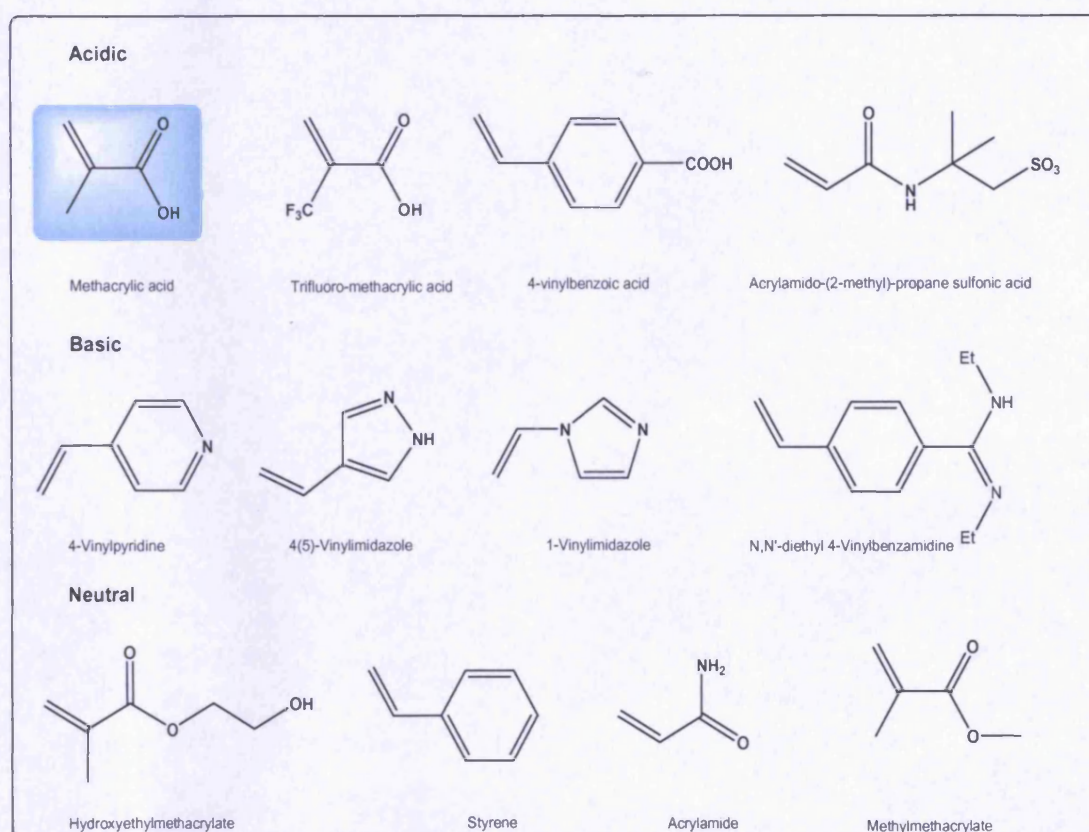


Figure 1.10: Representation of functional monomers for non covalent molecular imprinting.

Trifluoromethacrylic acid (TFMAA) is a stronger acid than MAA due to its electronegative fluorines, so that TFMAA is capable of forming stronger ionic interactions¹³³. Frequently, other acidic monomers are

employed such as sulphonates, phosphonates, phosphates. These are particularly used to form formal ion pairs when carrying out imprinting under aqueous conditions¹³⁴.

From the basic monomers, the vinylpyridines or vinylimidazoles are the most widely used as they can participate in the formation of hydrogen bonds and can also form ionic interactions with acidic template molecules¹³⁵⁻¹³⁶.

For some applications, it is advantageous to use “neutral” monomers, e.g. styrene or acrylamide¹³⁷, the latter has been used in imprinting of proteins in aqueous systems¹³⁸ and has shown high selectivity in the imprinting of amides and carboxylic acids¹³⁹.

In most examples only one functional monomer is used in a particular polymer. However, a combination of two or more functional monomers, has, in a few instances, given polymers with better recognition capabilities than that observed from the corresponding copolymers¹³⁹.

In covalent imprinting the number of functional monomers that can be used is more limited. Boronic esters are the most commonly used in this type of imprinting¹⁴⁰.

1.2.5.3 CROSSLINKING AGENT

The major fraction (80-95% by weight) of most MIPs is made up by the crosslinking agent, which is necessary to afford the required rigidity and selectivity. In an imprinted polymer, the cross-linker has three main functions: i) to control the morphology of the polymer matrix; ii) to stabilise the imprinted binding site; iii) to impart mechanical stability to the polymer matrix¹²². The most commonly used cross-linkers are ethyleneglycol dimethacrylate (EGDMA) and divinylbenzene (DVB),

which both contain only two polymerizable vinyl groups. Others cross-linking monomers have been used that possess more than two acrylate groups, these include trimethylolpropane trimethacrylate (TRIM)¹⁴¹ and pentaerythritol triacrylate (PETRA)¹⁴². These monomers produce polymers of greater rigidity¹²². This rigidity has been shown to lead to MIPs with higher capacities and selectivities than those prepared with EGDMA¹⁴³. The choice of cross-linker is also dependent upon the template and solvent. For example, methylene-*bis*-acrylamide has been used to crosslink protein imprinted polymers where the solvent used has been water¹⁴⁴. In addition, Spivak and co-workers have introduced a hybrid¹⁴⁵ of a crosslinker-functional monomer. In this way, the degree of cross-linking is maximized without imposing restrictions on functional group concentrations.

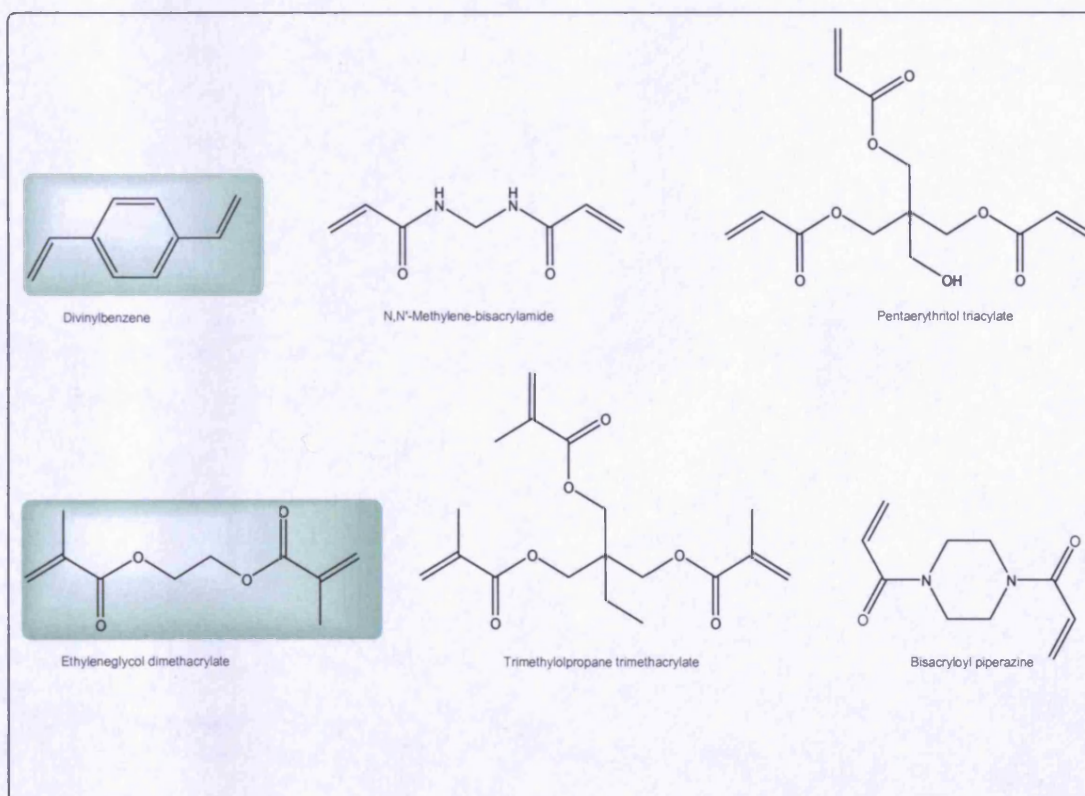


Figure 1.11: Selection of common cross-linkers used in molecular imprinting protocols.

1.2.5.4 POROGENS

Apart from dissolving all the components of the prepolymerisation mixture, the solvent has two other important roles. The first is in the formation of the pre-polymer complex. For polar non-covalent interactions such as ionic or hydrogen bonds, non polar solvents are preferred in order to drive the template and functional monomer toward complex formation¹⁴⁶. When there is reliance on polar non-covalent interactions, the use of polar solvents, especially those capable of hydrogen bonding, inhibits the formation and stability of non-covalent pre-polymerisation complexes¹⁴⁶. The second effect is that the solvent is responsible for the creation of pores in macroporous polymers. For this reason it is quite common to refer to the solvent as the “porogen”. The use of thermodynamically good solvent tends to lead to polymers with well-developed pore structures and high surface areas, whilst use of a thermodynamically poor solvent leads to polymers with poorly developed pore structures and low surface area¹²². Sellergren and Shea¹⁴⁷ evaluated MIPs templated with L-phenylalanine anilide using porogens and concluded that enantioselectivity is improved for polymers made with relatively nonpolar porogens, having a poor hydrogen bonding capacity¹⁴⁷.

In order to maximise the strength of polar, i.e. electrostatic interactions between the template and the functional monomer(s) in organic media, an aprotic solvent of low to medium polarity is normally chosen to act as the porogen. Normally these solvents have low dielectric constant, such as chloroform (4.806 at 20°C) and toluene (2.379 at 25°C). However, more polar solvents with higher dielectric constants, e.g. acetonitrile (30.5 at 20°C) or acetone (20.7 at 25°C), have wide application due to their great solvation properties, despite weakening the binding forces between the template and the functional monomers.

The imprinting of aqueous-based polymers remains a challenge due to the polar nature of water¹⁴⁸. However, a number of researchers have demonstrated efficacy in aqueous^{131,149} or partially aqueous environments¹⁵¹ and, recently, it was demonstrated that once the MIP has been synthesised in an apolar solvent, its rebinding in aqueous buffers by hydrophobic and metal coordination interactions was indeed possible, although the affinities and selectivities obtained were less than those for ligand binding in an optimal organic solvent^{150,151}. Certainly, these protocols cannot be used with all templates, but these studies have demonstrated that, against general belief, imprinting and the use of MIPs are possible in presence of water.

1.2.5.5 INITIATION METHODS

Generally MIPs are synthesised using radical polymerisation initiated either photochemically or thermally¹²². The most common initiator employed is the azobisisobutyronitriles (AIBN), which can be conveniently decomposed by photolysis (UV) or thermolysis to give two metastable radicals capable of initiating the growth of a number of vinyl monomers¹²². Azobisdimethylvaleronitrile (ABDV) has also been widely used, as it possess a thermal decomposition temperature lower than that of AIBN and allows thermal polymerisation to be initiated at 40^o81. Several studies have shown that polymerisation of MIPs at lower temperatures forms polymers with greater selectivity against polymers made at elevated temperatures¹⁵²⁻¹⁵⁴. The chemical structures of selected polymerization initiators are shown in Figure 1.12.

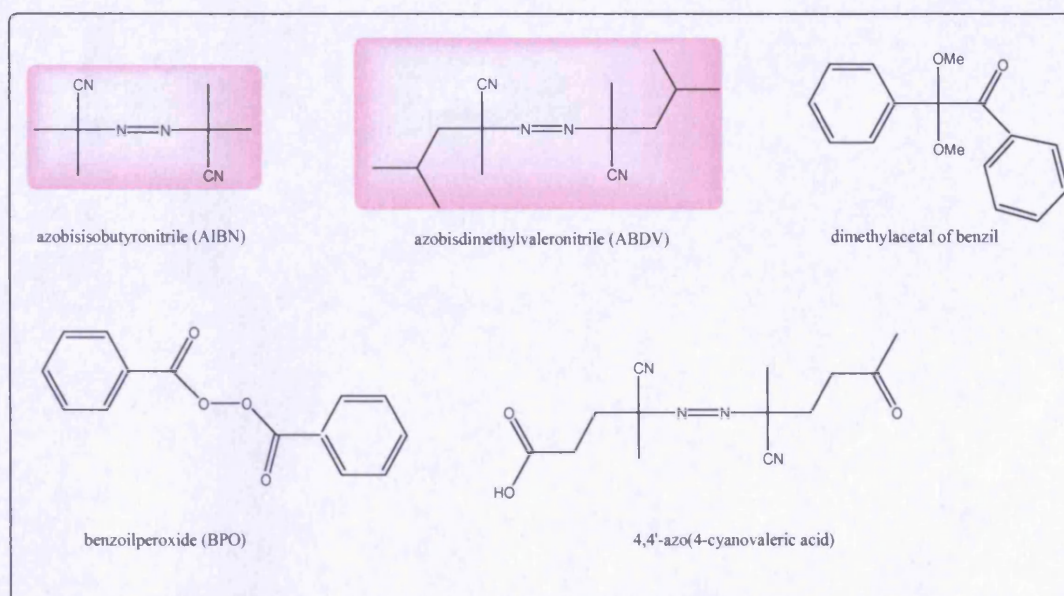


Figure 1.12: Chemical structures of selected chemical initiators.

The polymerisation process is characterised by three distinct stages: 1) initiation; 2) propagation and 3) termination. Importantly, oxygen gas slows down free radical polymerisation and, therefore, to avoid premature chain termination it is necessary to degas and purge the monomer mixture with an inert gas such as nitrogen or argon prior to polymerisation¹²².

1.2.6 CONSIDERATION IN THE DESIGN OF NON-COVALENT IMPRINTING SYSTEM

In the choice of a stoichiometric non-covalent approach to imprint our target molecule, several parameters have been taken into consideration. We have already discussed the advantages of the 'stoichiometric non-covalent interactions' against the non-covalent approach (section 1.2.4) and the importance of the nature and level of template, monomer(s), crosslinker(s), solvent(s) in the imprinting process. The other two factors that must be considered are:

- Type of interactions
- Thermodynamics of interaction

1.2.6.1 NON-COVALENT TYPE OF INTERACTIONS

Non covalent interactions can be described as interactions between two species that do not involve covalent bonds or the specific sharing of valence electrons¹⁵⁵. Associations of this nature cover a variable range of energies and depend explicitly on the structure and functionality of the species involved in the formed complex as well as the local environment of the complex¹⁵⁵. Table 1.3 lists some types of non covalent interactions that are important in molecular imprinting and their corresponding bond energies.

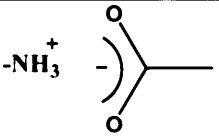
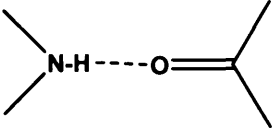
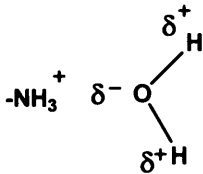
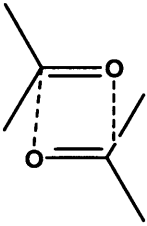
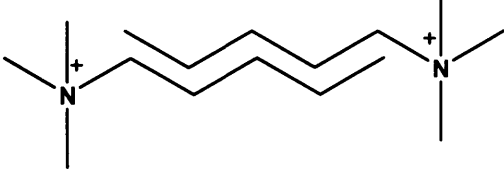
Type of interaction	Example	Approximate bond energy
Charge-charge		~60 kJ/mol
Hydrogen bond		~40 kJ/mol
Charge-dipole		~8 kJ/mol
Dipole-dipole		~1 kJ/mol
Van der Waals		0.1-1 kJ/mol

Table 1.3: Example of the most common non covalent interactions and approximate bond energies, (Adapted from Ref.158).

For non covalent imprinting, the most important monomer-template interactions are hydrogen bonding, ionic interactions, dipole-dipole interactions, Van der Waals (VDW) forces and hydrophobic forces¹⁵⁶.

Hydrogen bonding is the most important mechanism of interaction between the template and the functional monomer.

The hydrogen bond is really a special case of dipole forces. A hydrogen bond is the attractive force between the hydrogen attached to an electronegative atom of one molecule and an electronegative atom of a different molecule¹⁵⁷. Usually the electronegative atom is oxygen, nitrogen, or fluorine, which has a partial negative charge. The hydrogen then has the partial positive charge. Hydrogen bonding is usually stronger than normal dipole forces between molecules¹⁵⁷. The strength of a typical hydrogen bond is between 10 and 40 kJ/mol, which is much stronger than typical VDW interactions (~1kJ/mol) but still considerably weaker than covalent bonds (~500kJ/mol)¹⁵⁸. The length of hydrogen bonds depends on bond strength, temperature and pressure and typically its length in water is 197 pm (1.97 Å). Usually van der Waals forces play a minor role in typical imprinting procedures, as these interactions types do not display high binding energies¹⁵⁸.

Hydrophobicity implies the dislike of a molecular unit for water. Water is electrically polarized, and is able to form hydrogen bonds internally, which gives it many of its unique physical properties. But, since hydrophobes are not electrically polarized, and because they are unable to form hydrogen bonds, water repels hydrophobes, in favor of bonding with itself¹⁶⁰. However, such rearrangements are highly entropically unfavorable. A consequence of this hydrophobic effect is a relatively strong attractive interaction between two hydrophobic moieties in water compared to their interaction in a hydrocarbon-based solvent¹⁵⁸.

1.2.6.2 THERMODYNAMIC CONSIDERATIONS

The formation of monomer-template complexes in the pre-polymerization mixture plays a role in determining the quality and performance of the polymer product and it is controlled by thermodynamics principles. Nicholls, in a series of papers¹⁵⁹⁻¹⁶¹, re-interpretating the general theory for describing molecular recognition phenomena, Equation 1.1, with respect to molecular imprinting system, Equation 1.2, postulated that this thermodynamic treatment can be used to identify factors influencing site formation and binding of a ligand to a MIP receptor site¹⁶⁰.

$$\Delta G_{\text{bind}} = \Delta G_{\text{t+r}} + \Delta G_{\text{r}} + \Delta G_{\text{h}} + \Delta G_{\text{vib}} + \sum \Delta G_{\text{p}} + \Delta G_{\text{conf}} + \Delta G_{\text{vdw}} \quad \text{Eq.1.1}$$

$$\Delta G_{\text{bind}} = \Delta G_{\text{t+r}} + \Delta G_{\text{r}} + \Delta G_{\text{h}} + \Delta G_{\text{vib}} + \sum \Delta G_{\text{p}} \quad \text{Eq.1.2}$$

Where the Gibbs free energy changes are:

ΔG_{bind}	complex formation
$\Delta G_{\text{t+r}}$	translational and rotational
ΔG_{r}	restriction of rotors upon complexation
ΔG_{h}	hydrophobic interactions
ΔG_{vib}	residual soft vibrational modes
$\sum \Delta G_{\text{p}}$	the sum of interacting polar group contributions
ΔG_{conf}	adverse conformational changes
ΔG_{vdw}	unfavorable van der Waals interactions

By considering the various terms in this thermodynamic model, Equation 1.2, the following conclusions may be drawn in regard to the design of MIPs.

The $\Delta G_{\text{t+r}}$ term, in Equation 1.2, reflects the change in translational and rotational Gibbs free energy associated with combining two or more free entities in a complex¹⁶⁰ and imply that the greater the number of these

entities for complexation with the template, the lower will be the stability of the complex¹⁶². ΔG_r refers to the internal rotation free energy and indicates that the selectivities observed for MIPs prepared with rigid templates are superior to those of less rigid structures. The implication of $\sum \Delta G_p$, the sum of the free energy contributions from all electrostatic interactions, is that the stronger the interaction between the template and the monomer, the more stable is the resulting polymer¹⁶¹. ΔG_h refers to the hydrophobic interactions and indicates that the stability of complex formation in water is improved by the strength of interactions between hydrophobic portions of the template structure and suitable hydrophobic functional monomers. In relation to the other terms described in the Equation 1.2, ΔG_{vib} indicates that the homogeneity of the final adduct depends on the temperature used for the polymerization process; ΔG_{conf} and ΔG_{vdw} reflect the need to have a right conformation of template and an effective solvation in order to form solution adducts¹⁶². These last terms can be valued using molecular modelling¹⁶². In conclusion, the position of the equilibrium for formation of self-assembled solution adducts between templates and monomers, ΔG_{bind} , determines the number and degree of receptor site heterogeneity. Therefore, the use of non-covalent template-functional monomer interactions is a direct consequence of the extent of template complexation and of its stability¹⁶².

1.2.7 APPLICATIONS OF MOLECULAR IMPRINTING

The spectacular versatility of the molecularly imprinted polymers has seen them adopted in a wide range of applications, from chiral chromatographic separations^{163,164} to the binding of ligands with a specificity emulating the one of antibodies^{165,166}.

1.2.7.1 CHROMATOGRAPHY

Molecularly imprinting has been used to prepare separation materials with predetermined selectivity. A wide range of print molecules, from small molecules, such as drugs^{59,106}, amino acids and carbohydrates^{167,168}, to larger entities, such as proteins¹⁶⁹, have been pursued which employ several different techniques, such as high performance liquid chromatography¹⁵⁴ (HPLC), thin layer chromatography¹⁷⁰ (TLC), capillary electrophoresis⁷⁵ (CE) and capillary electrochromatography¹⁷¹ (CEC). Chiral separations have been a major area of investigation, and molecularly imprinted materials have been extensively employed as chiral stationary phases in HPLC¹⁶⁴. However, sometimes the use of MIPs as chiral stationary phases presented limitations due to the broad and asymmetric peak shapes, caused by the heterogeneity of the sites and irregular particle size distribution and due to the low saturation capacities. Different approaches have been described to overcome these problems which included improvement of the column packing technique¹⁷², the preparation of the polymer in situ in the HPLC column¹⁷³ and the production of more spherical particles¹⁷⁴ to allow a better distribution of the packed material.

1.2.7.2 CATALYSIS AND ARTIFICIAL ENZYMES

One of the most intriguing challenges for the use of molecularly imprinted polymer is their use as enzyme mimics. To date, four different approaches have been pursued: i) the use of transition state analogues as templates¹⁷⁵, ii) the use of coenzyme analogues for providing a useful predetermined catalytic mechanism¹⁷⁶, iii) the use of coordination compounds for mediation of catalytic reactions¹⁷⁷ and iv) the use of designed “bait-and switch” strategy¹⁷⁸ which involves preparing molecular imprints against a suitable molecule, where

interaction with a potentially catalytic functional group results in an appropriate reciprocal arrangement of groups in the resulting polymer.

Polymer catalytic materials potentially have significant advantages upon other systems, particularly biological systems, due to excellent thermal stability and resistance to extreme environments. In addition, their preparation and the recovery of the catalytic product can be straightforward¹⁷⁹.

Therefore, catalytic MIPs may be highly advantageous for industrial continuous transformation and/or conversion reactions, where temperature and solvent regimes are often such that biological catalysts are rapidly denatured or destroyed^{64,81}.

1.2.7.3 BIOSENSOR

MIPs have also been used as recognition elements in sensors⁷⁶. They have great potential to compete with antibodies and enzymes in this field since biological molecules can exhibit limited stability even in relatively mild environments⁷². MIP sensing systems are highly adaptable and have been linked to a range of different transduction systems including electrochemical¹⁸⁰, pH¹⁸¹, luminescence¹⁸² and fluorescence¹⁸³ (Figure 1.13). Molecularly imprinted polymers for sensor technology present advantages very similar to those for antibody mimics: they are very stable and robust with the potential of performing in harsh environments¹⁸⁴.

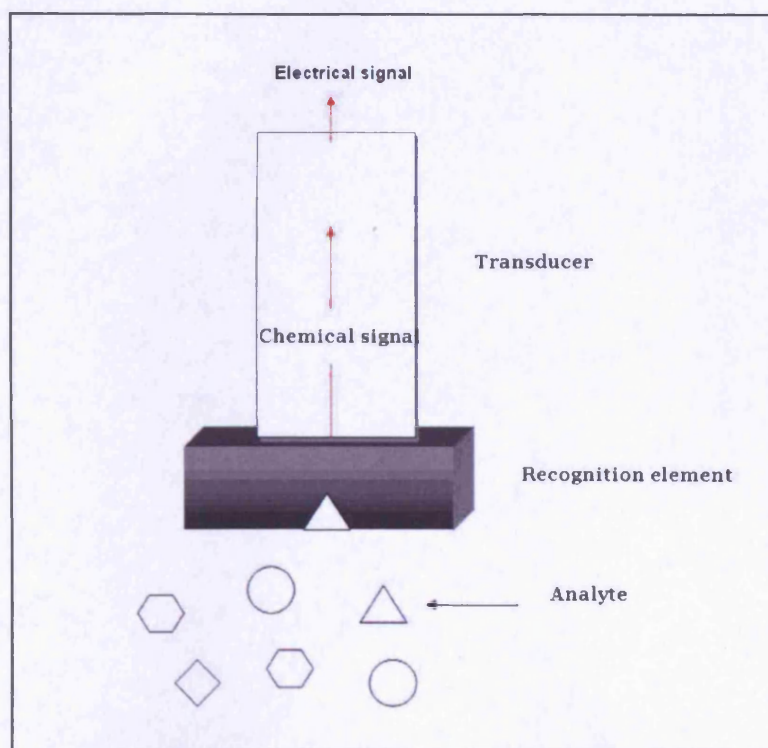


Figure 1.13: Scheme of biosensor device.

1.2.7.4 PSEUDOIMMUNO ASSAY

A number of studies have demonstrated that molecularly imprinted polymers can serve as artificial versions of natural antibodies and can be used as recognition elements in immunoassays. The first molecularly imprinted 'antibody replacement' radioassay was reported by Vlatakis *et al*⁵⁶. This study describes MIPs, specific against the tranquillizer diazepam and the bronchodilator theophylline, which demonstrated comparable cross-reactivity profiles to standard antibodies. Subsequently, similar studies have been reported for the analysis of other compounds, such as: caffeine¹⁸⁵, theophylline¹⁸⁶, propranolol¹³¹, morphine¹⁴⁹, Leu-enkephaline¹⁸⁷, penicillin G¹⁸⁸ and many others⁸¹.

In order to avoid the use of radiolabels, alternative approaches have also been developed which use fluorescent, electroactive, or enzyme-

labelled probes and an increasing number of non-radiolabel MIPs have been produced¹⁸⁹⁻¹⁹¹. Moreover, researches have also focussed on preparing MIPs in new formats for easier handling or compatibility with standard instrumentation, e.g. microplates¹⁶⁶. They include the preparation and use of magnetic MIP beads¹⁹², fine particles (< 1 μ m)¹⁹³, microspheres¹⁹³, immobilized templates¹⁹⁴, thin polymer films on glass¹⁹⁵, thin layers on microtiter plate wells¹⁹⁶. Additional advantages of MIP over antibodies for this form of assay is that they can be used in both aqueous and non-aqueous systems and there is no need for conjugation of the template to an immunogenic carrier⁸¹. Despite the obvious advantages, the standard issues associated with molecular imprinting, that is polyclonality, low comparative affinities compared to antibodies and the requirements for a large amount of the template in their preparation¹⁶⁶ still apply.

1.3 CONCLUSION

The success of the molecular imprinting approach has led to a dramatic increase in the number of molecular imprinting research articles (Figure 1.14) and has resulted in the exploitation of a range of new approaches for preparing imprinted materials in an increasingly wide range of formats for a broad range of applications. Particularly significant has been the recent improvements towards aqueous compatibility and an increased understanding of the processes of recognition. As a greater understanding of the fundamental processes underpinning molecular imprinting become better understood so confidence in the science has increased. It now seems more likely that the obvious potential of molecular imprinting will be realised and that in the coming years a number of new and exciting commercial products are likely to appear.

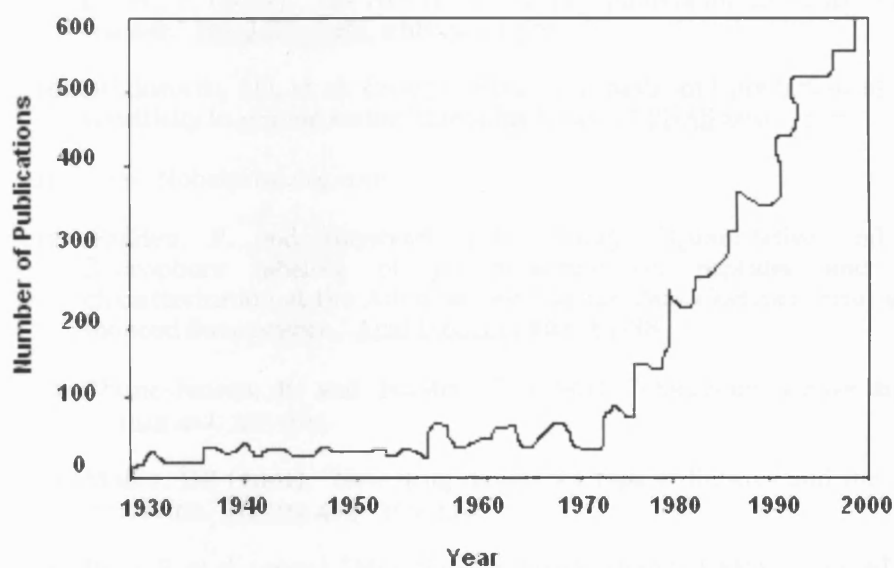


Figure 1.14: The number of articles published from 1931-2003. (Data obtained and adapted from the Society for Molecular Imprinting, ref.197)

BIBLIOGRAPHY

1. Williams, D.M. and Cole, P. (2001). "Kinase chips hit the proteomics era." Trends Biochem.Sci. **26**(5): 271-273.
2. Garnak, M. and Reeves, H.C. (1979). "Phosphorylation of isocitrate dehydrogenase of Escherichia Coli." Science **203**: 1111-1112.
3. Kennelly, P.J. (2002). "Protein kinases and protein phosphatases in prokaryotes: a genomic perspective." FEMS Microbiology Letters **206**: 1-8.
4. Hunter, T. (2000). "Signaling-2000 and beyond." Cell **100**: 113-127.
5. Cohen, P. (2000). "The regulation of protein function by multisite phosphorylation- a 25 years update." Trends Biochem.Sci. **25**: 596.
6. Sjaastad, M.D. and Nelson, W.J. (1997). "Integrin-mediated calcium signaling and regulation of cell adhesion by intracellular calcium." Bioessays **19**: 47.
7. Cantrell, D. (1996). "T cell antigen receptor signal transduction pathways." Annu.Rev.Immunol. **14**:259.
8. Cohen, P. (2002), "The origins of protein phosphorylation." Nature Cell Biology **4**: 127-130.
9. Cohen, P. (2001). "The role of protein phosphorylation in human health and disease." Eur.J.Biochem. **268**: 5001-5010.
10. Brinkworth, I.O. et al. (2003). "Structural basis and prediction of substrate specificity in protein serine/threonine kinases." PNAS **100**: 74-79.
11. [www. Nobelprize.org.com](http://www.Nobelprize.org.com)
12. Fadden, P. and Haystead, T.A.J. (1995). "Quantitative and selective fluorophore labeling of phosphoserine on peptides and proteins: characterization at the Attomole level by capillary electrophoresis and laser-induced fluorescence." Anal Biochem **225**: 81-88
13. Blume-Jensen, P. and Hunter, T. (2001). "Oncogenic kinase signalling." Nature **411**: 355-365.
14. Moller, DE (2001). "New drug targets for type 2 diabetes and the metabolic syndrome." Nature **414**: 356-359.
15. Blair, E. et al. (2001). "Mutations in the $\gamma 2$ subunit of AMP-activated protein kinase cause familial hypertrophic cardiomyopathy: evidence for the central role of energy compromise in disease pathogenesis." Hum. Mol. Genet. **10**: 1215-1220.
16. Narumiya, S. et al. (2000). "Use and properties of ROCK-specific inhibitor Y-27632." Methods Enzymol. **325**: 273-284.
17. Finkelman, E.H. (2002). "Glycogen synthase kinase 3: an emerging therapeutic target." Trends Mol Med **8**: 126-132.

18. Adamczyk, M. et al. (2001). "Selective analysis of phosphopeptides within a protein mixture by chemical modification, reversible biotinylation and mass spectrometry." Rapid Commun. Mass Spectrom. **15**: 1481-1488.
19. Davies, S.P. et al. (2000). "Specificity and mechanism of action of some commonly used protein kinase inhibitors." Biochem.J. **351**: 95-105.
20. Ross, H. et al. (2002). "A non radio-active method for the assay of many serine/threonine-specific protein kinases." Biochem.J. **366**: 977-981.
21. Liu, J. et al. (1991). "Calcineurin is a common target of cyclophilin-cyclosporin A and FKBP-FK506 complexes." Cell **66**: 807-815.
22. Brown, E.J. et al. (1994). "A mammalian protein targeted by G1-arresting rapamycin-receptor complex." Nature **369**: 756-758.
23. Yan, J.X. et al. (1998). "Protein phosphorylation: technologies for the identification of phosphoamino acids." Journal of Chromatography A **808**: 23-41.
24. Cohen, P. (2002). "Protein kinases-The major drug targets of the twenty-first century?" Nat.Rev., Drug Discov. **1**: 309-315.
25. Adams, A. J. (2001). "Kinetic and Catalytic Mechanisms of Protein Kinases." Chem.Rev. **101**: 2271-2290.
26. David, B. et al. (1991). "Chemical approaches to reversible protein phosphorylation" EMBO J. **10**: 317.
27. Rossomando A. et al. (1992). "Identification of Tyr-185 as the site of tyrosine autophosphorylation of recombinant mitogen-activated protein kinase p42mapk". Proc.Natl.Acad.Sci. **89**: 5221.
28. Shen, K. et al. (2005). "Protein kinase structure and function analysis with chemical tools." Biochimica et Biophysica Acta **1754**: 65-78.
29. Ting, A.Y. et al. (2001). "Phage-display evolution of tyrosine kinases with altered nucleotide specificity." Biopolymers **60**: 220-228.
30. Pearson, R.B. and Kemp, B.E. (1991). "Protein kinase phosphorylation site sequence and consensus specificity motifs:tabulations." Methods Enzymol. **200**: 62.
31. Wu, J. et al. (1994). "Identifying substrate motifs of protein kinases by a random library approach." Biochemistry **33**: 14825.
32. Dombradi, V. (2002). "Structure and function of protein phosphatases." Eur.J.Biochem. **269**: 1049.
33. Hunter, T. (1995). "Protein kinases and phosphatases: the yin and yang of protein phosphorylation and signaling." Cell **80**: 225-236.
34. Wera, S. and Hemmings, B.A. (1995). "Serine/threonine protein phosphatases." Biochem.J. **311**: 17-29.
35. Cohen, P. and Cohen, P.T.W. (1989). "Protein phosphatases come of age." Biol.Chem.J **264**: 21435-21438.

36. Cohen, P. (1989). "The structure and regulation of protein phosphatases." Annu.Rev.Biochem. **58**: 453-508.
37. Barford, D. et al. (1998). "The structure and mechanism of protein phosphatases: insight into catalysis and regulation." Annu.Rev.Biophys.Biomol.Struct. **27**: 133-164.
38. Garrison, J. C. (1992). Protein phosphorylation-A practical approach, Oxford university Press.
39. Mohanraj, D. et al. (1996). "Expression and Radiolabeling of Recombinant Proteins Containing a Phosphorylation Motif." Protein expression and purification **8**: 175-182.
40. McIlroy, B.K. et al. (1991). "A continuous fluorescence assay for protein kinase C." Anal.Biochem. **195**: 148-152.
41. Yeh, R-H et al. (2002). "Real Time Visualization of Protein Kinase Activity in living cells." Biol.Chem **277**: 11527-11532.
42. Kurokawa, K. et al. (2001). "A pair of fluorescent resonance energy transfer-based probes for tyrosine phosphorylation of the CrkII adaptor protein in Vivo." Biol.Chem **276**: 31305-31310.
43. Yan, J. X. (1997). "High sample throughput phosphoamino acid analysis of proteins separated by one-and two-dimensional gel electrophoresis." Journal of Chromatography A **764**: 201-210.
44. Ojida, A. et al. (2002). "First artificial receptors and chemosensors toward phosphorylated peptide in aqueous solution." J. Am.Chem.Soc. **124**: 6256-6258.
45. Akita, S. et al. (2005). "On-bead fluorescence assay for serine/threonine kinases." Organic Letters **7**(25): 5565-5568.
46. Shults, M.D. et al. (2005). "A multiplexed homogeneous fluorescence-based assay for protein kinase activity in cell lysates." Nature Methods: 1-7.
47. Chen, C-A et al. (2002). "Design and synthesis of a fluorescent reporter of protein kinase activity." J. Am.Chem.Soc. **124**: 3840-3841.
48. Shults, M.D. and Imperiali, B. (2003). "Versatile Fluorescence Probes of Protein Kinase Activity." J. Am.Chem.Soc. **125**: 14248-14249.
49. Von Ahsen, O. and Bomer, U. (2005). "High-Throughput screening for kinase inhibitors." ChemBioChem **6**: 481-490.
50. <http://www.mesoscale.com>
51. <http://www.piercenet.com>
52. <http://www.cambrex.com>
53. Lesaichere, M.L. (2002). "Antibody-based fluorescence detection of kinase activity on a peptide array." Bioorganic&Medicinal Chemistry letters **12**: 2085-2088.
54. Wang, J.Y.J. (1988). "Antibodies for phosphotyrosine: analytical and preparative tool for tyrosyl-phosphorylated proteins." Anal.Biochem. **172**: 1.

55. Mallat, E. et al. (2001). "A novel surface plasmon resonance immunosensor for 2,4,6-trinitrotoluene (TNT) based on indirect competitive immunoreactor." Trends Anal Chem **20**: 124-132.
56. Yu, J.H. et al. (2003). "Determination of theophylline in drugs and tea on nanosized cobalt phthalocyanine particles modified carbon electrode." Biosens Bioelectron **19**: 401-409.
57. Supernault, J.M. et al. (2004). Phosphokinase assay. US, WO 2004/081534 A2.
58. Ramstrom, O. et al. (1994). "Synthetic peptide receptor mimics-highly stereoselective recognition in non-covalent molecularly imprinted polymers." Tetrahedron Asymmetry **5**: 649-656.
59. Andersson, L. et al. (1995). "Mimics of the binding-sites of opioid receptors obtained by molecular imprinting of enkephalin and morphine." Proc.Natl.Acad.Sci. **92**: 4788-4792.
60. Ramstrom, O. et al. (1996). "Chiral recognition in adrenergic receptor binding mimics prepared by molecular imprinting." J.Molec.Recog.: 691-696.
61. Vlatakis, G. et al. (1993). "Drug assay using antibody mimics made by molecular imprinting." Nature 645-647.
62. Ramstrom, O. et al. (1996). "Artificial antibodies to corticosteroids prepared by molecular imprinting." Chem.Biol.: 471-477.
63. Haupt, K. et al. (1998). "Herbicide assay using an imprinted polymer based system analogous to competitive fluoroimmunoassays." Anal.Chem. **70**: 628-631.
64. Kandimalla, V.B. and Hunagxian, J. (2004). "Molecular imprinting: a dynamic technique for diverse applications in analytical chemistry." Anal.Bioanal.Chem. **380**: 587-605.
65. Polyakov M. et al. (1933). "On the structure of silica." Zhur.Fiz.Khim. **4**: 454.
66. Pauling, L. (1940). "A theory of the structure and process of formation of antibodies." J.Am.Chem.Soc. **62**: 2643-2657.
67. Dickey, F. (1955). "Specific adsorption." J.Phys.Chem **59**: 695-707.
68. Dickey, F. (1949). "The preparation of specific adsorbents." Proc.Natl.Acad.Sci. **35**(5): 227-229.
69. Morrison, J. et al. (1959). "The nature of the specificity of adsorption of alkyl orange dyes on silica gel." Can.J.Chem. **37**: 1986-1995.
70. Beckett, A. and Youseff, H. (1963). "Active sites in stereoselective adsorbents as models of drug receptors and enzyme active sites." J.Pharm.Pharmacol. **15**: 253T-266T.
71. Bartels, A. (1967). "On the order in silica gel with specific adsorption power." J.Chromatogr. **30**: 113-116.

72. Allender, C. J. et al. (1999). "Molecularly imprinted polymers-preparation, biomedical applications and technical challenges." Progress in Medicinal Chemistry **36**: 235-261.
73. Piletsky, S. et al. (1995). "Atrazine sensing by molecularly imprinted membranes." Biosensors and Bioelectronics **10**: 959-964.
74. Dhal, P. K. and Arnold, F. H. (1991). "Template-mediated synthesis of metal-complexing polymers for molecular recognition." J.Am.Chem.Soc. **113**: 7417-7418.
75. Brüggemann, O. et al. (1997). "Comparison of polymer coatings of capillaries for capillary electrophoresis with respect to their applicability to molecular imprinting and electrochromatography." J.Chromatogr.A **781**: 43-53.
76. Kriz, D. and Mosbach, K. (1995). "Competitive amperometric morphine sensor-based on an agarose immobilized molecularly imprinted polymer." Anal. Chim.Acta **300**: 71-75.
77. Vulfson, et al. (1997). "Assembling the molecular cast." Chemistry in Britain **32**: 23-26.
78. Wulff, G. (1995). "Molecular imprinting in cross-linked materials with the aid of molecular templates-a way towards artificial antibodies." Angew.Chem. **34**: 1812-1832.
79. Shea (1994). "Molecular imprinting of synthetic network polymers. The de-novo synthesis of macromolecular binding and catalytic sites." Trends in Polymer Science **2**: 166-173.
80. Mayes, A. J. and Whitcombe, M. J. (2005). "Synthetic strategies for the generation of molecularly imprinted organic polymers." Advanced Drug Delivery Reviews **57**: 1742-1778.
81. Alexander, C. et al. (2006). "Molecular imprinting science and technology: a survey of the literature for the years up to and including 2003." J.Molec.Recog. **19**: 106-180.
82. Wulff, G. and Sahran, A. (1972). "The use of polymer with enzyme-analogous structures for the resolution of racemates." Angew.Chem. **11**: 341.
83. Wulff, G. (1993). Biorecognition in molecularly imprinted polymers. Concept, chemistry, and application. Molecular interaction in bioseparations. T.Ngo. New York, Plenum Press: 363-381.
84. Wulff, G. et al. (1982). Affinity chromatography and related techniques. T. Gribnau. Amsterdam, Elsevier: 207-216.
85. Wulff, G. (1982). "Selective binding to polymers via covalent bonds - the construction of chiral cavities as specific receptor-sites." Pure Appl.Chem. **54**: 2093-2102.
86. Sellergren, B. and Andersson, L. (1990). "Molecular recognition in macroporous polymers prepared by a substrate-analog imprinting strategy." J.Org.Chem. **55**: 3381-3383.
87. Whitcombe, M. et al. (1994). Separations for biotechnology. Spec.Publ.R.Soc.Chem. D. L. Pile. **158**: 565.

88. Damen, J. and Neckers, D.J. (1980). "On the memory of synthesized vinyl polymers for their origins." Tetrahedron Letters **21**: 1913-1916.
89. Wulff, G. et al. (1986). "Molecular recognition through the exact placement of functional-groups on rigid matrices via a template approach." J.Am.Chem.Soc. **108**: 1089-1091.
90. Shea, K. et al. (1990). "Synthesis and characterisation of highly crosslinked polyacrylamides and polymethacrylamides-a new class of macroporous polyamides." Macromolecules **23**: 4497-4507.
91. Shea, D. J. and Dougherty, T.K. (1986). "Molecular recognition on synthetic amorphous surfaces-the influence of functional-group positioning on the effectiveness of molecular recognition." J.Am.Chem.Soc. **108**: 1091-1093.
92. Shea, K. J. et al. (1989). "Fluorescence probes for evaluating chain solvation in network polymers." Macromolecules **22**: 1722-1730.
93. Shea, K. J. and Sasaki, D.Y. (1989). "On the control of microenvironment shape of functionalised network polymers prepared by template polymerisation." J.Am.Chem.Soc. **111**: 3442-3444.
94. Marty, J. et al. (1999). "New molecular imprinting materials: liquid crystalline networks." Macromolecules **32**: 8674-8677.
95. Sarhan, A. and Wulff, G. (1982). "Enzyme-analog built polymers. 13. On the introduction of amino and boronic acid groups into chiral polymer cavities." Makromolekulare Chemie-Macromolecular Chemistry And Physics **183**: 85-92.
96. Wulff, G. and Vietmeier, J. (1989). "Enzyme-analogue built polymers .26. Enantioselective synthesis of amino-acids using polymers possessing chiral cavities obtained by an imprinting procedure with template molecules." Makromolekulare Chemie-Macromolecular Chemistry And Physics **190**: 1727-1735.
97. Shea, K.J. and Thompson, E.A. (1978). "Template synthesis of macromolecules. Selective functionalization of an organic polymer." J.Org.Chem. **43**: 4253-4255.
98. Shea, K. et al. (1980). "Template synthesis of macromolecules. Synthesis and chemistry of functionalised macroporous polydivinylbenzene." J.Am.Chem.Soc. **102**: 3149-3155.
99. Damen, J. and Neckers, D.J. (1980). "Stereoselective synthesis via a photochemical template effect." J.Am.Chem.Soc. **102**: 3265-3267.
100. Damen, J. and Neckers, D.J. (1980). "Memory of synthesised vinyl polymers for their origins." J.Am.Chem.Soc. **45**: 1382-1387.
101. Mosbach, K. and Arshady, R. (1981). "Synthesis of substrate-selective polymers by host-guest polymerisation." Makromol. Chem. **182**: 687-692.
102. Dong, H. et al. (2003). "Syntheses of steroid-based molecularly imprinted polymers and their molecular recognition study with spectrometric detection." Spectrochim.Acta **59**: 279-284.

103. Kempe, M. and Mosbach, K. (1994). "Direct resolution of naproxen on a noncovalently molecularly imprinted chiral stationary-phase." J.Chromatogr.A **664**: 276-279.
104. Wulff, G. and Haarer, J. (1991). "Enzyme-analog built polymers .29. The preparation of defined chiral cavities for the racemic-resolution of free sugars." Makromolekulare Chemie-Macromolecular Chemistry And Physics **192**: 1329-1338.
105. Vlatakis, G. et al (1993). "Drug assay using antibody mimics made by molecular imprinting." Nature **361**: 645-647.
106. Shea, K. et al. (1993). "Polymer complements to nucleotide bases - selective binding of adenine-derivatives to imprinted polymers." Journal Of The American Chemical Society **115**: 3368-3369.
107. Whitcombe, M. et al. (1995). "A new method for the introduction of recognition site functionality into polymers prepared by molecular imprinting-synthesis and characterisation of polymeric receptors for cholesterol." J.Am.Chem.Soc. **117**: 7105-7111.
108. Hwang, C. and Lee, W.C. (2002). "Chromatographic characteristics of cholesterol-imprinted polymers prepared by covalent and non-covalent imprinting methods." J.Chromatogr.A **962**: 69-78.
109. Percival, C. et al. (2002). "Molecular imprinted polymer coated QCM for the detection of nandrolone." Analyst **127**: 1024-1026.
110. Petcu, M. et al. (2001). "Molecular imprinting of a small substituted phenol of biological importance." Anal.Chim.Acta **435**: 49-55.
111. Bass, J. et al. (2003). "Thermolytic synthesis of imprinted amines in bulk silica." Chem.Mater. **15**: 2757-2763.
112. Graham, A. et al. (2002). "Development and characterisation of molecularly imprinted sol gel materials for the selective detection of DDT." Anal. Chem. **74**: 458-467.
113. Perez, N. et al. (2000). "Molecularly imprinted nanoparticles prepared by aqueous suspension polymerisation." J.Appl.Polymer.Sci. **77**: 1851-1859.
114. Zimmerman, S. et al. (2003). "Molecular imprinting inside dendrimers." J.Am.Chem.Soc. **125**: 13504-13518.
115. Kirsche, N. and Whitcombe, M. (2005). The semi-covalent approach. Molecularly Imprinted Materials: Science and Technology. M. Yan, Ramstrom, O. New York.
116. Ye, L. and Mosbach, K. (2001). "The technique of molecular imprinting-Principle, state of art, and future aspects." Journal of Inclusion Phenomena and Macrocyclic Chemistry **41**: 107-113.
117. Wulff, G. and Biffis, A. (2001). Techniques and instrumentation in analytical chemistry. Molecularly imprinted polymers: Man-made mimics of antibodies and their applications in analytical chemistry. Sellaergren. Amsterdam, Elsevier. **23**: 71-111.

118. Wulff, G. (2005). The covalent and other stoichiometric approaches. Molecular imprinted materials: Science and technology. M. Yan, Ramstrom, O. New York: 59-92.
119. Wulff, G. and Knorr, K (2002). "Stoichiometric noncovalent interaction in molecular imprinting." Bioseparation **10**: 257-276.
120. Wulff, G. and Schonfeld, F. (1998). "Polymerisable amidines-adhesion mediators and binding sites for molecular imprinting." Adv.Mater. **10**: 957-959.
121. Wulff, G. (1986). "Molecular recognition in polymers prepared by imprinting with template." Polymeric Reagents and Catalysts.: 186-230.
122. Cormark, P. and Zurutuza Elorza, A. (2004). "Molecularly imprinted polymers: synthesis and characterisation." J.Chromatogr.B **804**: 173-182.
123. Bowmann, M. et al. (1998). " A high-throughput screening technique employing molecularly imprinted polymers as biomimetic selectors in "Drug-development assay approaches including molecular imprinting and biomarkers"." Meth.Surv. **25**: 37-43.
124. Matsui, J. et al. (1996). "Highly stereoselective molecularly imprinted polymer synthetic receptors for cinchona alkaloids." Tetrahedron-Asymmetry **7**: 1357-1361.
125. Nicholls, I. A. (1995). "Thermodynamic considerations for the design of and ligand recognition by molecularly imprinted polymers." Chem.Lett.: 1035-1036.
126. Takeuchi, T. et al. (1996). "Molecular imprinting: An approach to "tailor-made" synthetic polymers with biomimetic functions." Acta Polymerica **47**: 471-480.
127. Ramstrom, O. (2005). Synthesis and selection of functional and structural monomers. Molecularly imprinted materials: Science and technology. M. Yan, Ramstrom, O. New York: 181-224.
128. Wulff, G. (1995). "Molecular imprinting in cross-linked materials with the aid of molecular templates - a way towards artificial antibodies." Angew. Chem., Int. Ed. **34**: 1812-1832.
129. Shi, H. et al. (1999). "Template-imprinted nanostructured surfaces for protein recognition." Nature **398**: 593.
130. Aherne, A. et al. (1996). "Bacteria-mediated lithography of polymer surfaces." J.Am.Chem.Soc. **118**: 8771.
131. Andersson, L.I. (1996). "Application of molecular imprinting to the development of aqueous buffer and organic solvent based radioligand binding assays for (S)-propranolol." Anal.Chem. **68**: 111-117.
132. Hart, B. R. et al. (2000). "Discrimination between enantiomers of structurally related molecules: Separation of benzodiazepines by molecularly imprinted polymers." Journal Of The American Chemical Society **122**: 460-465.
133. Matsui, J. et al. (1997). "2-(trifluoromethyl)acrylic acid: a novel functional monomer in noncovalent molecular imprinting." Anal. Chim.Acta **343**: 1-4.

134. Kempe, M. et al. (1993). "Chiral separation using molecularly imprinted heteroaromatic polymers." Journal of Molecular Recognition **6**: 25-29.
135. Yu, C. and Mosbach, K. (1997). "Molecular imprinting utilizing an amide group for hydrogen bonding leading to highly efficient polymers." J.Org.Chem. **62**: 4057-4064.
136. Liao, J. et al. (1996). "Novel support with artificially created recognition for the selective removal of proteins and for affinity chromatography." Chromatographia **42**: 259-262.
137. Yu, C. and Mosbach, K. (1997). "Molecular imprinting utilizing an amide functional group for hydrogen bonding leading to highly efficient polymers." Journal Of Organic Chemistry **62**: 4057-4064.
138. Ramstrom, O. et al. (1993). "Recognition sites incorporating both pyridinyl and carboxy functionalities prepared by molecular imprinting." J.Org.Chem. **58**: 7562-7564.
139. Meng, Z. et al. (1999). "High performance cocktail functional monomer for making molecule imprinting polymer." Anal.Sci. **15**: 141-144.
140. Wulff, G. et al. (1986). "Enzyme-analog built polymers .19. Racemic-resolution on polymers containing chiral cavities." Journal Of Liquid Chromatography **9**: 385-405.
141. Kempe, M. and Mosbach, K. (1995). "Receptor binding mimetics: a novel molecularly imprinted polymer." Tetrahedron Letters **36**: 3563-3566.
142. Kempe, M. (1996). "Antibody-mimicking polymers as chiral stationary phases in HPLC." Anal.Chem. **68**: 1948-1953.
143. Tong, D. et al. (2001). "Some studies of the chromatographic properties of gels for selective sorption of proteins." Chromatographia **54**: 7-14.
144. Sibrian-Vazquez, M. and Spivak, D. (2003). "Improving the strategy and performance of molecularly imprinted polymers using cross-linking functional monomers." J.Org.Chem. **20**.
145. Spivak, D. (2005). Selectivity in molecularly imprinted matrices. Molecularly imprinted materials: Science and Technology. M. Yan, Ramstrom,O. New York: 395-418.
146. Yilmaz, E. et al. (2005). The noncovalent approach. Molecularly imprinted materials: science and Technology. M. Yan, Ramstrom,O. New York.
147. Sellergren, B. and Shea, K. (1993). "Influence of polymer morphology on the ability of imprinted network polymers to resolve enantiomers." J.Chromatogr. **635**: 31-49.
148. Andersson, L.I. et al. (1995). "Mimics of the binding sites of opioid receptors obtained by molecular imprinting of enkephalin and morphine." Proc.Natl.Acad.Sci. **92**: 4788-4792.
149. Haupt, K. et al. (1998). "Assay system for the herbicide 2,4-dichlorophenoxyacetic acid using a molecularly imprinted polymer as an artificial recognition element." Anal.Chem. **70**: 628-631.

150. Piletsky, S. et al. (1999). "Combined hydrophobic and electrostatic interaction-based recognition in molecularly imprinted polymers." Macromolecules **32**: 633-636.
151. Striegler, S. (2003). "Carbohydrate recognition in cross-linked sugar-templated poly(acrylates)." Macromolecules **36**: 1310-1317.
152. O'Shannessy, D. et al. (1989). "Molecular imprinting of amino-acid derivatives at low temperature using photolytic homolysis of azobisnitriles." Anal.Biochem. **177**: 144-149.
153. Spivak, D. and Shea, K.J. (1997). "Evaluation of binding and origins of specificity of 9-ethyladenine imprinted polymers." J.Am.Chem.Soc. **119**: 4388-4393.
154. O'Shannessy, D. et al. (1989). "Recent advances in the preparation and use of molecularly imprinted polymers for enantiomeric resolution of amino acid derivatives." J.Chromatogr. **470**: 391-399.
155. Shug, K.A. and Lindner, W. (2005). "Noncovalent binding between guanidinium and anionic groups: focus on biological and synthetic-based arginine/guanidinium interactions with phosph[on]ate and sulf[on]ate residues." Chem.Rev. **105**: 67-113.
156. Yilmaz, E. et al. (2005). "The noncovalent approach." Molecularly Imprinted Materials: Science and Technology.
157. Jeffrey, G.A. (1997). An Introduction to Hydrogen Bonding.
158. Ben-Na'im, Aryeh. Hydrophobic Interaction. New York, Plenum Press.
159. Nicholls, I.A. et al. (2001). "Can we rationally design molecularly imprinted polymers?" Analytica Chimica Acta **435**: 9-18.
160. Nicholls, I.A. (1998). "Towards the rational design of molecularly imprinted polymers." Journal of Molecular Recognition **11**: 79-82.
161. Nicholls, I.A. and Andersson, S.H. (2001). "Thermodynamic principles underlying molecularly imprinted polymer formulation and ligand recognition" in Molecularly imprinted Polymers: Man-made mimics of antibodies and their applications in analytical chemistry.
162. Holroyd, S.E. et al. (1993). "Rational design and binding of modified cell-wall peptides to Vancomycin-group antibiotics: factorising free energy contributions to binding." Tetrahedron **49**: 9171-9182.
163. Kempe, M. and Mosbach, K. (1995). "Molecular imprinting used for chiral separations." J.Chromatogr.A **694**: 3-13.
164. Remcho, V. and Tan, Z.J. (1999). "MIPs as chromatographic stationary phases for molecular recognition." Anal. Chem. **71**: A248-A255.
165. Ansell, R. (2005). Applications of MIPs as antibody mimics in immunoassays. Molecularly Imprinted Materials: Science and Technology. M. Yan, Ramstrom, O. New York.
166. Yilmaz, E. et al. (2000). "The use of imprinted polymers as recognition elements in biosensors and binding assays." Novel Approaches in Biosensors and Rapid Diagnostic Assays: 193-209.

167. Mayes, A. et al. (1994). "Sugar binding polymers showing high anomeric and epimeric discrimination obtained by noncovalent molecular imprinting." Analytical Biochemistry **222**: 483-488.
168. Sellergren, B. et al. (1985). "Molecular imprinting of amino-acid derivatives in macroporous polymers - demonstration of substrate-selectivity and enantio-selectivity by chromatographic resolution of racemic mixtures of amino-acid derivatives." Journal of Chromatography **347**: 1-10.
169. Kempe, M. et al. (1995). "An approach towards surface imprinting using the enzyme ribonuclease A." J.Molec.Recog. **8**: 35-39.
170. Kriz, D. et al. (1994). "Thin layer chromatography based on the molecular imprinting technique." Anal.Chem. **66**: 2636-2639.
171. Spiegel, P. et al. (2003). "Molecularly imprinted polymers in capillary electrochromatography: recent developments and future trends." Electrophoresis **24**: 3892-3899.
172. Andersson, H. et al. (1999). "Study of the nature of recognition in molecularly imprinted polymers II [1] - Influence of monomer-template ratio and sample load on retention and selectivity." J.Chromatogr.A **848**: 39-49.
173. Sellergren, B. (1994). "Imprinted dispersion polymers - a new class of easily accessible affinity stationary phases." J.Chromatogr.A **673**: 133-141.
174. Glad, M. et al. (1995). "Molecularly imprinted composite polymers based on trimethylolpropane trimethacrylate (TRIM) Particles for efficient enantiomeric separations." Reactive Polymers **25**: 47-54.
175. Robinson, D. and Mosbach, K. (1989). "Molecular imprinting of a transition-state analog leads to a polymer exhibiting esteroytic activity." Journal Of The Chemical Society-Chemical Communications: 969-970.
176. Andersson, L. I. and Mosbach, K. (1989). "Molecular imprinting of the coenzyme-substrate analog N-pyridoxyl-L-phenylalaninamide." Makromolekulare Chemie-Rapid Communications **10**: 491-495.
177. Shimada, T. et al. (1994). "Footprint catalysis .10. Surface modification of molecular footprint catalysts and its effects on their molecular recognition and catalysis." Bulletin Of The Chemical Society Of Japan **67**: 227-235.
178. Beach J. V. and Shea, K. J. (1994). "Designed catalysts - A synthetic network polymer that catalyzes the dehydrofluorination of 4-fluoro-4-(p-nitrophenyl)butan-2-one." Journal Of The American Chemical Society **116**: 379-380.
179. Severin, K. (2005). Applications of molecularly imprinted materials as enzyme mimics. Molecularly Imprinted Materials: Science and Technology. M. Yan, Ramstrom, O. New York.
180. Hedborg, E. et al. (1993). "Some studies of molecularly-imprinted polymer membranes in combination with field-effect devices." Sensors And Actuators A-Physical **37-8**: 796-799.

181. Chen, G. et al. (1997). "A glucose sensing polymer." Abstracts Of Papers Of The American Chemical Society **213**: 176-177.
182. Jenkins, A. et al. (1997). "Polymer based lanthanide luminescent sensors for the detection of nerve agents." Analytical Communications **34**: 221-224.
183. Piletsky, S. et al. (1997). "Optical detection system for triazine based on molecularly-imprinted polymers." Analytical Letters **30**: 445-455.
184. Mosbach, K. and Ramstrom, O. (1996). "The emerging technique of molecular imprinting and its future impact on biotechnology." Biotechnology **14**: 163-170.
185. Ye, L. et al. (2000). "Synthesis and characterisation of molecularly imprinted microspheres." Macromolecules **33**: 8239-8245.
186. Yilmaz, E. et al. (2000). "The use of immobilized templates-A new approach in molecular imprinting." Angew.Chem. **39**: 2115-2118.
187. Andersson, L. et al. (1996). "Molecular imprinting of the endogenous neuropeptide Leu(5)-enkephalin and some derivatives." Macromol.Rapid Commun. **17**: 65-71.
188. Cederfur, J. et al. (2003). "Synthesis and screening of a molecularly imprinted polymer library targeted for penicillin G." J.Comb.Chem **5**: 67-72.
189. Suarez-Rodriguez et al. (2001). "Fluorescent competitive flow-through assay for chloramphenicol using molecularly imprinted polymers." Biosensors and Bioelectronics **16**: 955-961.
190. Piletsky, S. et al. (2001). "Substitution of antibodies and receptors with molecularly imprinted polymers in enzyme-linked and fluorescent assays." Biosensors and Bioelectronics **16**: 701-707.
191. Haupt, K. (1999). "Molecularly imprinted sorbent assays and the use of non-related probes." Reactive Polymers **41**: 125-131.
192. Mayes, A. and Mosbach, K. (1996). "Molecularly imprinted polymer beads: suspension polymerisation using a liquid perfluorocarbon as the dispersing phase." Anal. Chem. **68**: 3769-3774.
193. Ye, L. et al. (1999). "Molecularly imprinted monodisperse microspheres for competitive radioassay." Anal. Commun. **36**: 35-38.
194. Yilmaz, E. et al. (2000). "The use of immobilized templates- a new approach in molecular imprinting." Angev.Chem.
195. Marx, S. and Liron, Z. (2001). "Molecular imprinting in thin films of organic-inorganic hybrid sol-gel and acrylic polymers." Chem.Mat. **13**: 3624-3630.
196. Piletsky, S. et al. (2000). "Chemical grafting of molecularly imprinted homopolymers to the surface of microplates. Application of artificial adrenergic receptor in enzyme-linked assay for β -agonists determination." Anal. Chem. **72**: 4381-4385.

197. Website of the Society for Molecular Imprinting, <http://www.smi.tu-berlin.de/>

Chapter 2

Aims and objectives

2.1 AIM

The aim of this project was to develop a selective synthetic molecularly imprinted receptor that demonstrated high affinity for serine phosphorylated peptides. It was important that the receptor had minimal affinity for the non-phosphorylated form and also that binding to phosphoserine was independent of adjacent amino acid residues. In addition, it was important that the system should function in a near aqueous environment.

2.2 OBJECTIVES

- i. Development of a general procedure for the design of MIPs with improved affinity and selectivity.
- ii. To design and synthesise a template able to mimic 'peptide incorporated' phosphoserine.
- iii. To synthesise the functional monomer *N,N'*-diethyl-4-vinylbenzamidine.
- iv. To investigate by computational analysis monomer-template interaction.
- v. Synthesis of appropriate molecularly imprinted polymers.
- vi. Equilibrium evaluation of template affinity and characterisation of selectivity.
- vii. Optimise aqueous performance of the MIP.
- viii. Evaluate the enantio-selectivity of the optimised system.
- ix. To evaluate the affinity and specificity of the MIP for a serine-phosphorylated peptide.

Chapter 3

Design and synthesis of the template and the functional monomer

3.1 MIP DESIGN

The first goal of this project was to identify a suitable template and an appropriate monomer system from which to prepare a MIP that possesses the characteristics set out in the objectives of this project listed in Chapter 2. The first step in this process was to evaluate previous molecular imprinting studies in which the template molecule contained a phosphate or related functional group.

3.1.1 IMPRINTING OF PHOSPHATES OR PHOSPHONATES

The literature contains a few reports on the imprinting of phosphate or phosphonate esters but no reports on the imprinting of phosphorylated serine. These studies focus on the detection of pesticides and toxic chemical warfare nerve agents. In 1999 Jenkins *et al.*¹ combined molecular imprinting with a sensitized lanthanide luminescence to create the basis for a sensor that was capable of selectively monitoring the hydrolysis product of the nerve agent Soman in water (Figure 3.1).

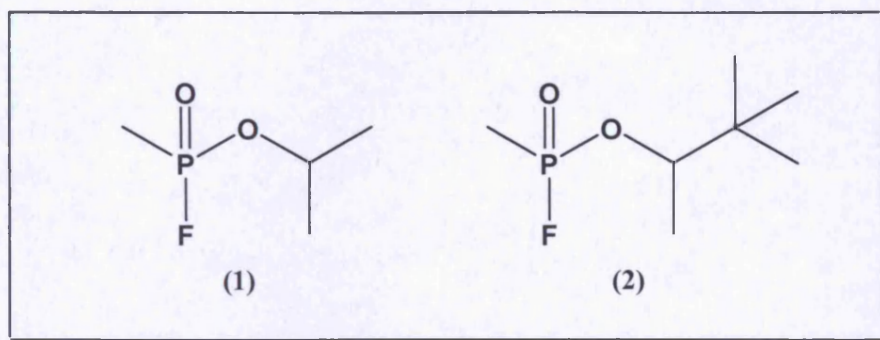


Figure 3.1: Chemical warfare nerve agents Sarin (1) and Soman (2).

Following these studies, Meng Zi-Hui *et al.*² were able, not only to imprint the nerve agents pinacolyl methylphosphonate, ethyl methylphosphonate and methane phosphonic acid, but also, by taking the advantage of their crossreactivity, they were able to recognise the degradation product of other nerve agents (Figure 3.2).

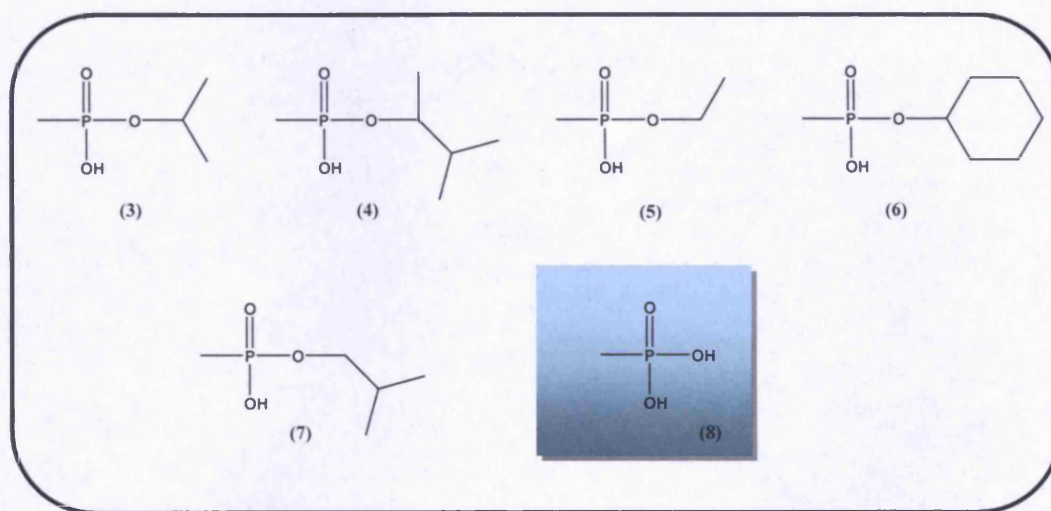


Figure 3.2: The molecular structures of the degradation products of nerve agents. Isopropyl methylphosphonate (3), pinacolyl methylphosphonate (4), ethyl methylphosphonate (5), cyclohexyl methylphosphonate (6) and isobutyl methylphosphonate (7) are the degradation products of the main nerve agents: Sarin, Soman, VX, GF and Russian VX. Methylphosphonic acid (8) is the final degradation product of all nerve agents and their products.

Moller *et al.*³ reported the use of molecular imprinting to prepare a solid-phase extraction (SPE) MIP that was used to selectively extract diphenyl phosphate from biological samples, such as human blood and urine. Diphenyl phosphate was identified as the major degradation product of the flame retardant additive triphenyl phosphate which was found to induce several biological responses, including allergenic effects (Figure 3.3). Diphenyl phosphate esters are highly polar and acidic compounds, which are difficult to extract from aqueous samples using conventional extraction methods. Thus, the combined use of molecular imprinting solid-phase extraction (MISPE) and ion pairing-LC-ES-MS-MS was reported as a fast and easy clean-up method for acidic diphosphate esters in complex matrices.

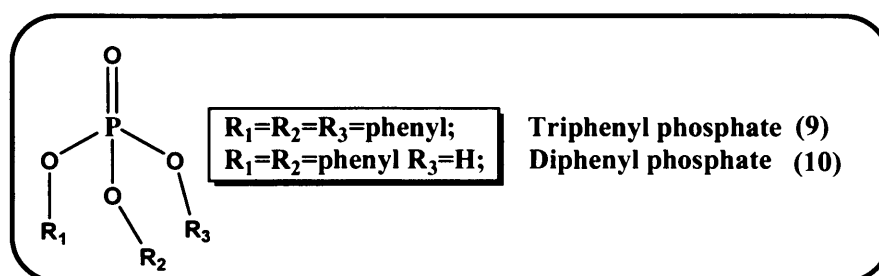


Figure 3.3: Structures of triphenyl (9) and diphenyl (10) phosphates.

Recently, Sellergren *et al.*⁴ successfully demonstrated the non-covalent molecular imprinting of phosphorus esters containing a single hydrogen bond acceptor site using a urea-based functional monomer (Figure 3.4). In particular, they developed a different approach using an excess of template compared with the functional monomer, in order to increase the imprinting effect in non-polar and polar mobile phase.

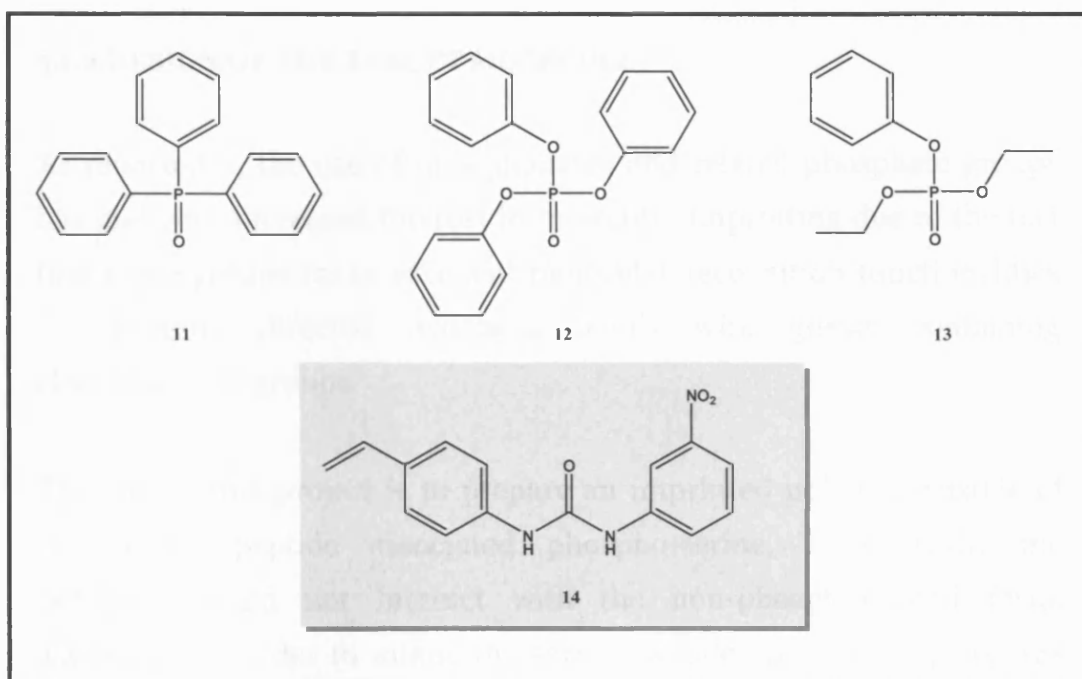


Figure 3.4: Chemical structures of the urea-based functional monomer (14) and the templates: triphenyl phosphine oxide (11), phosphorus ester triphenyl phosphate (12) and phosphorus ester diethylphenyl phosphate (13).

3.1.2 DESIGN OF THE TARGET MOLECULE

As reported¹⁻⁴, the use of phosphonates and related phosphate groups has met with increased interest in molecular imprinting due to the fact that these groups make excellent molecular recognition functionalities for forming directed hydrogen bonds with guests containing electropositive groups.

The aim of this project is to prepare an imprinted polymer capable of recognising peptide associated phospho-serine. Importantly, the polymer should not interact with the non-phosphorylated form. Therefore, in order to mimic the serine peptide bond, a template was designed with the amino group protected by t-butyloxycarbonyl (Boc) and the carboxyl group esterified with a methyl group. The esterification was aimed to imitate the amide function in the peptide linkages. In fact, like the amide group, the ester group is water-soluble and is planar with bond angles about the carbonyl tending to 120°.

Thus, the natural isomer (L) of Boc-serine methyl ester was selected for the next step of phosphorylation and for the molecularly imprinting process.

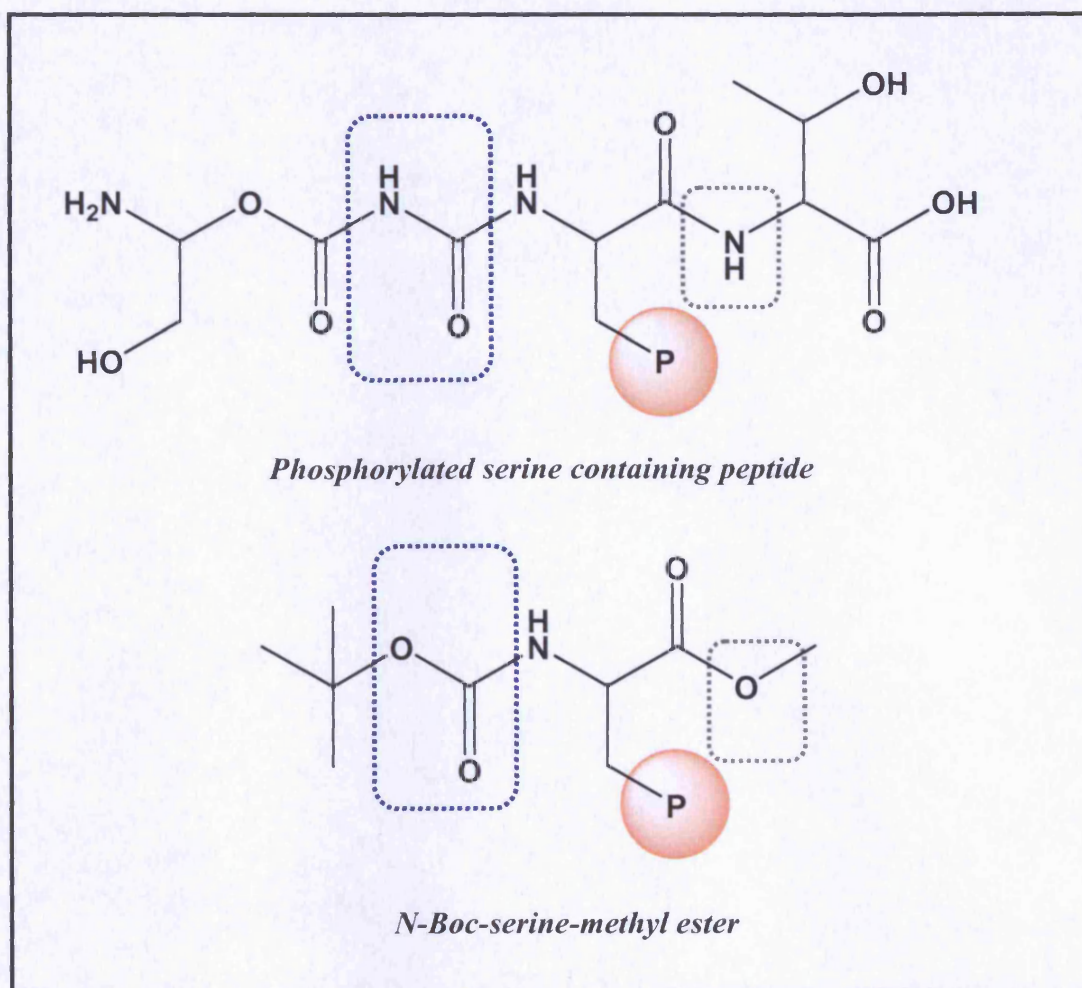


Figure 3.5: Boc-phospho-L-serine methyl ester chosen as target molecule.

3.1.3 RATIONALE BEHIND THE CHOICE OF THE AMIDINE AS THE FUNCTIONAL MONOMER

3.1.3.1 BIOLOGICAL AND SYNTHETIC RECEPTORS

Non-covalent binding interactions play an important role in Nature. The interactions in the antigen-antibody reaction are mainly based on non-covalent interactions between ionic and polar groups of the amino acids, and proteins rely on hydrogen bonding for their secondary and tertiary structures and for the molecular recognition of hormones and synthetic drugs at receptor binding sites. Since molecular recognition plays such an important role in life, it is not surprising that chemists have thought to prepare artificial receptor molecules combining the recognition abilities of natural systems with the flexibility or rigidity possible through the modern synthetic chemistry. In modern drug design, the guanidinium moiety of arginine is a biological receptor system often mimicked and replaced by an amidine, which works quite well since amidines and guanidines are strong organic bases. The biological activity of many amidines is attributed to a cationic hydrogen-bond donor group that can act as binding sites for both carboxylate and phosphates. The amidine pharmacophore is found in a range of pharmaceutical drugs; benzamidine, in particular, has replaced arginine in various synthetic analogues of natural hormones⁵.

3.1.3.2 APPLICATIONS OF AMIDINE-BASED MOLECULARLY IMPRINTED POLYMERS

The use of the amidine as receptor in molecularly imprinted polymers has been investigated by several workers. Wulff *et al.*⁶ were the first group to develop amidine-based MIP. Amidinium binding sites were used for the preparation of chiral imprints with optically active dicarboxylic acid as templates⁶. These imprinted polymers were able to discriminate between template enantiomers. Another application of

imprinted polymers with amidinium binding sites is for catalysis in the investigation of the alkaline hydrolysis of ester, carbonates and carbamates⁷⁻¹⁰. These polymers resulted in significant enhancements in the rates of ester hydrolysis by 102-235 times faster relative to the solution reactions. In the case of carbonates and carbamates, the hydrolysis brought about by the imprinted polymers was 588 and 400-3860 faster, respectively¹. More recently the feasibility of using benzamidine based molecular imprinted polymers as sensitive material for chiral sensors has been demonstrated¹¹. In this study benzamidine polymers were prepared on the surface of optical transducers. These systems were then probed using reflectometric interference spectroscopy in order to evaluate template binding.

On the basis of these previously reported studies, the benzamidine-phosphate interaction was selected as an appropriate approach with which to achieve the desired 'MIP-phosphate' selectivity.

3.1.4 CONCLUSION

Boc-phospho-L-serine methyl ester and a suitable benzamidine containing monomer were chosen respectively as template and functional monomer. However, as these compounds were not commercially available, an initial objective was to synthesise and obtain them with high purity.

3.2 SYNTHESIS OF THE TEMPLATE MOLECULE

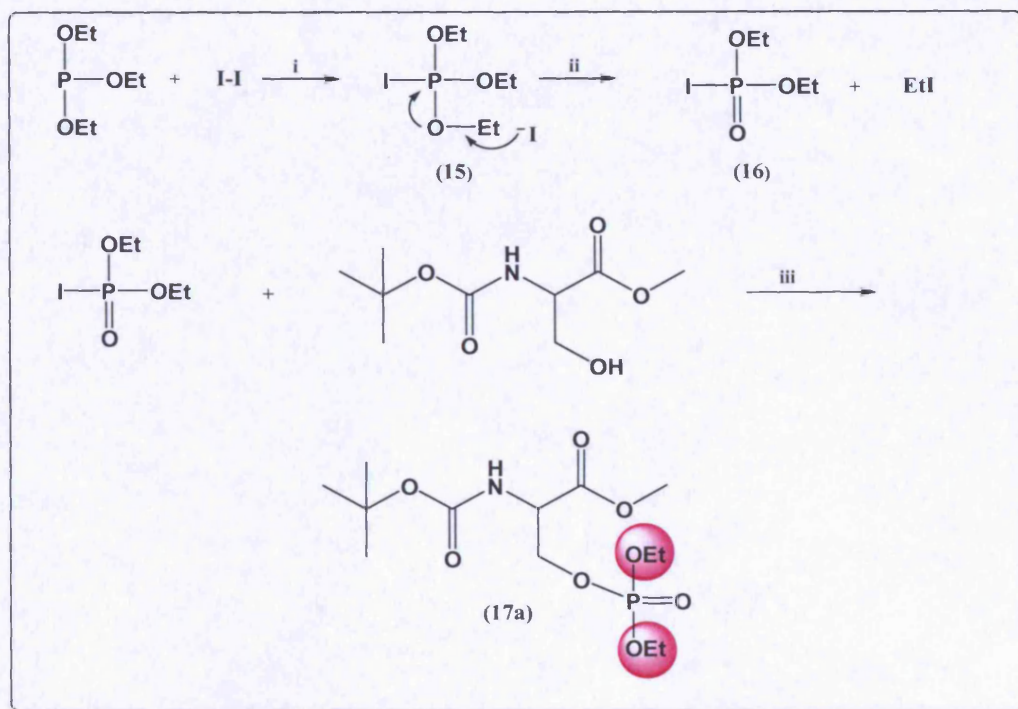
3.2.1 INTRODUCTION

To prepare the template molecule Boc-phospho-L-serine-methyl ester from Boc-L-serine-methyl ester, a number of different phosphorylation approaches were investigated under a range of conditions. The product was finally obtained using a procedure that used a phosphoramidate as the source of phosphate. This was reacted with the starter material, Boc-L-serine methyl ester, to give the final pure compound chosen as target, Boc-phospho-L-serine-methyl ester, in good yield. Full experimental details of the procedures are given in Appendix I.

3.2.2 PHOSPHORYLATION METHODS

3.2.2.1 ARBUZOV REACTION

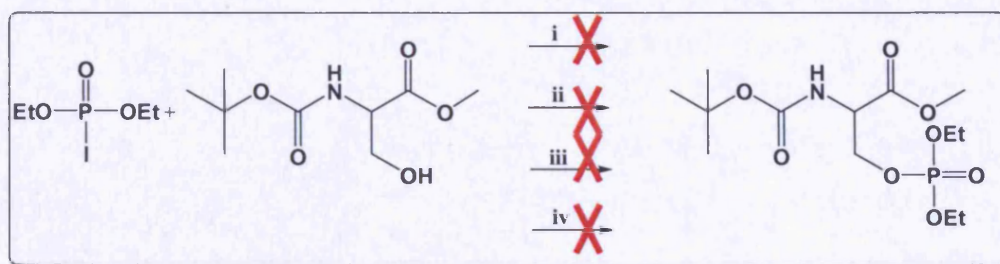
The first procedure attempted was that of Jeffrey K. Stowell and Theodore S. Widlansky¹², who reported the synthesis of phosphate esters *via* the activation of trialkyl phosphite with molecular iodine. Using this method, the phosphorylation of phenols as well as primary and secondary alcohols was accomplished in virtually quantitative yields under mild conditions. We have explored this reaction as a potential use for the phosphorylation of OH group of Boc-L-serine methyl ester. In one experiment, triethyl phosphite was oxidized with iodine to obtain the phosphorylating agent that was added then to the Boc-L-serine methyl ester (Scheme 3.1).



Scheme 3.1: Arbuzov Reaction for the phosphorylation of Boc-L-serine methyl ester.

Reagent and conditions: (i) CH_2Cl_2 , 0°C , 5 min.; (ii) 25°C , 30 min.; (iii) Pyridine, CH_2Cl_2 , 4 hrs

This synthesis was deemed unsuccessful due to the absence of any additional spot on a TLC plate. The procedure was therefore modified, increasing the reaction time and modifying the temperature but, even in this case, TLC showed only starting material. The reaction was then carried out increasing the equivalents of phosphorylated agent $\text{P}(\text{OEt})_3$ (Scheme 3.2).



Scheme 3.2 : Attempted phosphorylations.

Reagents and conditions: (i) Iodine, pyridine, dichloromethane, 25°C, 4 hrs; (ii) Iodine, pyridine, dichloromethane, 0°C, 4 hrs; (iii) Iodine, pyridine, dichloromethane, 0°C, 4 hrs, 4 eq. phosphite; (iv) Iodine, pyridine, dichloromethane, 24 hrs.

The product recovered was identified by ^{31}P -NMR as containing a phosphorus peak inherent to the intermediate (**17a**) but, after column chromatography, the NMR showed that the purified product lost its phosphate group (Table 3.1).

Table 3.1: Synthetic variations and phosphorus shifts (δ ^{31}P -NMR data) for Arbuzov Reaction.

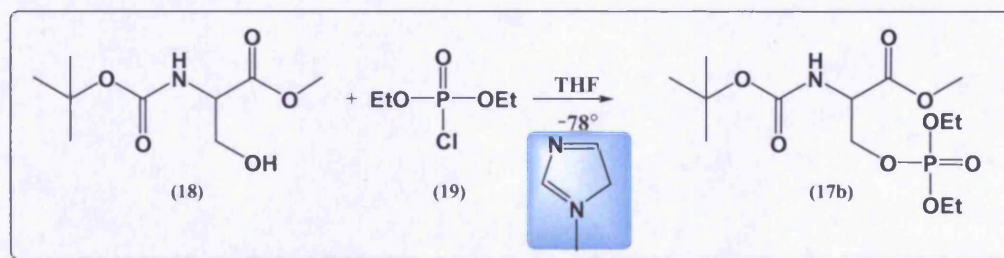
Sample #	Equivalent Boc-serine	Equivalent $\text{P}(\text{OEt})_3$	Reaction Time	T	$\delta^{31}\text{P}(\text{CDCl}_3)$ before chromatography	Observations
1	1	1	4 hours	25°	-11.995	Final product with similar Rf as the starting material
2	1	1	4 hours	0°	-11.880	TLC showed only starting material
3	1	4	4 hours	0°	-11.833	Small amount isolated by column chromatography but not containing phosphorus
4	1	1	overnight	0°	-11.832	Only a trace of product observed by TLC

As it was not possible to synthesise the Boc-phospho-L-serine methyl ester using this reaction, possible alternative routes have been carried out.

These procedures entailed the use of alternative phosphorylating agents and bases.

3.2.2.2 PHOSPHORYLATION USING NMI AS BASE

In this attempt, diethyl chlorophosphate was used instead of triethyl phosphate in presence of N-methylimidazole (NMI) as base (Scheme 3.3).

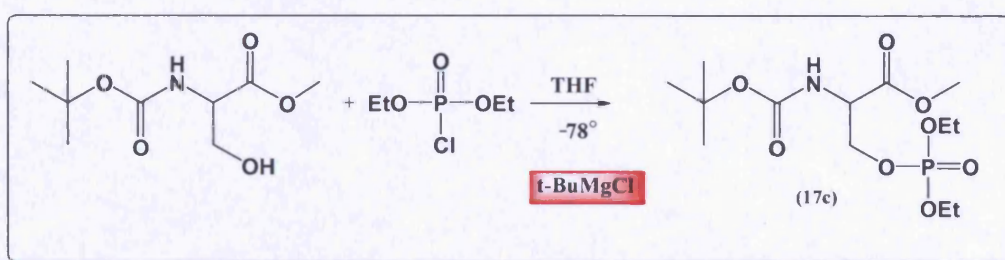


Scheme 3.3: Attempted synthesis using NMI as base.

In this case, the NMI acted as a catalyst; in fact it reacted with the phosphorylating agent to form a better leaving group for the successive step of phosphorylation. As the starting material could not be seen on TLC, the reaction was followed using ^{31}P -NMR that showed, at the final step, a peak at around -11.961 ppm. This result confirmed that the intermediate diethylphosphoserine was not obtained, as the chemical shift detected was typical of a pyrophosphate.

3.2.2.3 PHOSPHORYLATION USING A GRIGNARD REAGENT

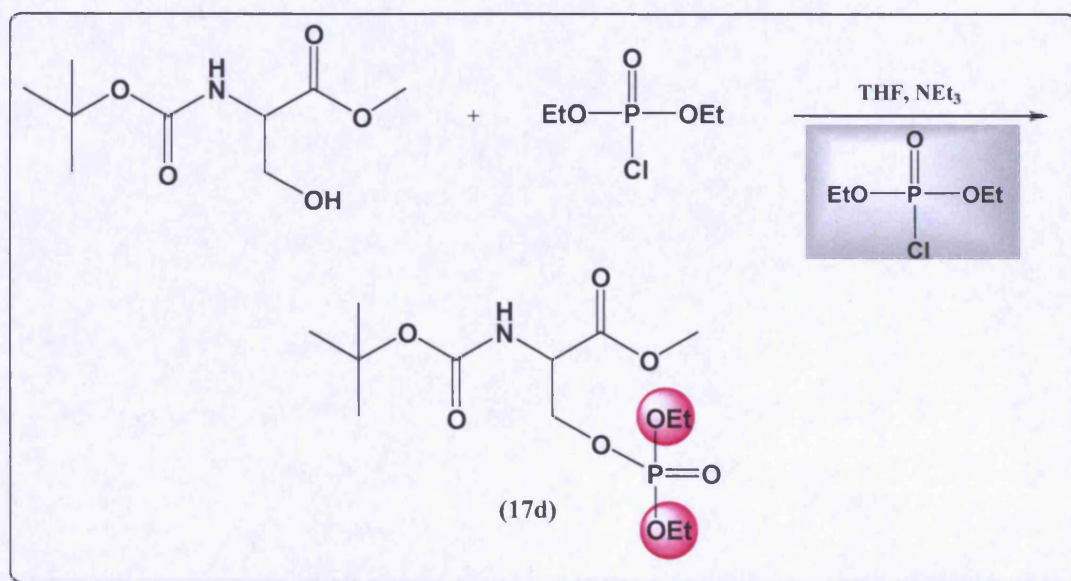
The third method involved the use of a Grignard reagent as stronger base (Scheme 3.4). After adding diethyl chlorophosphate to a solution of starting material in presence of 2.5 equivalents of *tert*-butylmagnesium chloride, the reaction was left stirring for 2 hours. The reaction was followed by ^{31}P -NMR that showed a persistent peak at 5.6 ppm, similar to that of starter material suggesting that no reaction took place.



Scheme 3.4: Phosphorylation method by using the Grignard reagent.

3.2.2.4 PHOSPHORYLATION USING TRIETHYLAMINE AS BASE

This method is a modification of the previous approach (section 3.2.2.3) and used triethylamine as base instead of a Grignard Reagent. Importantly, in this approach a second addition of the phosphorylating agent was made after 3 hours (Scheme 3.5).



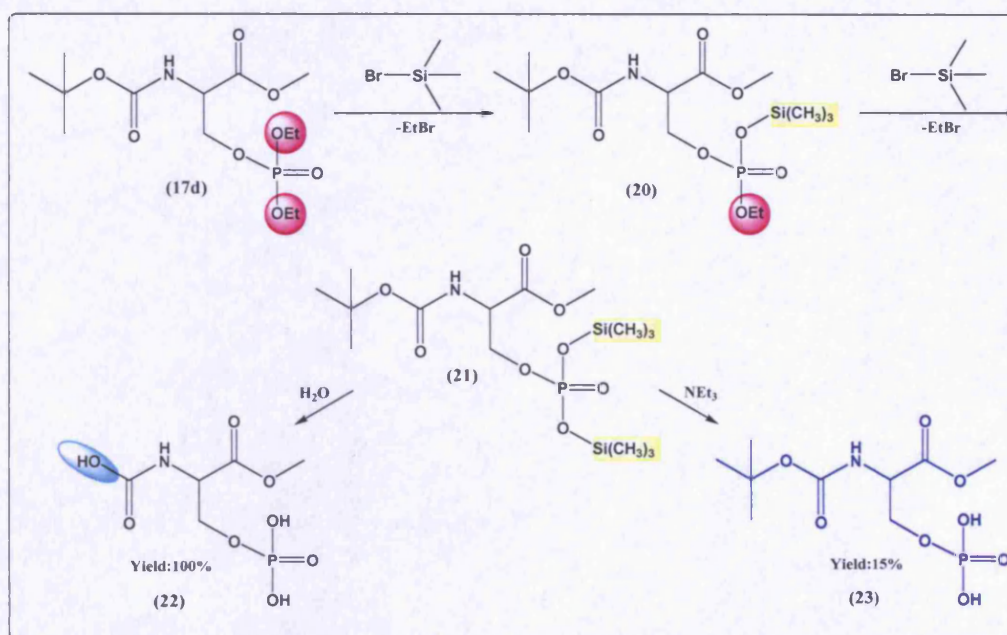
Scheme 3.5: Alternative synthesis for serine phosphorylation.

Using this approach Boc-diethyl-phospho-L-serine methyl ester (**17d**), was obtained in very low yield. Deprotection of this product was then attempted using the method described in 3.2.2.5

3.2.2.5 DEPROTECTION OF DIETHYLPHOSPHO-BOC-L-SERINE METHYL ESTER BY TRIMETHYLSILYL BROMIDE

The deprotection of phosphoester was carried out using trimethylsilyl bromide in two steps by a mechanism well known in literature¹³⁻¹⁵. The reaction is believed to occur *via* a mechanism involving nucleophilic attack of the phosphoryl oxygen on silicon followed by dealkylation of a phosphonium intermediate¹³ (Scheme 3.6). The silyl groups attached to phosphorus can be readily removed under mild conditions leading to the formation of a free phosphorus acid. Using this reagent, deprotection of the phosphoester was achieved; however, under the conditions employed, the Boc group was also cleaved. It was proposed that the loss of the Boc group was due to the formation of acidic P-OH groups following deprotection.

In order to avoid the decomposition of the phosphoserine methylester adduct and to improve its solubility, we replaced acetonitrile with dimethylformamide (DMF) and used triethylamine as a base to neutralise the P-OH groups. In this way, the acidity of OH groups was reduced and $^1\text{H-NMR}$ confirmed the presence of the Boc group. The desired final compound was obtained, but in very low yields (15%).



Scheme 3.6: Deprotection of diethyl phospho-boc-serine methyl ester.

3.2.2.6 SYNTHESIS OF BOC-PHOSPHO-L-SERINE METHYL ESTER BY USING *N,N'*-DIISOPROPYL-BIS-(4-CHLOROBENZYL)-PHOSPHORAMIDATE

This approach was based on previously reported methods¹⁶⁻²⁰ and used *N,N'*-diisopropyl-bis-(4-chlorobenzyl) phosphoramidite as a phosphorylating agent. The phosphoramidite (Figure 3.6) was prepared from PCl₃ in a three-steps procedure and purified by short column chromatography (Scheme 3.7).

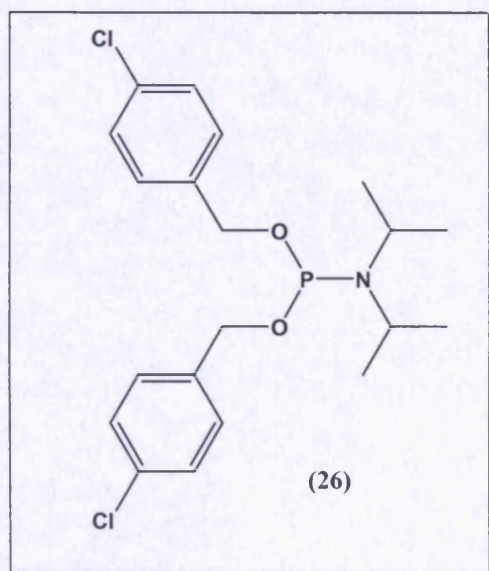
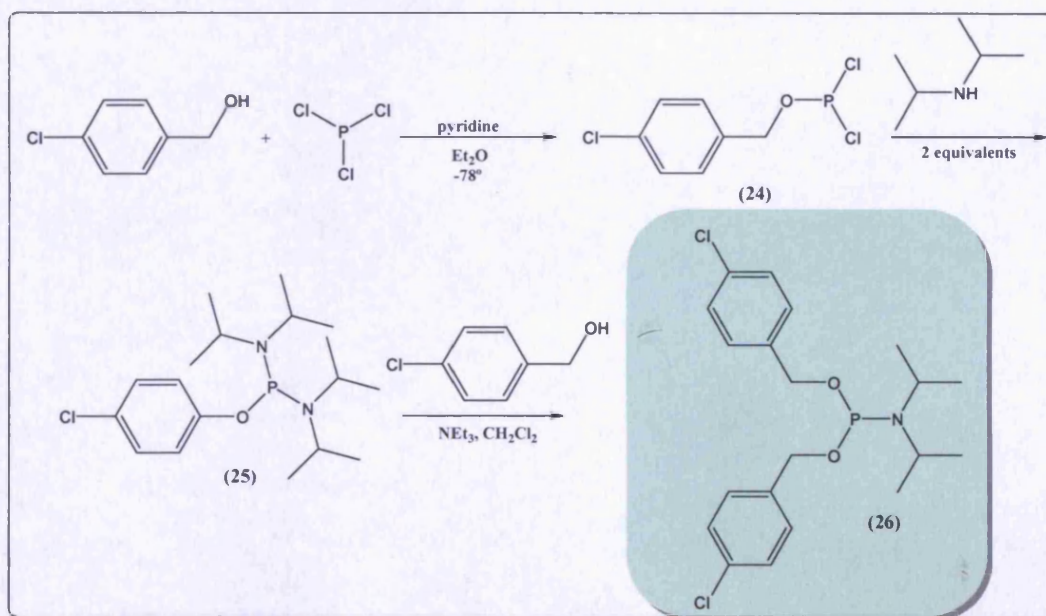


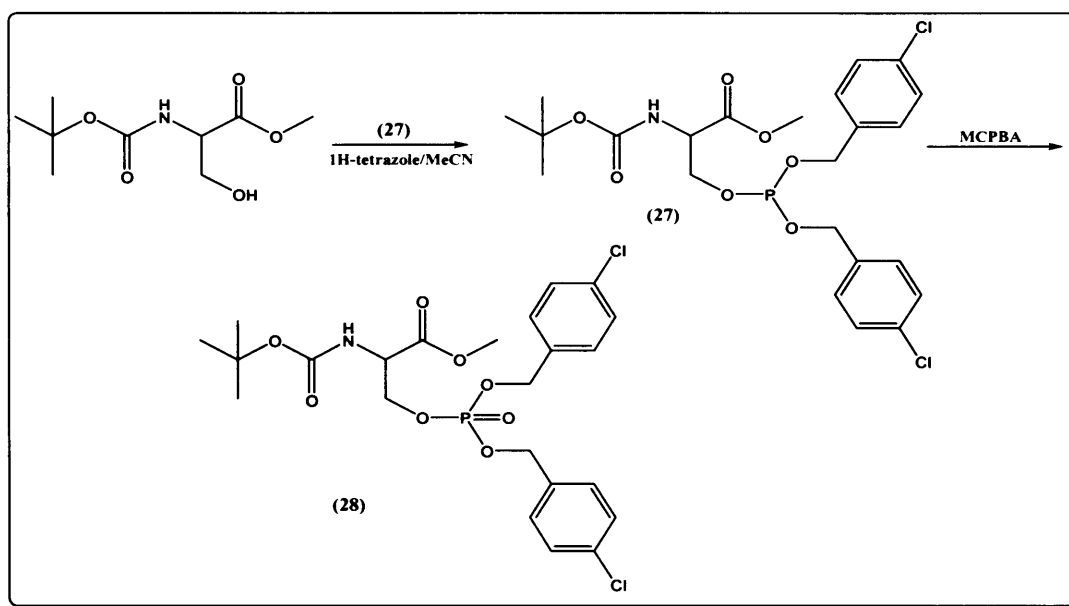
Figure 3.6: Chemical structure of *N,N*-diisopropyl-bis-(4-chloro)-benzyl phosphoramidite

The product was obtained as an easy to handle waxy solid, which crystallised readily due to the presence of the 4-chlorobenzyl groups.



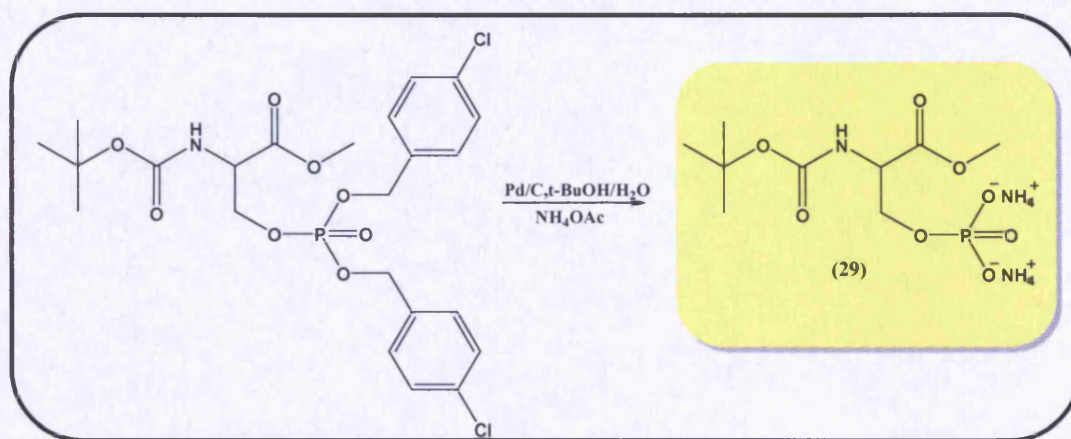
Scheme 3.7: Preparation of the phosphoramidite by three step reactions.

The phosphoramidite (**27**) was then used to phosphorylate the hydroxyl group of Boc-L-serine-methyl ester. To introduce the phosphate moiety, a solution of the protected amino acid and 1H-tetrazole in acetonitrile was treated with *N,N'*-diisopropyl-bis-(4-chlorobenzyl) phosphoramidite, followed by oxidation with meta-chloroperbenzoic acid (MCPBA) to give the intermediate Boc-phospho-4-chloro-(dibenzyl)-L-serine methyl ester (**28**).



Scheme 3.8: Synthesis of the intermediate Boc-phospho-4-chloro-(dibenzyl)-L-serine methyl ester (**28**), made by addition of phosphoramidite (**27**) to the Boc-L-serine methyl ester in the appropriate conditions.

The benzyl groups were removed quantitatively by catalytic hydrogenation on Pd/C giving the desired phosphorylated amino acid in 77% yield (**29**).



Scheme 3.9: Final step of the synthesis of Boc-phospho-L-serine methyl ester (**29**).

Importantly, the hydrogenation was carried out using a solution of ammonium acetate in *t*-BuOH/H₂O. Under basic conditions, the hydrogenation gives rise to the formation of the phosphate salt. Whilst under neutral conditions, the protonated phosphate would bring about cleavage of the Boc group.

3.2.3 HYDROGENATION METHODS

Hydrogenation, as previously reported in section 3.2.2.6, gave the desired Boc-phospho-L-serine methyl ester in good yield (77%).

Initially, palladium (5%) was used as a catalyst and the reaction was monitored by TLC. At the end of the reaction, the product solution was filtered, evaporated to dryness and analyzed by ¹H, ³¹P-NMR and mass spectrum (ES⁻). Unfortunately, no traces of the desired compound were observed. Instead, the major product was shown to be the mono chlorobenzyl phosphate (Figure 3.7).

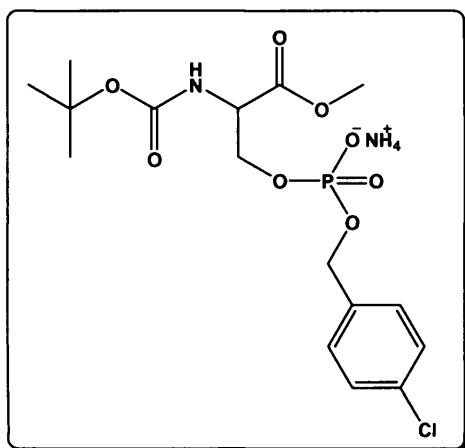


Figure 3.7: Structure of the monobenzyl Boc-phospho-L-methyl ester.

The hydrogenation was subsequently repeated using a larger amount of catalyst and for a longer period of time. Under these conditions, the ^1H -NMR and the mass spectrum showed that a small amount of Boc-phospho-L-serine methyl ester was obtained.

To improve the yield of the final compound, the previous reaction was repeated using palladium (10%). In addition, Pancaldi reagent was used in order to improve the efficiency of TLC visualisation. After 24 hours, the reduction was complete and the target compound was obtained in moderate yield (60%).

In order to reduce the reaction time, an additional modification was made. Palladium (10%) was added to Boc-phospho-L-dibenzyl-serine methyl ester (**28**) in a solution of ammonium acetate in $\text{H}_2\text{O}/t\text{-BuOH}$ (1:2) and treated with hydrogen gas (2 atm). After 2 - 3 hours the catalyst was filtered off over celite (the reaction was followed by TLC). The solvent was removed and the obtained crude product was analysed by ^1H , ^{31}P NMR which confirmed the complete deprotection of the benzyl groups. This third approach appeared to be the most efficient, providing an overall yield of Boc-phospho-serine methyl ester of 77% from Boc-phospho-L-dibenzyl-serine methyl ester (**28**).

3.2.4 PURIFICATION OF BOC-PHOSPHO-L-SERINE METHYL ESTER

The key spectroscopic evidence of the successful synthesis of Boc-phospho-L-serine methyl ester was provided by mass spectrometry (ESI⁻), indicating the presence of the molecular peak at 298.1 m/z, and NMR.

¹H-NMR gave information about the number of protons, chemical shifts and coupling constants. ¹H,¹H-COSY was mainly used to confirm adjacent protons through coupling constants association. ¹³C-NMR showed the number of carbons and ¹³C-DEPT 135 showed different peaks for each carbon according to the number of attached protons.

Careful analysis of the ¹H-NMR showed the presence of signals inherent to the benzyl groups of the phosphoramidate at 7.5 ppm and also two signals at 1.2 ppm and 2.9 ppm due to the presence of some remaining triethyl ammonium salt and two signals at 1.2 ppm and 3.5 ppm due to a residue of diisopropyl amine (Figure 3.8). Therefore, additional purification procedures were carried out to remove these contaminants.

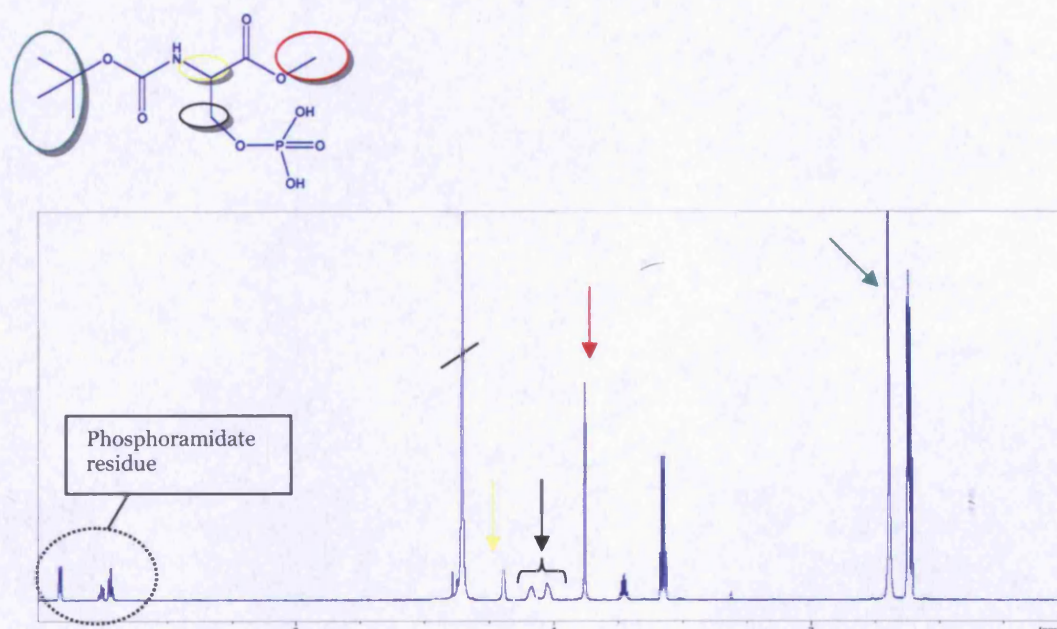


Figure 3.8: ¹H-NMR of Boc-phospho-L-serine methyl ester after hydrogenation.

The mixture was purified by preparative HPLC (reverse phase C₁₈ ODS₂, 25x100mm, 300 Angstrom; mobile phase 100% H₂O; flow rate: 20mL/min; wavelength= 210 nm), providing a final compound with high purity. The fractions containing the pure product were collected and freeze-dried. ¹H-NMR analysis indicated the complete disappearance of the signals corresponding to the benzyl groups and to the diisopropyl amine (Figure 3.9).

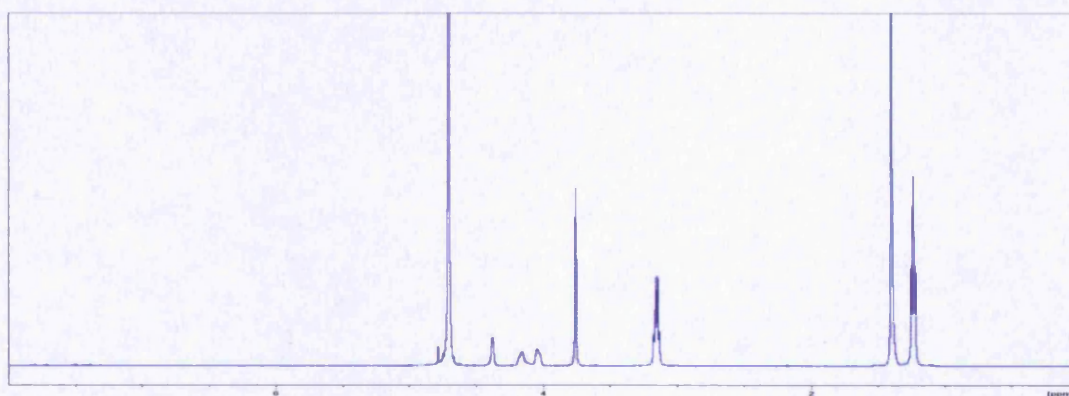


Figure 3.9: ¹H-NMR of Boc-phospho-serine methyl ester after preparative HPLC.

An additional purification step was carried out to remove the two signals at 1.2 ppm and 2.9 ppm inherent to the triplet and quartet of the triethyl ammonium salt (Figure 3.10). As it was not possible to separate the product from the triethylamine by solvent extraction or crystallisation, a cation exchange resin was employed where one ion (Na⁺) replaced the other (⁺NHEt₃) in a highly efficient exchange process. After activating the resin by washing firstly with water and finally with NaOH(aq) 1N, the template, dissolved in water, was added to the Buchner funnel containing the resin. The template was recovered and dried and the residue checked by NMR. ³¹P-NMR showed a single peak at 1.4 ppm. This shift was marginally greater than that observed for the triethylammonium salt of the product. The ¹H-NMR spectrum further confirmed the structure of the product and demonstrated the loss of the triethylamine species (Figure 3.11).

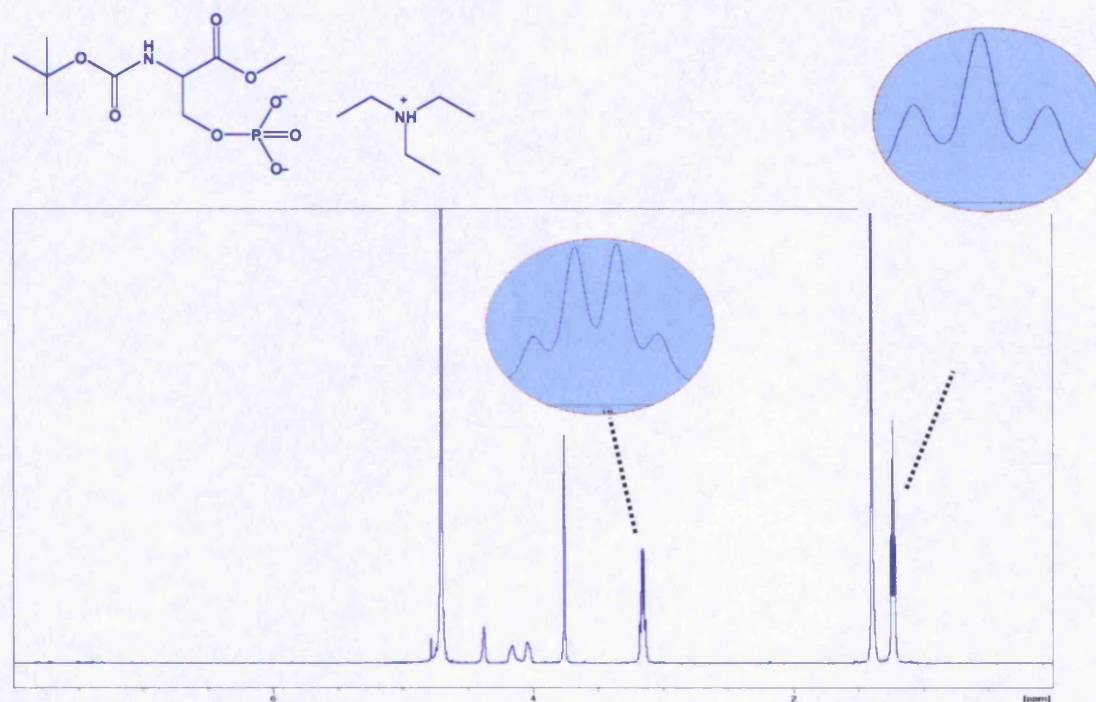


Figure 3.10: ¹H-NMR spectrum in D₂O of Boc-serine methyl ester before treatment with ion exchange resin.

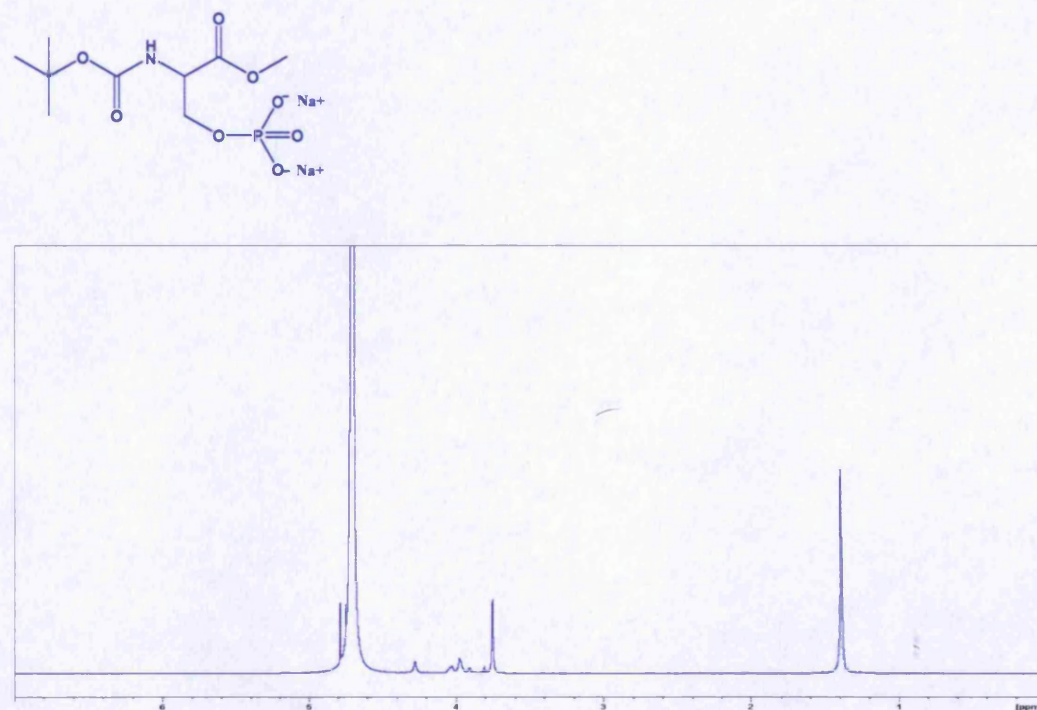


Figure 3.11: ¹H-NMR spectrum in D₂O of Boc-phospho-L-serine methyl ester after treatment with ion exchange resin.

LC-Mass spectroscopy analysis (GE Healthcare instrument (Ettan System: waters Q-TOF-2 MS, 2790 LC); Mobile phase: 50mmol Ammonium acetate pH7.6/CH₃CN 1:1; flow rate 1ml/min; Column: Gemini 110A C₁₈ 50x2mm 5μ: ES⁻ infusion) was subsequently performed to demonstrate the purity of the final compound. The spectrum showed a single peak at 4.8 minutes (Figure 3.12) of MS 298, which was the molecular weight of the Boc-phospho-L-serine methyl ester (Figure 3.13). Only a peak inherent to our target and dimers at 597/896 were seen on the spectrum and no evidence of impurities was observed.

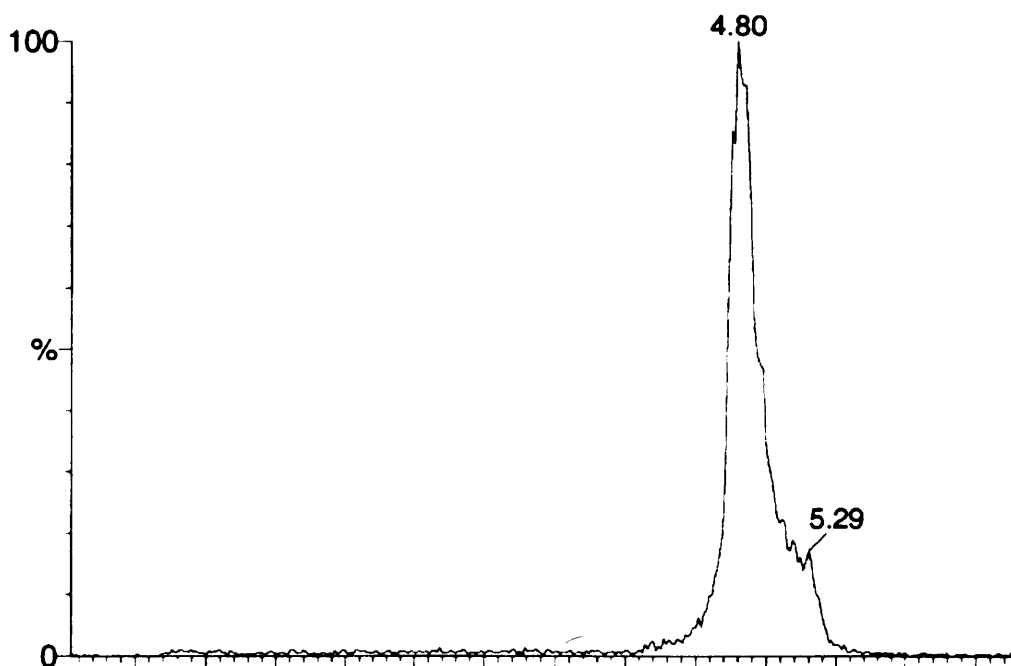


Figure 3.12: Retention time at 4.80 of Boc-phospho-L-serine methyl ester observed in the LC.

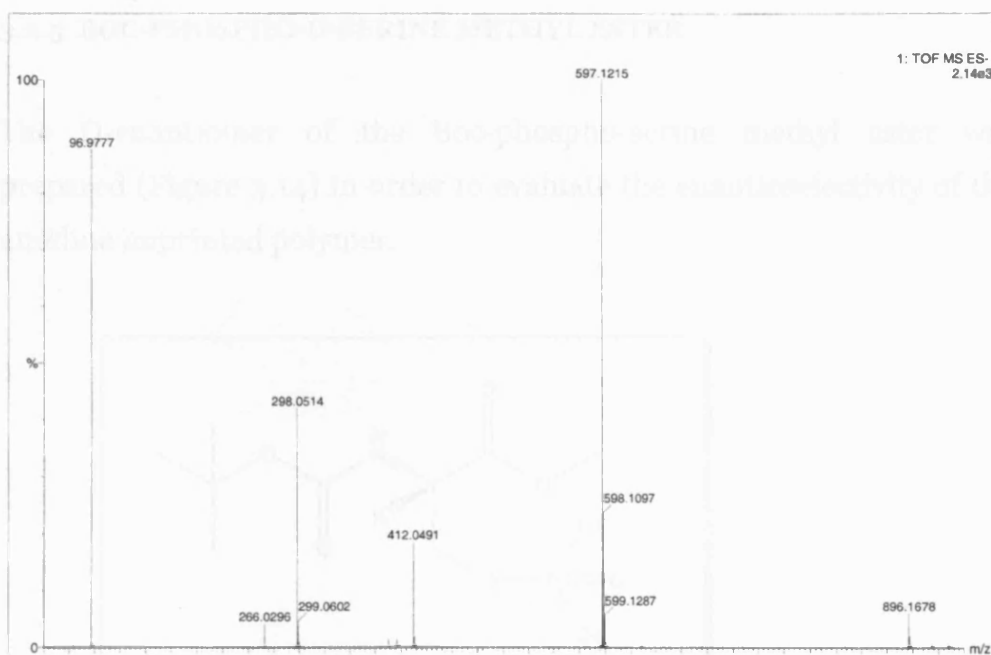


Figure 3.13: Mass spectrometry of Boc-phospho-L-serine methyl ester. Peak at 298 inherent to the template and at 597 and 896 inherent to the dimers.

3.3.1 SYNTHESIS OF THE D-ENANTIOMER

The phosphorylation of the Boc-D-serine methyl ester was carried out following the same procedure as for the L-enantiomer (section 3.2.2.6). However, as the Boc-D-serine methyl ester was not commercially available, the first step of the synthesis made entailed the reformation of the Boc-D-serine by addition of methyl iodide in presence of solid potassium carbonate. This reaction was followed by K_2CO_3 which showed after purification the presence of ester (MW 146) which was purified with 20% diisopropyl ether on 50% ethoxide on a 10% yield. The successful introduction of the methyl group was confirmed by the presence of a signal at about 3.6 ppm in the $^1\text{H-NMR}$ and a peak at 298 m/z in the mass spectrum. The Boc-D-serine methyl ester was quantitatively converted to Boc-phospho-D-serine methyl ester upon treatment with the N,N -diisopropyl-*tert*-butylbenzyl phosphoramidite and subsequent deprotection in presence of Pd(dppf)Cl $_2$.

3.2.5 BOC-PHOSPHO-D-SERINE METHYL ESTER

The D-enantiomer of the Boc-phospho-serine methyl ester was prepared (Figure 3.14) in order to evaluate the enantioselectivity of the amidine imprinted polymer.

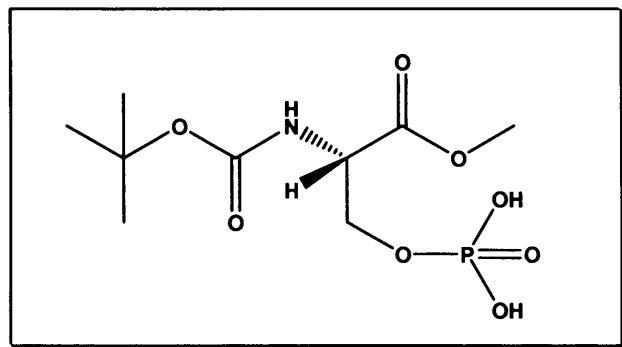
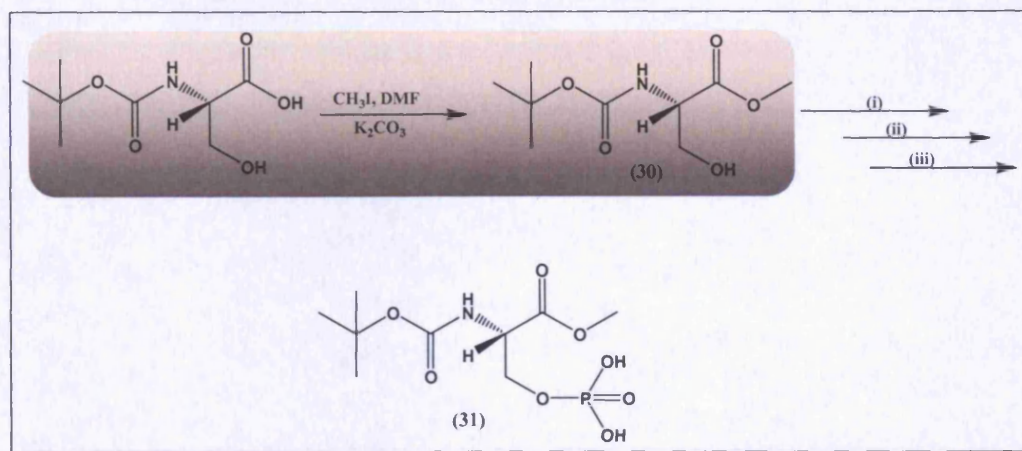


Figure 3.14: Structure of Boc-phospho-D-serine methyl ester.

3.2.5.1 SYNTHESIS OF THE D-ENANTIOMER

The phosphorylation of the Boc-D-serine methyl ester was carried out following the same procedure as the one employed for the L-enantiomer (section 3.2.2.6). However, as the Boc-D-serine methyl ester was not commercially available, the first step of the synthetic route entailed the esterification of the Boc-D-serine by addition of methyl iodide in presence of solid potassium carbonate. The reaction was followed by TLC which showed after one hour the clean formation of ester ($R_f = 0.38$ visualized with 20% phosphomolybdic acid in 80% ethanol) with 83% yield. The successful introduction of the methyl group was confirmed by the presence of a signal at about 3.2 ppm in the $^1\text{H-NMR}$ and a peak at 220 m/z in the mass spectrum. The Boc-D-serine methyl ester was quantitatively converted to Boc-phospho-D-serine methyl ester, upon treatment with the N,N-diisopropyl-bis-(4-chloro)-benzyl phosphoramidite and subsequent deprotection in presence of Palladium

as catalyst (section 3.2.3). The target compound was characterised by NMR and mass spectrometry, and was found to be pure and consistent with the expected structure.



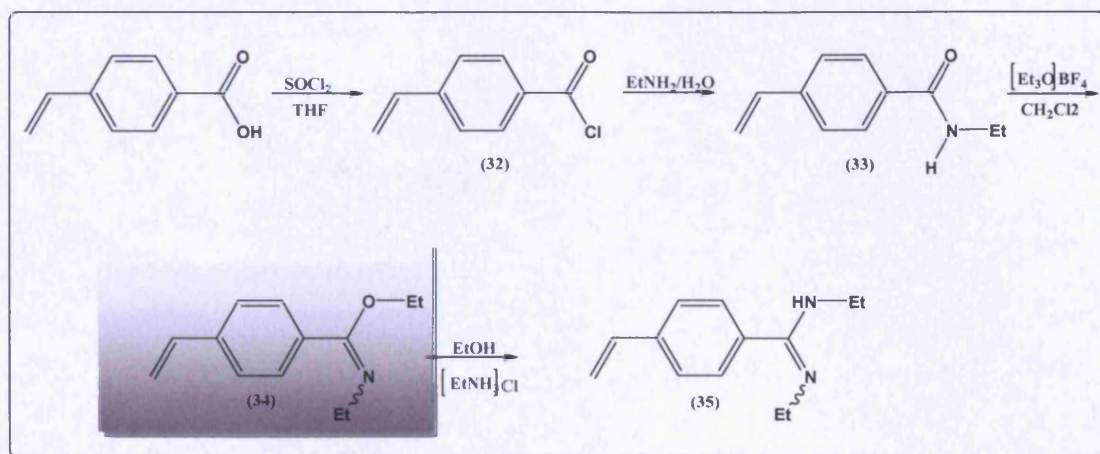
Scheme 3.10: Boc-D-serine esterification and phosphorylation.

Reagents and conditions: (i) *N,N'*-diisopropyl-bis-(4-chloro)-benzylphosphoramidite, 1H-tetrazole/MeCN; (ii) meta-chloroperbenzoic acid (MCPBA); (iii) Pd 10%, H₂O/*t*-BuOH.

3.3 SYNTHESIS OF THE *N,N'*-DIETHYL-4-VINYLBENZAMIDINE

In this study *N,N'*-diethyl-4-vinyl benzamide was used to stoichiometrically interact with the phosphate group of the template. It was already known that amidines form strong complexes with carboxylic acid, phosphonates and phosphates^{8,10}. However, systematic investigations have shown that unsubstituted amidines often form insoluble complexes with carboxylic acids. This drawback can be overcome by using *N,N'*-dialkylated benzamidines. Out of a large series of compounds *N,N'*-diethyl-4-vinyl benzamide had been shown to be the most favourable binding monomer, due to solubility even in non-polar solvents like chloroform and benzene⁸. Other investigations showed that the amidinium monomer forms complexes with carboxylic acid and phosphonic monoesters in acetonitrile with high association constants^{6,7}. In less polar solvents, like toluene, the association constant is even higher⁷. Therefore, *N,N'*-diethyl-4-vinyl benzamide represented a good candidate to bind Boc-phospho-serine methyl ester for a number of reasons: *N,N'*-disubstituted amidine is more soluble in non-polar organic solvents, it has a higher stability towards hydrolysis and aggregation through intermolecular hydrogen bonds is generally suppressed⁸. Moreover, the substituted amidine offers advantages in binding studies, particularly in non-polar solvents or if weak binding interactions are expected¹.

N,N'-diethyl-4-vinyl benzamide was synthesised using a 4 steps reaction starting from 4-vinyl benzoic acid⁵ (Scheme 3.11).



Scheme 3.11: Amidine synthesis.

Reaction of the 4-vinyl benzoic acid with SOCl_2 gave the acid chloride which was treated with aqueous ethylamine to obtain (33). The amidine was then converted to benzimidate (34) by treatment with triethyl oxonium tetrafluoroborate. Stirring with ethylamine hydrochloride produced the *N,N'*-diethyl-4-vinyl benzamidinium (35) in good yield. The synthesis was difficult to accomplish due to the presence of a secondary product, discovered after studying the integration of the proton peaks in the NMR of (34), formed by hydrolysis during extraction with ice-cold aqueous NaOH (6M) and ice-cold ether (Figure 3.15).

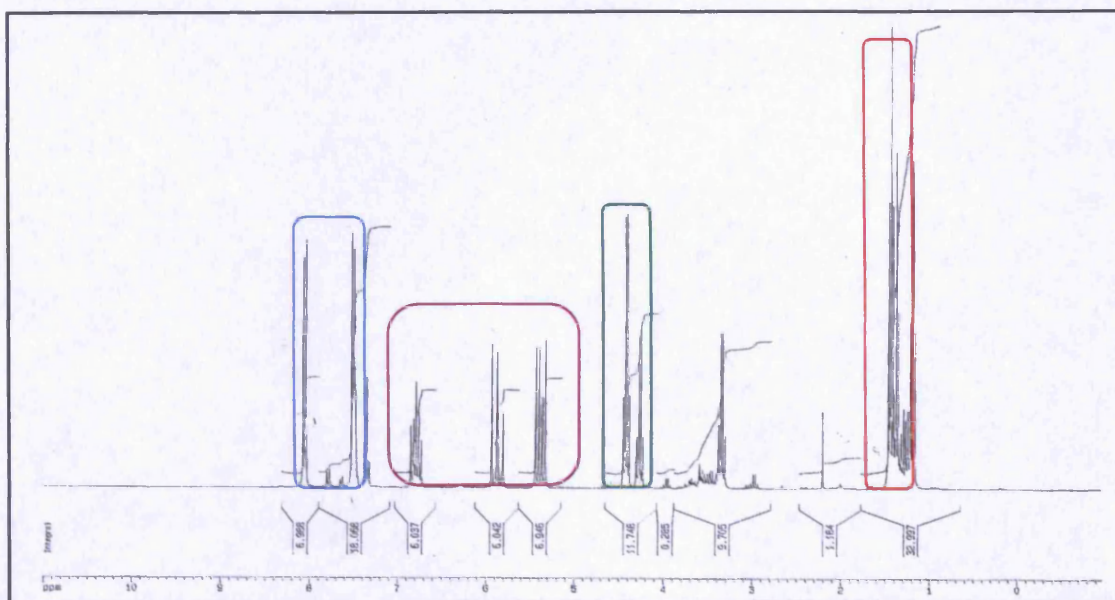
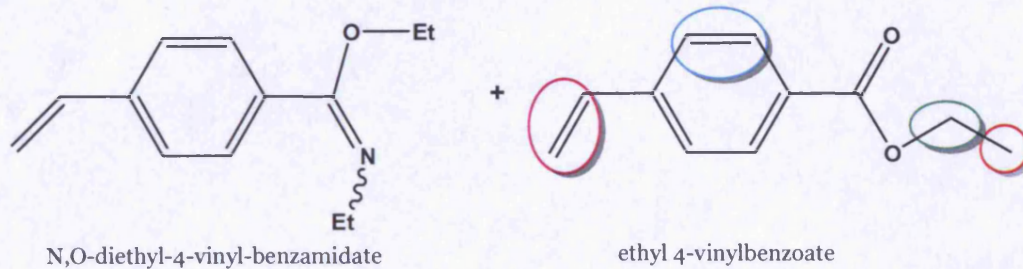


Figure 3.15: $^1\text{H-NMR}$ of N,O-diethyl-4-vinylbenzamidate and ethyl 4-vinyl benzoate.

The problem was overcome by extracting the residue using a weaker base. In this case this was achieved using ice-cold sodium bicarbonate and ice-cold ether. Proton NMR showed that under these conditions only the desired product was formed (Figure 3.16). A small amount of starting material was removed by distillation.

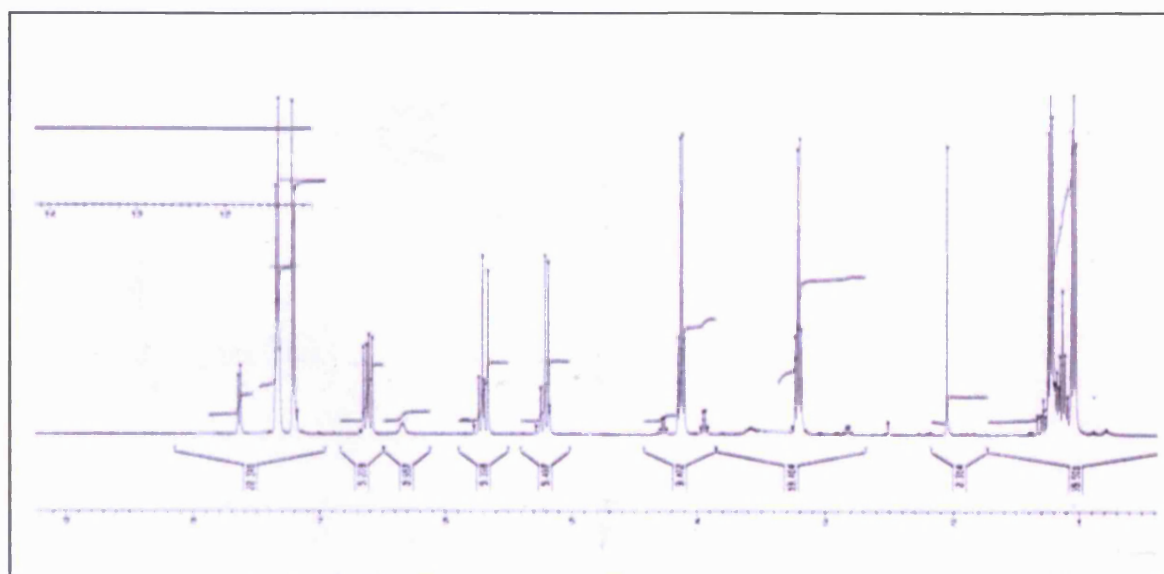
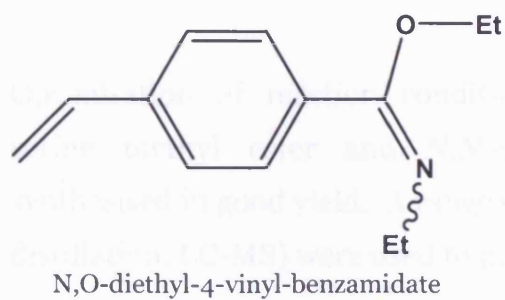


Figure 3.16: ¹H-NMR of N,O-diethyl-4-vinyl-benzamidate (**34**).

With 4 synthetic steps this method yielded *N,N'*-diethyl-4-vinyl benzamidine in 64%.

3.4 CONCLUSIONS

Optimisation of reaction conditions resulted in Boc-phospho-L/D-serine methyl ester and *N,N'*-diethyl-4-vinyl benzamidine being synthesised in good yield. A range of techniques (i.e. HPLC preparative, distillation, LC-MS) were used to purify the products.

BIBLIOGRAPHY

1. Jenkins, A.L. et al. (1999). "Polymer- based lanthanide luminescent sensor for detection of the hydrolysis product of the nerve agent Soman in water." Anal.Chem. **71**: 373-378.
2. Zi-Hui, M. and Qin, L. (2001). "Determination of degradation products of nerve agents in human serum by solid phase extraction using molecularly imprinting polymer." Analytica Chimica Acta **435**: 121-127.
3. Moller, K. et al. (2001). "Synthesis and evaluation of molecular imprinting polymers for extracting hydrolysis products of organophosphate flame retardants." Journal of Chromatography A **938**: 121-130.
4. Hall, A.J. et al. (2005). "Non-covalent imprinting of phosphorus esters." Analytica Chimica Acta **538**: 9-14.
5. Kraft, A. et al. (2002). "Hydrogen bonding between benzoic acid and an *N,N'*-diethyl-substituted benzamidine." Tetrahedron **58**: 3499-3505.
6. Wulff, G. and Shonfeld, R. (1998). "Polymerizable amidines-adhesion mediators and binding sites for molecular imprinting." Advanced Materials **10**: 957-959.
7. Wulff, G. et al. (1997). "Enzyme models based on molecularly imprinted polymers with strong esterase activity." Angew.Chem.Int.Ed.Engl. **18**: 1962-1964.
8. Strikovskiy, A.G. et al. (2000). "Catalytic molecularly imprinted polymers using conventional bulk polymerization or suspension polymerization: selective hydrolysis of diphenyl carbonate and diphenyl carbamate." J.Am.Chem.Soc. **122**: 6295-6296.
9. Jong-Man, K. et al. (2001). "Cholesterol esterase activity of a molecularly imprinted polymer." Macromol.Chem.Phys. **202**: 1105-1108.
10. Wulff, G. et al. (1998). "Molecular imprinting for the preparation of enzyme-analogous polymers." American Chemical Society: 10-28
11. Nopper, D. et al. (2003). "Amidine-based molecularly imprinted polymers- new sensitive elements for chiral chemosensors." Anal.Bioanal.Chem. **377**: 608-613.
12. Stowell, J.K. and Widlanski, T.S. (1995). "A new method for the phosphorylation of alcohols and phenols." Tetrahedron Letters **36**: 1825-1826.
13. McKenna, C.E. et al. (1977). "The facile dealkylation of phosphonic acid dialkyl esters by bromotrimethylsilane." Tetrahedron Letters **2**: 155-158.
14. Hughes, J.L. and Leopold, E.J. (1993). "Cleavage and deprotection of peptides from MBHA-resin with bromotrimethylsilane." Tetrahedron Letters **34**: 7713-7716.
15. Chojnowski, J. et al. (1978). "The selective displacement of O-Alkyl by trialkylsilyl in some derivatives of acids of phosphorus." Chem.Comm.: 777-778.
16. De Bont, H.B.A. et al. (1990). Recl.Trav.Chim.Pays-Bas **109**: 27-28.

17. Perich, J.W. and Johns, R.B. (1988). "Di-t-butyl N,N'-diethylphosphoramidate and dibenzyl N,N'-diethylphosphoramidate. Highly reactive reagents for the "phosphite-triester" phosphorylation of serine containing peptides." Tetrahedron Letters **29**(119): 2369-2372.
18. Perich, J.W. et al. (1986). "Solution-phase synthesis of an O-phosphoseryl-containing peptide using phenyl phosphotriester protection." Tetrahedron Letters **27**(12): 1373-1376.
19. Bannwarth, W. and Trzeciak, A. (1987). "A simple and effective chemical phosphorylation procedure for biomolecules." Helvetica Chimica Acta **70**.
20. Alewood, P.F. et al. (1984). "Preparation of N-(t-butoxycarbonyl)-O-(dibenzylphosphono)-L-serine." Aust.J.Chem. **37**: 429-433.

Chapter 4

Virtual analysis

Conformational analysis was used to identify the “preferred” conformation of the functional monomer, *N,N'*-diethyl-4-vinyl benzamidine, capable of interacting with the template molecule. The process involved the analysis of two conformers of the functional monomer, containing functional groups able to interact with the template by means of hydrogen bonds. The use of conformational analysis showed which isomer would present a stronger interaction with the template creating specific and strong binding sites.

4.1 MOLECULAR MECHANIC-THEORY

Conformational analysis is the study of molecular conformations and the effect that these have on the properties of the molecule. A set of molecular conformations is conventionally defined as those arrangements of atoms in space that can be inter-converted purely by rotation about single bonds (i.e. modifying torsion angles)¹. This definition is usually relaxed in recognition of the fact that small distortions in bond angles and bond lengths often accompany conformational changes¹. The objective of a conformational search is to identify the preferred conformations of a molecule and this is achieved by identification of conformers that present minima on the energy surface. Energy minimisation methods therefore play a crucial role in conformational analysis². The energy values calculated from molecular mechanics, however, cannot be considered as absolute physical quantities, but only as relative values to compare the energies of different conformations having the same connectivity, i.e. the same structure/complex or different complexes². In fact, molecular mechanic

energies have no meaning as absolute quantities and only comparison between different energy values, between two or more conformations, have meaning². Equation 4.1 is a simple equation used to determine energy in molecular mechanics calculations. The components of this energy are explained in Figure 4.1.

$$\text{Energy (E)} = E_{\text{stretch}} + E_{\text{bending}} + E_{\text{torsion}} + E_{\text{non-bonded interactions}} \quad \text{Eq. 4.1}$$

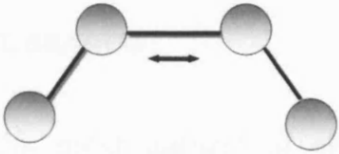
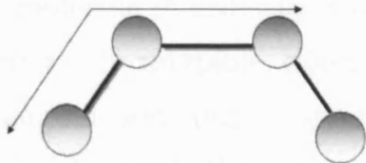
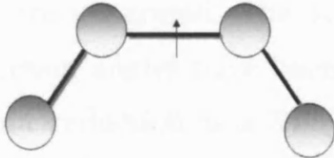
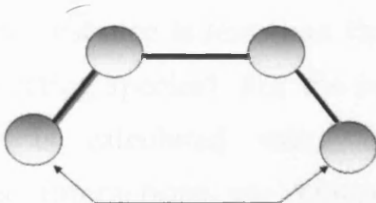
Stretching Energy	
Bending Energy	
Torsion Energy	
Non bonded Energy	

Figure 4.1: Molecular mechanic force fields include (i) stretching energy; (ii) bending energy; (iii) torsion energy; (iv) non bonded energy, which accounts for repulsion, van der Waals attraction and electrostatic interactions.

Solvation effects may also be important, and various schemes are now available for calculating the solvation free energy of a conformation, which can be added to the intramolecular energy³. Conformational search methods can be divided into the following categories:

- Systematic search
- Monte Carlo or random approach
- Stochastic method

4.1.2 SYSTEMATIC CONFORMATIONAL SEARCH

The systematic search is perhaps the most natural of all different conformational analysis methods. It is performed by systematically varying each of the torsion angles of a molecule in order to cover a vast range of possible conformations². First, all rotatable bonds in the molecule are identified. The bond lengths and angles remain fixed throughout the calculation. Each of these bonds is then systematically rotated through 360° using a fixed increment. That means, during a full rotation of 360°, 12 conformations are generated. The search stops when all possible combinations of torsion angles have been generated and minimised. The first step in data reduction is a Van der Waals screening or, “bump check”. This is performed before the potential energy of the conformations is determined. The screening procedure excludes all conformations where any distance is less than the sum of the Van der Waals radii of the interacting species³. For the remaining conformers, the potential energy is calculated using molecular mechanics. In general, electrostatic interactions are ignored when calculating conformational energy, i.e. charges are not taken into account and the conformational analysis is performed *in vacuo*⁴. If the inclusion of electrostatic interactions into a conformational analysis is justified for a special case, then the whole process becomes much more complex.

When the conformational energies have been calculated for the remaining conformers, it is useful to further reduce the number of conformations by using an energy window⁴. This process removes conformations with energy significantly higher than those with energies close to the minimum. The value for this energy window depends on the size of the studied molecule as well as on the applied force field⁵.

Those conformations not excluded by the filtering steps, represent a complete ensemble of energetically accessible conformations for a particular molecule. An advantage of the systematic search is that the resulting set of conformers will contain most or all of the local minima⁵.

4.1.3 MONTE CARLO METHODS OR RANDOM SEARCH

In the Monte Carlo method, changes are assigned to the system by randomly modifying a few degrees of freedom at a time; the atoms are moved truly randomly, not deterministically².

A random search starts with an initial conformation, which is minimised with respect to the energy. An arbitrary number of torsional angles from the initial conformation are chosen and are varied by a random amount. The resulting conformation is minimized using molecular mechanics and the randomization process is carried out by using a criterion based on the energy to retain or discard this move⁵. If retained, the process is continued; if discarded, the process is restarted. The minimized conformation is then compared with the previously generated structures and, if there is no match to previously acquire minima, it is stored as a unique⁵. The process restarts again by randomly varying the torsion angles of a minimised structure and it continues until a set of low energy conformers has been generated a certain number of times⁵. The main advantage of random search methods is that, in principle molecules of any size can be successfully



treated. In practice, however, highly flexible molecules often do not give converging results, because the volume of the respective conformational space is too large³. Other useful applications for Monte Carlo search methods include investigation on cyclic systems, because ring systems in general are difficult to treat in systematic searches³.

4.1.4 STOCHASTIC CONFORMATIONAL SEARCH

The stochastic conformational search method is based upon random rotations of bonds (including ring bonds) and generates conformations by sampling local minima of the potential energy surface¹. In our study, we were especially interested in minimum points on the energy surface. Minimum energy arrangements of the atoms correspond to stable states of the system; any movement away from a minimum gives a configuration with a higher energy. There may be a very large number of minima on the energy surface. The minimum with the very lowest energy is known as the global energy minimum (Figure 4.2).

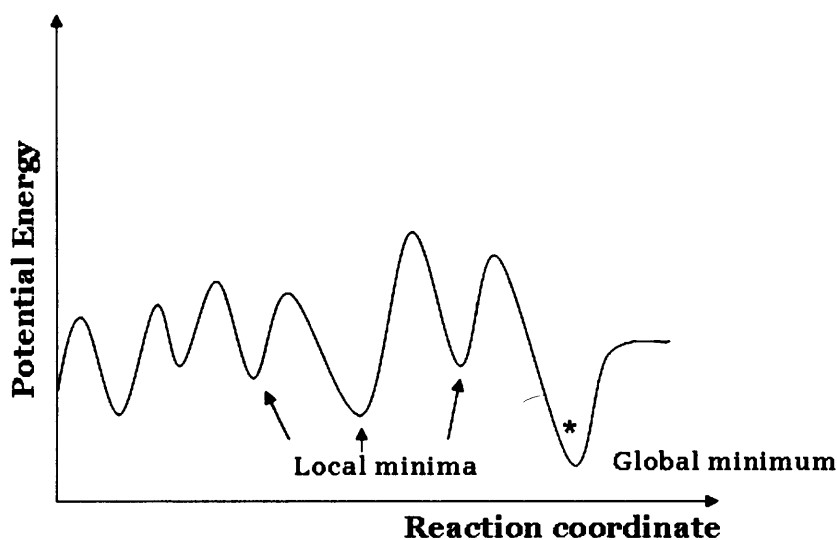


Figure 4.2: Plot of molecular conformations vs potential energy.

Unlike the systematic search, the minimization step inherent to the stochastic conformational search simulation cannot locate conformers that do not lie at potential energy minima⁶.

However, the stochastic search is a fast and powerful method for locating conformational minima for large flexible systems (ring and chains) and for those containing multiple chiral centres. The Stochastic conformational search algorithm proceeds as follows⁶:

1. Initialise the conformer list identifying all rotation bonds.
2. Rotate all rotation bonds (including ring bonds) to random dihedral angles (possibly biased towards certain multiples of 30 or 60 degrees).
3. Energy minimize the resulting conformation in dihedral angle space; that is, minimize energy by rotating bonds without changing bond lengths or angles.
4. Check the resulting conformation in order to determine if it had already been generated by comparing all atom positions using a predefined root-mean-square (RMS) tolerance. If the atom positions are within the RMS tolerance, discard the current conformation and increment the failure count; if no duplicate was found, put the current conformation into the list and set the failure count to zero.
5. When the number of failures to find new conformations exceeded 10.000 in a row, then stop.
6. Return to step 2.

4.2 CONFORMATIONAL STUDY OF AMIDINE ISOMERS

4.2.1 INTRODUCTION

N,N'-diethyl-4-vinyl benzamidine can exist in three conformations with an (E,E/cis), an (E,Z/trans) or a (Z,Z/cis inverted) stereochemistry at the partial C-N double bond (Figure 4.3).

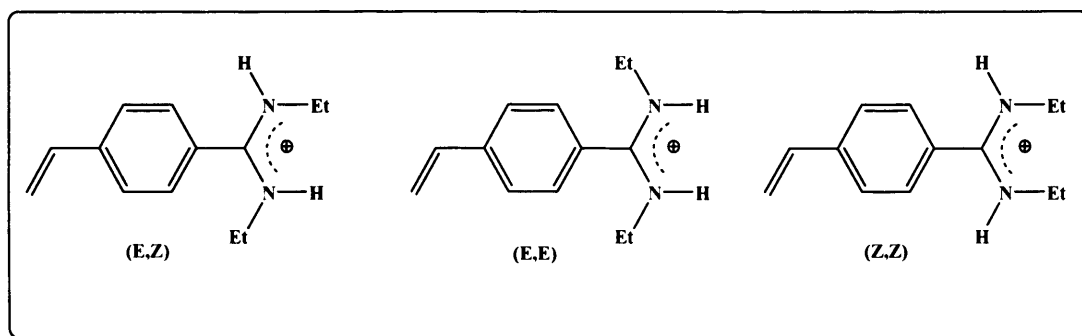


Figure 4.3: Conformers of *N,N'*-diethyl-4-vinyl benzamidine.

Since different conformations represent varying distances between the atoms or group rotating about the bond, and these distances determine the amount and type of interaction between adjacent atoms or groups, different conformations may represent different potential energies of the molecule. Therefore, our investigation aimed to study and identify the conformation which has the lowest energy.

4.2.2 METHODS

All calculations were carried out using the Molecular Operating Environment (MOE) program suite (version 2001.01, Chemical Computing Group Inc., Montreal, Canada). Conformational searches were performed using the stochastic approach, where all bonds included ring and side-group bonds were allowed to rotate randomly and simultaneously to generate new molecular conformations that were energetically evaluated. The calculations were initially run on the amidine in absence of template. The structure was minimised in order to find a set of atomic coordinates that corresponded to a local minimum of the molecular energy function. The same experiment was then repeated in presence of the Boc-phospho-L-serine methyl ester. Before running the conformational analysis, the two structures were minimised; the monomer was subsequently left free to rotate around the immobilised template in order to find the best (lowest energy) binding orientation of the amidine to the phosphate group.

4.2.3 RESULTS AND DISCUSSION

The results of the experiment showed that, when the search was performed in absence of the template, the E,Z/trans conformer was more stable, had a lower energy, than the E,E/cis conformer for both steric and electronic reasons. The E,E conformation also showed to have the highest energy and this value was even higher than the Z,Z form which represents the cis inverted conformation (Figure 4.4).

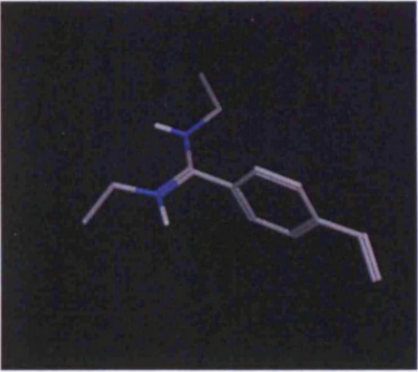
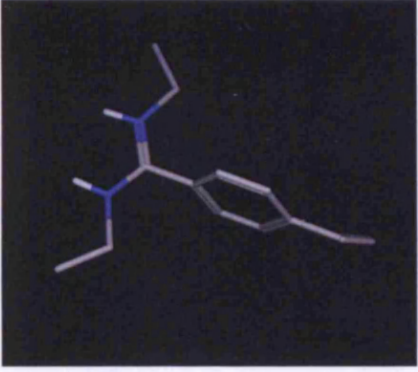
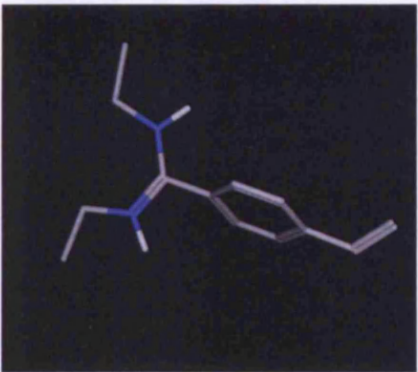
Molecule	E (Kcal mol ⁻¹)
	19.194033
(E,Z)	
	21.545439
(E,E)	
	20.601625
(Z,Z)	

Figure 4.4: Generated conformations and conformation energies.

When the template, Boc-phospho-L-serine methyl ester, was included in the analysis, a different result was observed due to the fact that not only the minimum-energy conformation of the single molecule had to be taken in consideration, but also the energy of the system. This time, the E,E conformer was found to have the lowest energy value, resulting to be the most favourable form to interact with the phosphate group through the formation of two hydrogen bonds (Figure 4.5).

In addition, the model suggested that when the E,E/cis form of the monomer interacted with the template, it was likely that an additional H bond was formed between the NH group of the serine and the third oxygen of the phosphate group (Figure 4.5).

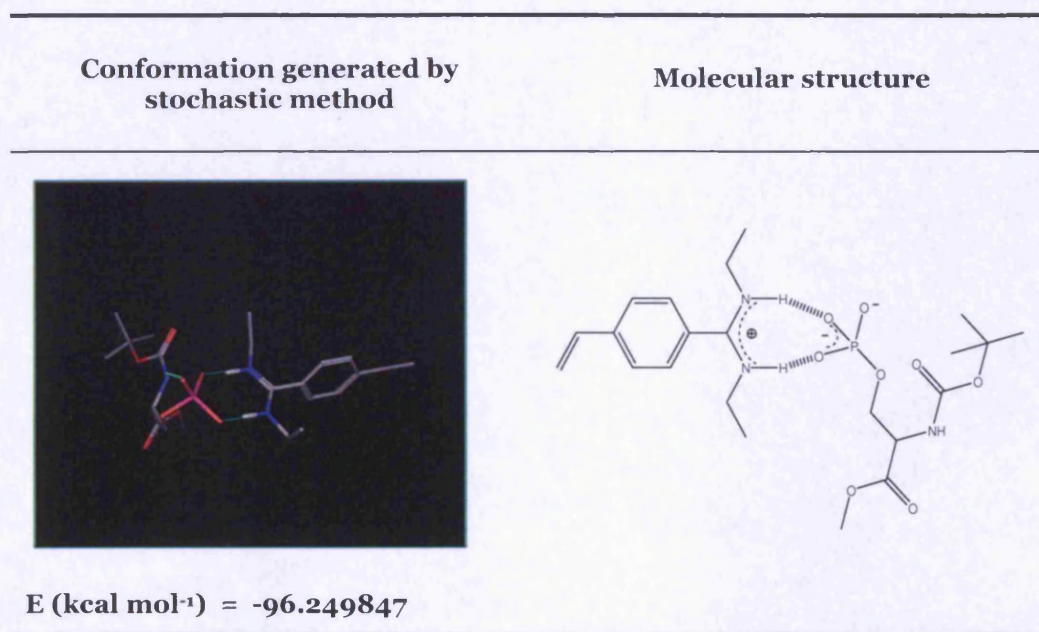


Figure 4.5: Conformation energy and molecular structure of (E,E)-N,N'-diethyl-4-vinyl benzamidine and Boc-phospho-L-serine methyl ester complex

In contrast, it was found that the link between the E,Z monomer and the template was possible through the formation of just one hydrogen bond and the complex had a higher energy value than that of the E,E-complex (Figure 4.6).

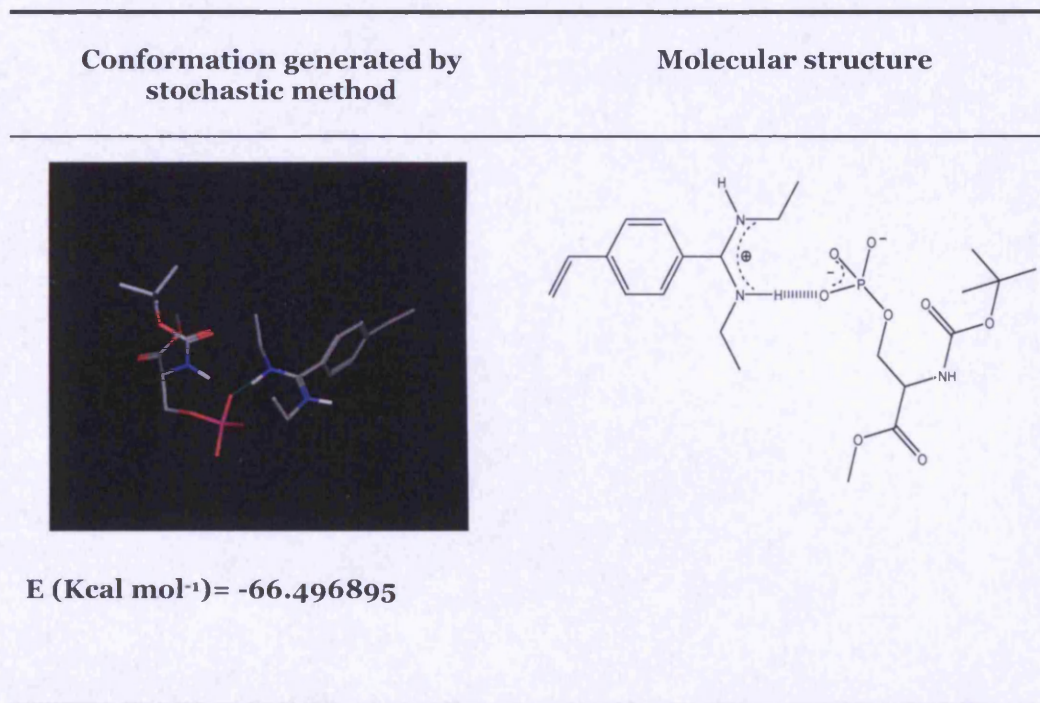


Figure 4.6: Conformation energy and molecular structure of (E,Z)-N,N'-diethyl-4-vinyl benzamidine and Boc-phospho-L-serine methyl ester complex.

4.2.4 CONCLUSION

Although in absence of template it was found that the E,Z conformer had the lowest energy, when the same experiment was run in presence of Boc-phospho-L-serine methyl ester, it was observed that the E,E conformer of the amidine showed the lowest energy value. This is summarised in figure 4.7.

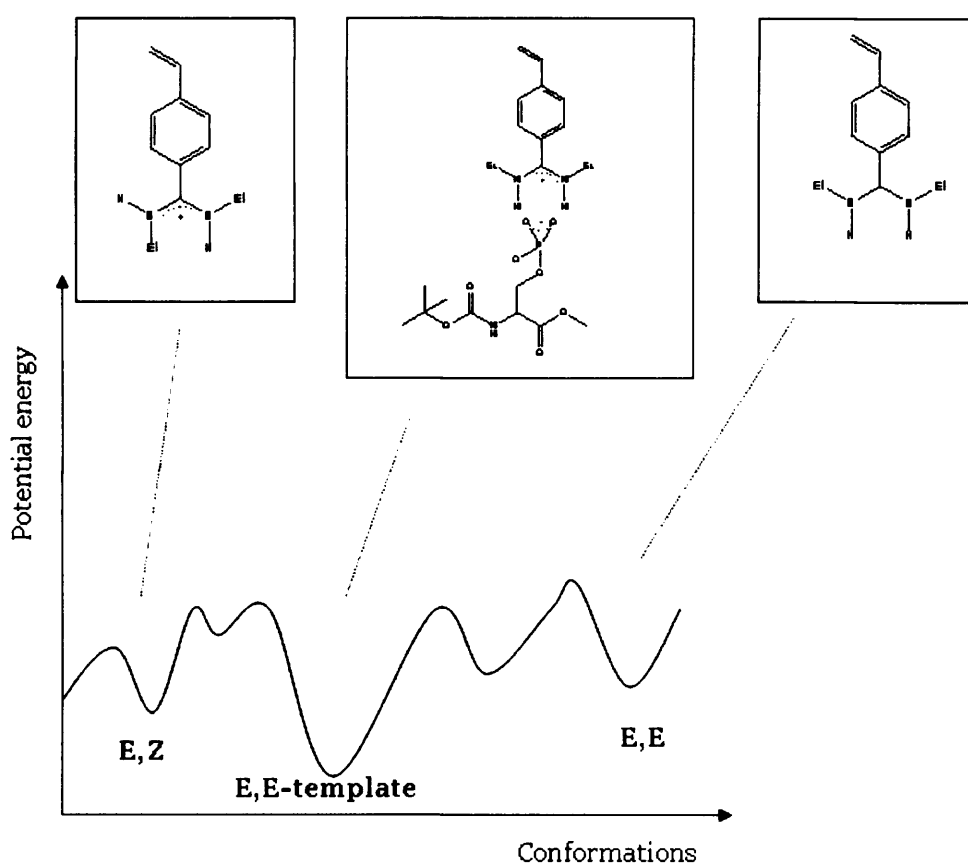


Figure 4.7: Potential energies of (E,E) and (E,Z) conformers of the amidine in absence of template and the preferential conformation (E,E) which bound the phosphate group of the Boc-L-serine methyl ester.

4.3 MOLECULAR DYNAMICS

4.3.1 INTRODUCTION

The previous studies of conformational analysis were performed *in vacuo*. The next step of this investigation regarded the modelling of the syn/anti monomer-template complex in presence of solvent and introducing temperature effects.

4.3.2 PRINCIPLES

A very common strategy to achieve this objective is the use of molecular dynamic simulations to explore conformational space. In general, molecular dynamic simulations are described as deterministic since given a set of initial coordinates and velocities with a force ($F(r)$) the evolution of the system is determined⁷.

The potential energy surface used in molecular dynamics is based on molecular mechanic models. It is, therefore, assumed that the atoms in the molecule interact with each other according to the rules of the employed force field⁷. The classical equations of motion, in molecular dynamics simulation, given by Newton's second law are solved (Equation 4.2):

$$\boxed{F_i(t) = m_i a_i(t)} \quad \text{Eq.4.2}$$

Where F_i is the force on atom i at time t , m_i is the mass of atom i , and a_i is the acceleration of atom i at time t .

As mentioned in section 4.1, the force field for a typical compound can be given as a sum of the various components including bond stretching and bending, torsional potentials, and non-bonded interactions. It is possible to calculate the forces between the atoms by taking the

derivative of the potential $V(r)$ given by the force fields⁸; this derivative can be used in the context of Newton's equation of motion (Equation 4.3):

$$m_i r_i = F_i = \Delta r_i V(r)$$

Eq.4.3

Here, the gradient of the potential energy function is used to calculate the forces on the atoms while the initial velocities on the atoms are generated randomly at the beginning of the dynamics run. Based on the initial atom with coordinates of the system, new atomic positions and velocities on the atoms can be predicted at time t and the atoms will be moved to these new positions⁷. As a result of this, a new conformation is created and this cycle will be iterated for a predefined number of time steps. In fact, molecular dynamic has no defined point of termination other than the amount of time that can be practically covered⁸.

4.3.3 METHOD

In this study, a molecular dynamics simulation in water was performed on the template-monomer complex using different starting conformations and a temperature (T) of 298° K. The experiment was carried out keeping the number of moles, T and the volume of the box containing the structures constant. The simulation was stopped when the total energy during the molecular dynamics runs appeared to be equilibrated and showed no further tendency to drift.

4.3.4 RESULTS

The results of these experiments showed once again that the E,E/cis conformer of the N,N'-diethyl-4-vinyl-benzamidine was the preferred form to interact with the phosphate group due to its lowest energy

compared to the higher value energy of the trans-template complex (Figure 4.8).

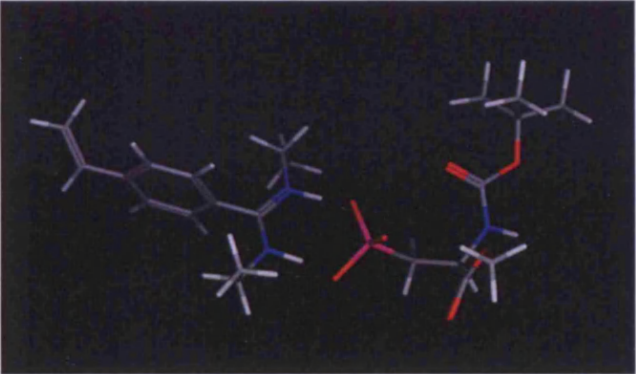
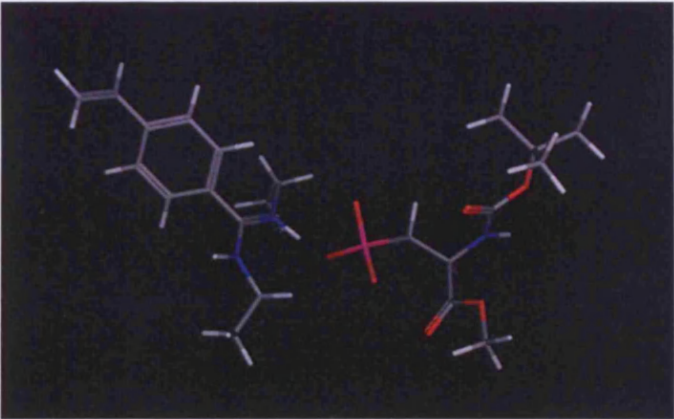
Molecule	U (Kcal/mol ⁻¹)
	-6928,8
(<i>E,E</i>) monomer-template complex	
	-6836,3
(<i>E,Z</i>) monomer-template complex	

Figure 4.8: Binding energies for *N,N'*-diethyl-4-vinyl benzamidine-Boc-phospho-L-serine methyl ester.

4.4 NMR SPECTROSCOPY

4.4.1 INTRODUCTION

The conformational behaviour of *N,N'*-diethyl-4-vinyl benzamidine was explored using a combination of molecular dynamics simulations and a range of NMR experiments. NMR studies were performed in order to distinguish between the different conformers of the amidine and to determine which was the major conformation in the presence of the template. It was observed that the different isomers could be easily differentiated by NMR depending on the temperature, on the solvent and on the presence of a coordinating counter-ion.

4.4.2 METHODS

NMR spectra were acquired on Bruker Avance 500 MHz, topspin 1.3.

The NMR measurements were recorded at different temperatures from 25°C to -32°C in CDCl₃ to isolate the two configurations (cis/trans) of the amidine.

¹H NMR experiments for *N,N'*-diethyl-4-vinyl benzamidine and Boc-phospho-L-serine methyl ester were performed using a host-guest ratio of 2:1 equivalents in protic solvents, MeOD and D₂O, and aprotic solvent DMSO.

4.4.3 RESULTS AND DISCUSSION

The main aim of this study was to correlate the information obtained by molecular simulations with that obtained by NMR in order to improve the accuracy of structural prediction. The realisation consisted of two approaches: (i) ¹H-NMR of the benzamidine at different temperatures;

(ii) $^1\text{H-NMR}$ of the benzamidine in presence of different counter ions (HCl and template) and different solvents.

4.4.3.1 NMR OF AMIDINE AT DIFFERENT TEMPERATURES

The $^1\text{H-NMR}$ of the amidine species was initially performed in CDCl_3 at room temperature. Two different triplet and quartet signals for both N -ethyl substituents were predicted (Figure 4.9); however, only the presence of two broad peaks at ~ 1.19 ppm and at ~ 3.30 ppm were observed due to the rapid interconversion of a conformer of the amidine into the other at room temperature (Figure 4.10).

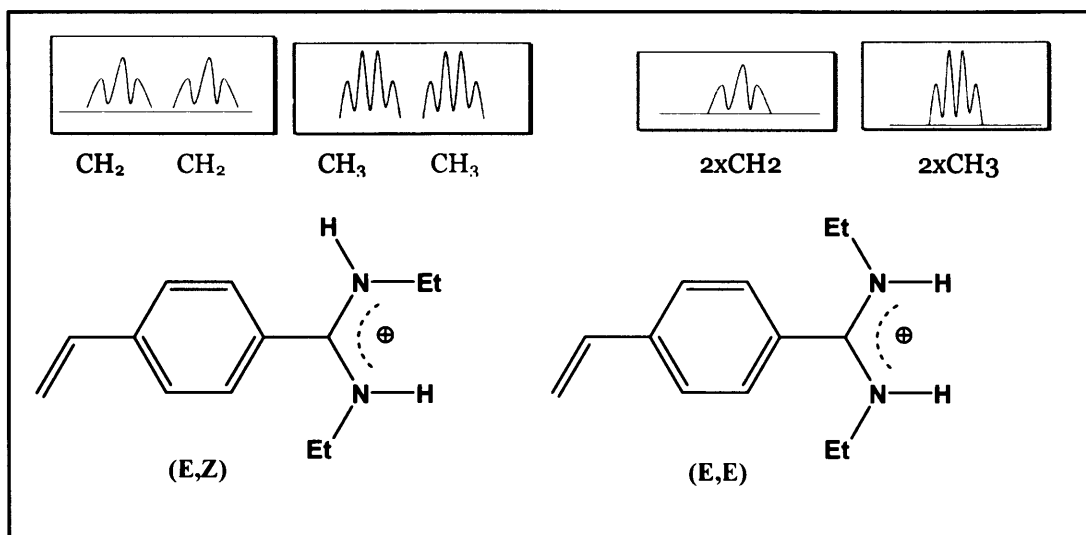


Figure 4.9: Predicted chemical shifts for the N -ethyl groups of the E,E and E,Z isomers.

Therefore, these initial NMR studies showed that a dynamic equilibrium between (E,E) and (E,Z) conformational isomers is frequently observed for N,N' -diethyl-4-vinyl benzamidine.

Subsequently, additional NMR experiments were carried out at different temperatures in an attempt to freeze and isolate the different isomers of the amidine. The results of this studies showed that starting from $T = -14^\circ\text{C}$, two different peaks for the CH_2 and two peaks for the

CH₃ of the N-ethyl groups were observed (Figure 4.11), indicating the prevalence of the E,Z/trans form of the amidine and suggesting that the rapid interconversion of the two conformers is controlled by temperature.

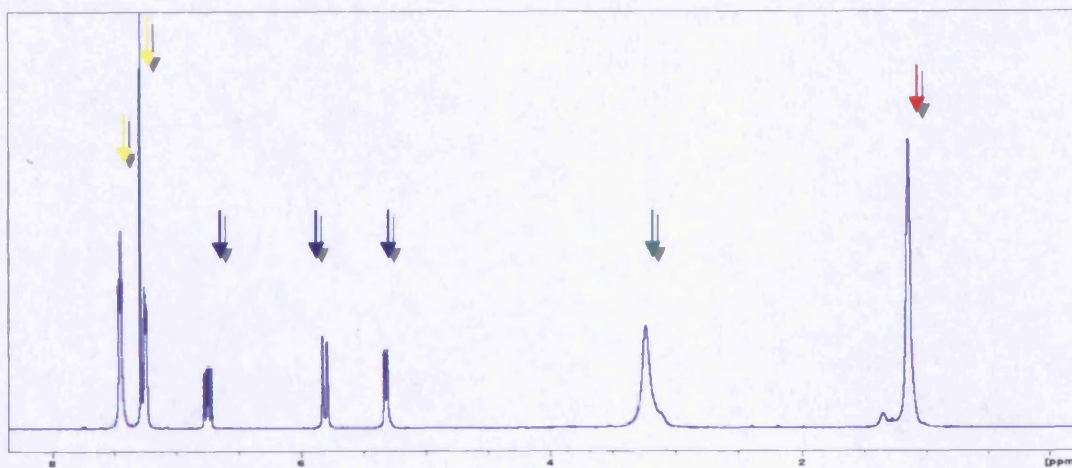
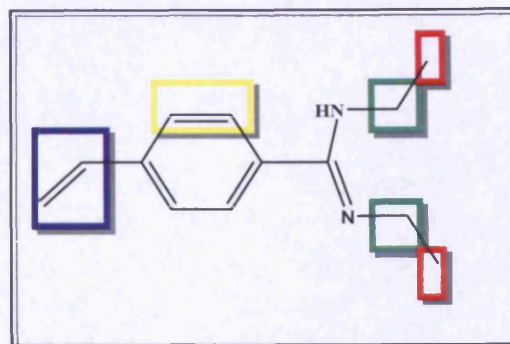


Figure 4.10: ¹H-NMR of *N,N'*-diethyl-4-vinyl benzamidinium in CDCl₃.

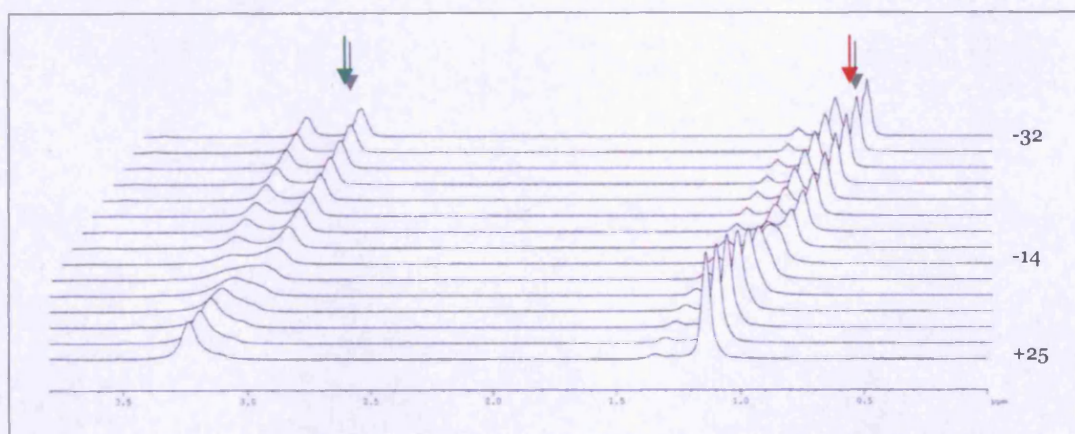


Figure 4.11: ¹H-NMR of *N,N'*-diethyl-4-vinyl benzamidinium in CDCl₃ at different temperatures. Signals at ~1.19 ppm and at ~ 3.30 ppm are inherent to the CH₃ and CH₂ of the two *N*-ethyl groups.

4.4.3.2 NMR STUDIES OF THE AMIDINE IN PRESENCE OF DIFFERENT COUNTER IONS AND SOLVENTS

In order to study the conformational behaviour of the amidine in presence of the template, ^1H -NMR experiments were performed using weak ligand (hydrochloride) and strong ligand (Boc-phospho-L-serine methyl ester).

The spectrum of the benzamidinium salt, prepared from the reaction with the hydrochloride, showed two sets of signals for the N-ethyl substituents indicating that the amidine existed exclusively as the (E,Z) isomer (Figure 4.12). In fact, in presence of a non-coordinating counterion, the amidine prefers the E,Z isomer in DMSO- d_6 , most likely for steric reason.

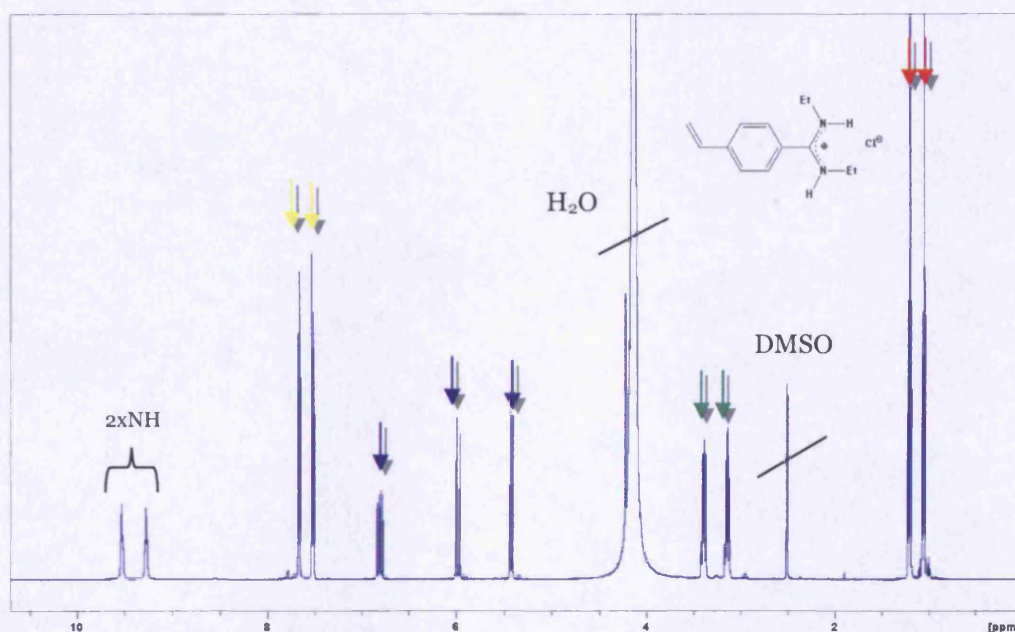


Figure 4.12: ^1H -NMR of amidinium chloride in DMSO.

When the same experiment was run in presence of Boc-phospho-L-serine methyl ester, it was observed that the two ethyl groups gave a

single set of $^1\text{H-NMR}$ signals. Both N-ethyl substituents produced a triplet and quartet indicative of an exclusively (E,E)-configured amidine, which was a consequence of strong binding interactions between the amidine and the phosphate.

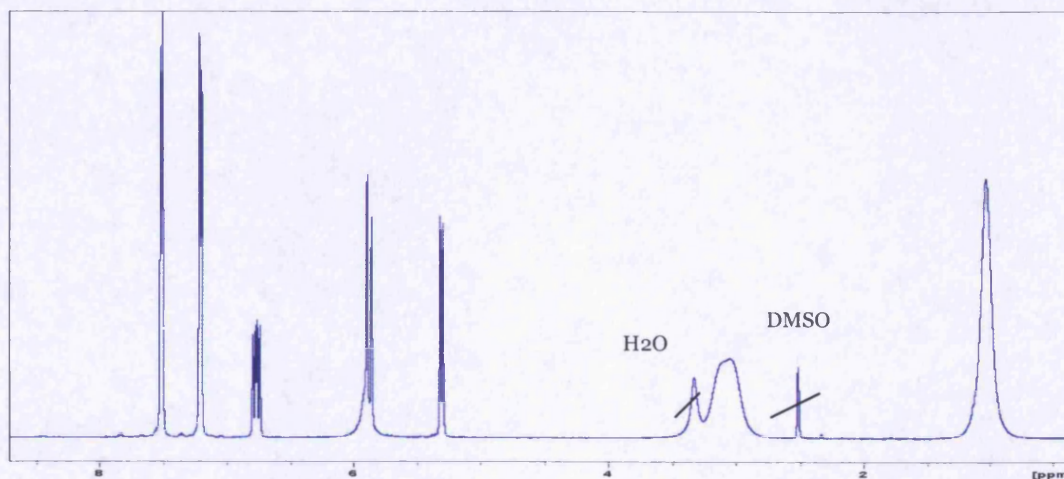


Figure 4.13: $^1\text{H-NMR}$ of amidine in DMSO.

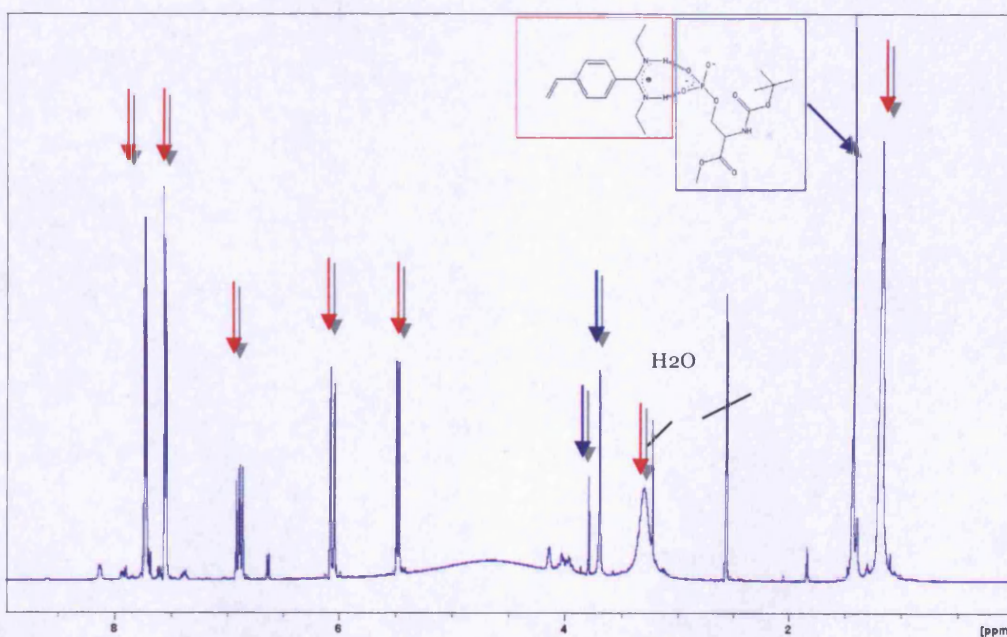


Figure 4.14: $^1\text{H-NMR}$ of monomer-template complex in DMSO.

However, the prevalence of one conformer with respect to the other was seen to depend not only on the type of counter ion, but also on the nature of the solvent employed. In fact, when the same experiment with the template was performed in presence of more protic solvents, like MeOH and H₂O, no complexation was observed so that the thermodynamically more stable (E,Z)-configured amidine prevailed under these conditions, which was confirmed by the presence of two different signals for both N-ethyl groups (Figure 4.15).

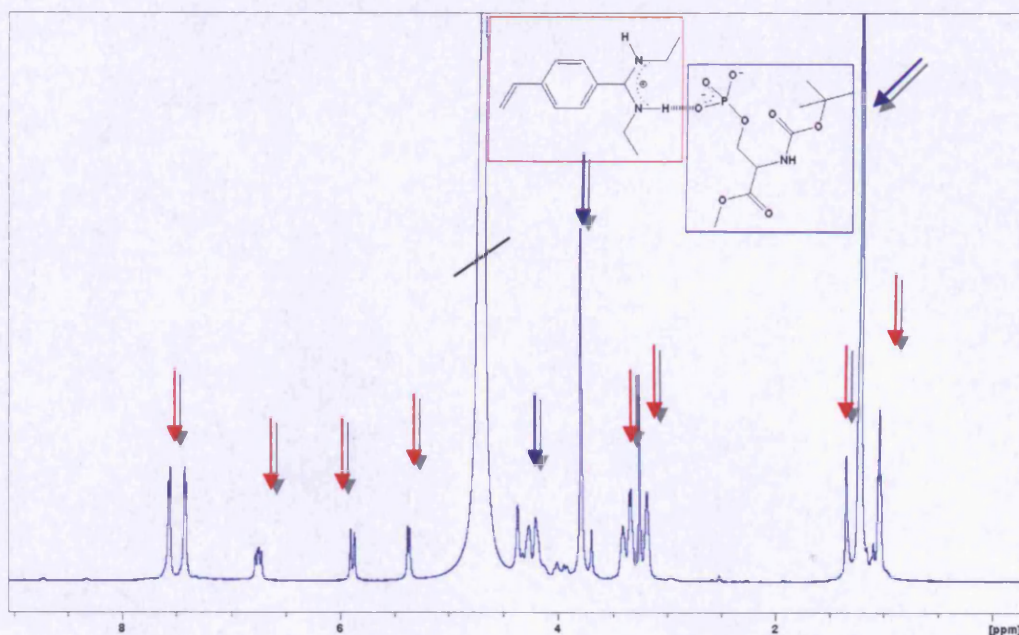


Figure 4.15: ¹H-NMR of template-monomer complex in D₂O.

4.4.4 CONCLUSIONS

The two isomeric forms of the amidine were isolated by freezing the compound at -14°C .

N,N'-diethyl-4-vinyl benzamidine was seen to form strong complexes with the phosphate serine in aprotic solvents such as dimethylsulfoxide. Additional NMR studies showed that only strong ligands, such as the phosphate group, were obviously able to force the *N,N'*-diethyl-substituted amidine into an (E,E) configuration. In contrast, the (E,Z) isomer was dominant in presence of weakly binding ligands (hydrochloride) that cannot bind to the amidine through two hydrogen bonds.

4.5 FURTHER DISCUSSION

The stochastic conformational search was used successfully to model the amidine since it accurately identified the lowest energy conformations in presence and in absence of template. This “global minimum” agrees with the conformation of amidine deduced experimentally in solution by NMR analysis.

The prevalence of the complex formation between the (E,E) isomer and the Boc-phospho-L-serine methyl ester, provided by molecular mechanics calculations in presence of water molecules, was indicative of a even stronger host-guest interaction during the polymerisation process, where the shielding effect due to the presence of water was absent. This hypothesis was confirmed by the experiments of ^1H -NMR in DMSO, where the aprotic nature of the solvent favoured the formation of two hydrogen bonds between the monomer and the template.

BIBLIOGRAPHY

1. Leach, A.R. "Molecular Modelling: Principles and Applications".
2. Holtje, H-D and Folkers, G. "Molecular modelling: Basic Principles and Applications".
3. MOE manual.
4. Allinger, N. L. et al (1989). "Molecular mechanics. The MM3 force field for hydrocarbons." J. Am.Chem.Soc. **111**: 8551-8566.
5. Burkert, U. and Allinger, N.L. (1982). Molecular Mechanics. Washington, American Chemical Society.
6. Hirst, D. (1990). A computational approach to chemistry. Oxford, Blackwell scientific publications.
7. Rapaport, D. (2004). The art of molecular dynamic simulation.
8. Lagona, A. (2001). Reaction and molecular dynamics.

Chapter 5

Preparation and characterisation of Boc-phospho-L-serine methyl ester molecularly imprinted polymer

5.1 INTRODUCTION

5.1.1 POLYMER AND POLYMERISATION

The term “polymer” derives from the Greek words: *polys* meaning *many* and *meros* meaning *parts*, and is used to describe a high molecular weight compound that has been formed by combining many smaller units. Paul Flory¹ states that “... perhaps the most significant structural characteristic of a long polymer chain is its capacity to assume an enormous array of configurations”. This means that the key feature which distinguishes polymers from other compounds is the repetition of many identical, similar, or complementary molecular subunits called monomers, linked by covalent, ionic, or even metallic bonds. The simplest polymer consists of mono-substituted carbon chains based on the $-\text{CH}_2\text{-CHR}$ repeat unit which is often formed from a vinyl group containing compound $\text{CH}_2=\text{CHR}$ (in this study an acrylate group is defined as ‘containing’ a vinyl group conjugated to a carbonyl group). In a linear polymer, the structural units are connected in a chain arrangement and they are linked to the rest of the polymer via two bonds. When the structural unit contains three bonds to the bulk of the polymer then the polymer is termed non-linear or ‘branched’². Polymers containing a single repeating unit are called homopolymers and those containing two or more different structural units are called copolymers².

A chemical reaction that results in the formation of a polymer is called a polymerisation reaction and can be classified by two different systems² :

1. Addition-Condensation system
2. Chain Growth-Step Growth system

The first system divides polymerisation into two types:

- 1.1) addition polymerisation
- 1.2) condensation polymerisation

Addition polymerisation involves the reaction of unsaturated monomers. These are able to link up with other monomers to form a repeating chain² (Figure 5.1). Condensation polymerisation is a process which occurs when two molecules join together, with the loss of a small molecule such as water, methanol or HCl (Figure 5.1).

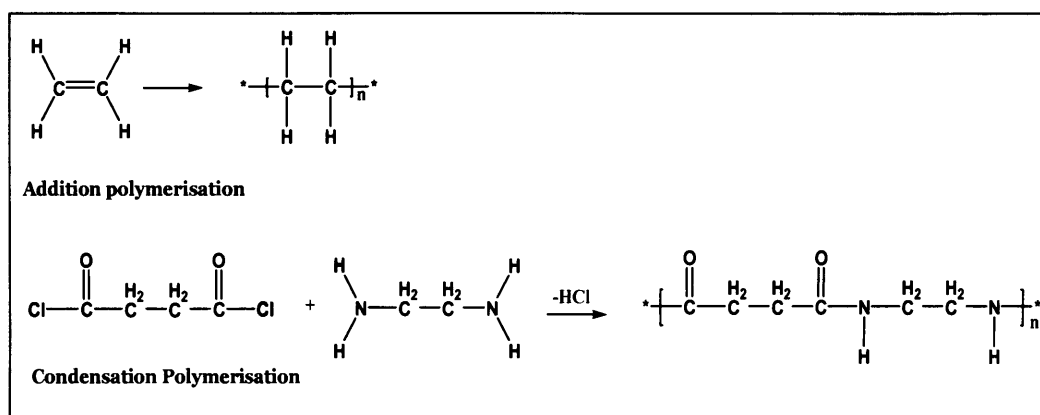


Figure 5.1: Addition-condensation system.

The other system categorizes polymers based on their mechanism. In a chain growth polymerisation, the polymers are produced by the addition of one monomer to another. In the step growth polymerisation, the polymers chains are formed by random union of monomer molecules to form dimers, trimers and higher species².

Reaction steps	Step-growth	Chain growth
Elimination of a small molecule	Often	Never
Initiator (for starting reaction)	Not necessary	Necessary
Propagation	(i) Two complementary end groups condense to form a linkage in the polymer chain thus formed. (ii) All complementary chain ends can react with each other	(i) An active end group yields again an active end group (chain reaction). (ii) Only initiated chains react with monomer.
Termination	Mostly not	As a rule

Table 5.1: Differences between step- and chain-growth polymerisation (Adapted from G.Challa³).

Molecularly imprinted polymers are usually prepared using either free radical polymerisation or radical co-polymerisation.

5.1.2 FREE RADICAL POLYMERISATION

Free radical polymerisations can be performed under mild conditions in solution and are very tolerant of functional groups in the monomers and impurities in the system⁴. The mechanism of free radical polymerisation is characterised by three distinct stages: (i) initiation, (ii) propagation and (iii) termination.

(i) Initiation: this step begins when an initiator decomposes into free radicals in the presence of monomers (Figure 5.2). The liability of

carbon-carbon double bonds in the monomer makes them susceptible to reaction with the unpaired electrons in the radical. In this reaction, the active centre of the radical takes one of the electrons from the double bond of the monomer, leaving an unpaired electron to appear as a new active centre at the end of the chain⁵. Addition can occur at either end of the monomer. A large number of initiators are available and normally they are used at low levels compared to the monomer, e.g. 1wt %, or 1mol % with respect to the total number of moles of polymerisable double bonds⁴. In a typical synthesis, between 60% and 100% of the free radicals undergo an initiation reaction with a monomer. The remaining radicals may join with each other or with an impurity instead of with a monomer⁵.

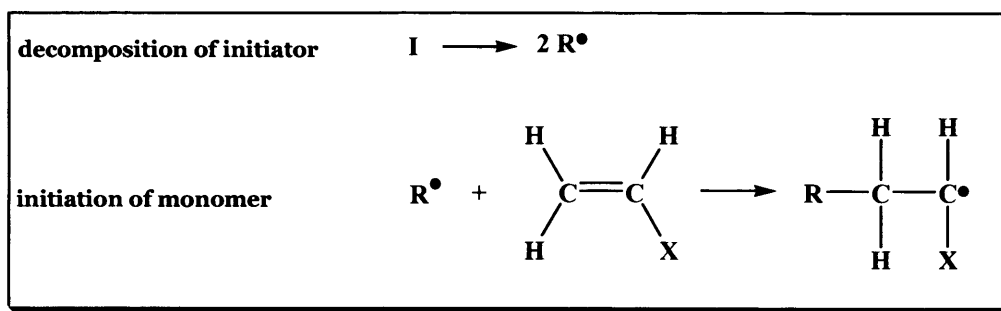


Figure 5.2: Initiation step.

(ii) Propagation: during the propagation stage, the process of electron transfer and consequent motion of the active centre down the chain proceeds (Figure 5.3). Importantly, in a typical free radical polymerisation the rate of propagation is usually much faster than the rate of initiation, so that as soon as a new polymer chain starts to grow it propagates to high molecular weight in a relatively short period of time before it terminates⁴. Therefore, high molecular weight product is present in the system even when the amount of monomer consumed is low⁴.

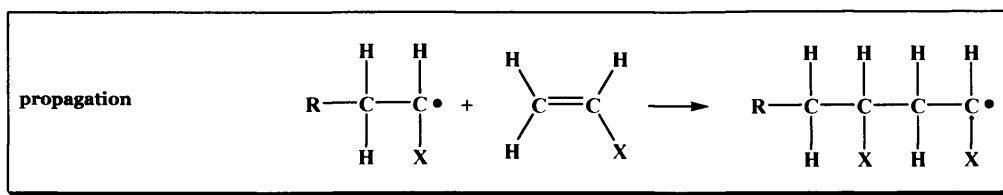


Figure 5.3: Propagation step.

(iii) Termination: termination occurs either by combination or disproportionation³ (Figure 5.4). Combination occurs when the polymer's growth is stopped by free electrons from two growing chains that join and form a single chain. Disproportionation halts the propagation reaction when a free radical strips a hydrogen atom from an active chain and a carbon-carbon double bond takes the place of the missing hydrogen². Disproportionation can also occur when the radical reacts with an impurity. This is why it is so important that polymerization be carried out under 'clean' conditions.

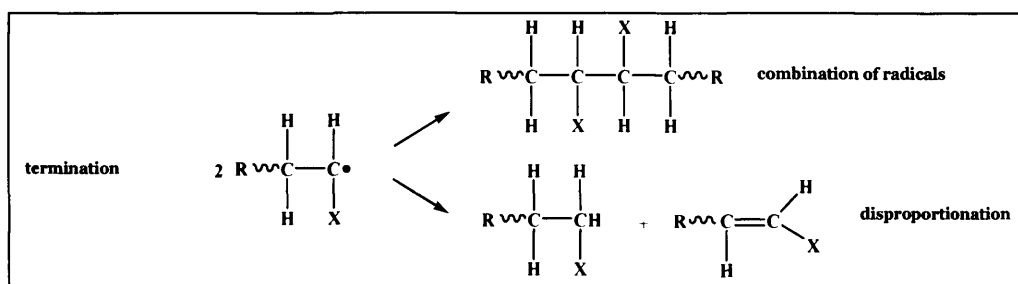


Figure 5.4: Termination step.

In the field of organic molecularly imprinted materials, vinyl polymerisation is the most common method used to give co-polymers. However, it is often highly desirable to simultaneously polymerise two or more vinyl acylate monomers within the same reaction vessel to give co-polymers⁴. This generates products with chemical properties distinct to the polymers obtained when monomers are polymerised independently, leading for example, to an increment of solubility in a thermodynamically compatible solvents⁵. Nevertheless, particular

attention must be paid to the relative reactivities of the monomers at the design stage of synthesis, as not all monomers are compatible with one another in copolymerisation⁴. More specifically, should the polymerisation rates of the co-monomers vary, then the composition of the resulting polymer will not mirror the composition of the reaction mixture composition, but it will have a composition that is a function both of initial monomer ratio and monomer reaction rate.

5.1.3 DESIGN OF A BOC-PHOSPHO-SERINE METHYL ESTER MOLECULARLY IMPRINTED POLYMER

A stoichiometric non-covalent approach (section 1.2.4) was chosen as method to imprint the Boc-phospho-L-serine methyl ester in the presence of *N,N'*-diethyl-4-vinyl-benzamidine functional monomer. In this way, fewer binding groups would be non-specifically distributed within the polymer.

The imprinted polymers were made using a six-stage procedure described as follows:

- i. *N,N'*-diethyl 4-vinyl benzamidine was selected as the functional monomer to interact with the template based on its ability to bind the target molecule. Its binding specificity was also studied by NMR titration and molecular modelling (Chapter 4).
- ii. The template molecule and the functional monomer were dissolved in a suitable solvent into 25 mL sealable injection vials. The vials were sonicated to aid dissolution of the components.
- iii. A large molar excess of cross-linking monomer was added together with a free radical initiator. Since oxygen retards free radical polymerizations, the solution was normally sparged with nitrogen or argon.

- iv. The polymerization was initiated by raising the temperature to 60°C or by exposure to UV irradiation.
- v. Before the molecularly imprinted polymer can be used, the template must be removed. Template removal is a fundamental issue in non-covalent MIPs, as slow bleeding of residual template can cause interferences with analyte detection. Although the use of analogues or “dummy templates”^{6,7} may help to overcome these problems, a study by Ellwanger *et al.*⁸ reported methods for complete template removal to minimize template bleed. This was achieved by washing the polymer with alternating large quantities of water containing acids (e.g. acetic acid) or bases (e.g. di-sodium hydrogen orthophosphate).
- vi. The prepared molecularly imprinted polymer was subject to work up which involved particle fragmentation and grading.

After polymerization, polymers were ground manually using a pestle and a mortar and the resulting particles were wet sieved in an appropriate solvent until the particle size was reduced to < 45 micron. In order to remove the fine particles (< ~10 micron), the recovered polymers were sedimented in acetonitrile (3 times for 4-6 hours). This process was influenced by the mass of polymer being treated. When sedimentation was complete, the supernatant was decanted from the cylinder and the remaining particles recovered by filtration (Whatman No1 filter paper). The particles were then left overnight to dry in a vacuum oven at 60°C and were subsequently sized by laser diffraction.

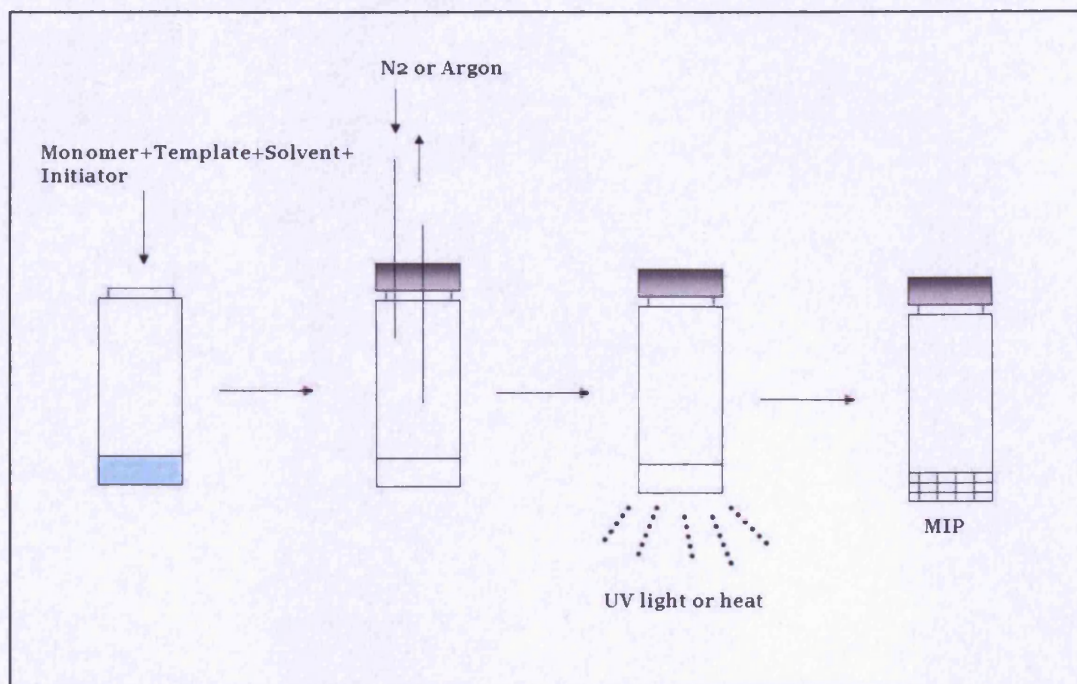


Figure 5.5: Scheme of MIP preparation.

5.1.4 CHARACTERISATION OF PARTICLE SIZE BY LASER DIFFRACTION

For a spherical, homogeneous particle, its size is usually and unambiguously described by its diameter⁹. Particles of irregular shape, which include MIP particles resulting from monolithic polymerisations, can be characterised in various ways. The microscope is the basic instrument for sizing small particles, however, it is common to use an automated approach, such as light-scattering or electrical resistance zone measurements. In this study, the particle size distribution of all polymers was determined by laser diffraction.

5.1.4.1 PRINCIPLES

The LASER diffraction (LAS) method involves the detection and analysis of the angular distribution of light produced by a LASER beam passing through a dilute dispersion of particles. Typically, a He-Ne LASER ($\lambda=632.8$ nm) in the 5 milliwatt (mW) to 10 mW range is

employed as the coherent light source. To be precise, light can be *scattered, diffracted* or *absorbed* by the dispersed particles¹⁰. Scattered light consists of reflected and refracted waves and depends on the form, size, and composition of the particles. Diffracted light arises from edge phenomena and is dependent only on the geometric shadow created by each particle: diffraction is independent of the composition of the particles. Absorption occurs when light is converted to heat or electrical energy by interaction with the particles, and is influenced by both size and composition. The so-called laser diffraction technique incorporates all three of these effects, but is generally limited to the more straightforward scattering angles. There are two different kinds of laser diffraction: the “wet method” (LAS-W) and the “dry” method (LAS-D). Differences between LAS-D and LAS-W methods arise primarily from the different ways in which the particles are dispersed in each case. In liquid it is possible to modify solution conditions, by changing pH or adding chemical dispersing agents for example, or break up aggregates using mechanical or ultrasonic energy. In the LAS-D method, a stream of compressed air (or a vacuum) is used to both disperse the particles and to transport them to the sensing zone¹⁰. This method of dispersion works well for large, non-colloidal-phase spheroids, where the interfacial contact area is small and the physical bonds holding the individual particles together are relatively weak. For the particles smaller than a micron and highly asymmetric, the higher surface-to-volume ratio results in more intimate and numerous contact points and, as a consequence, a greater driving force is needed to separate aggregated particles¹⁰.

In laser diffraction particle size analysis, a representative cloud or ‘ensemble’ of particles passes through a broadened beam of laser light which scatters the incident light onto a Fourier lens. This lens focuses the scattered light onto a detector array and, using an inversion algorithm, a particle size distribution is inferred from the collected diffracted light data¹¹ (Figure 5.6). Then the signals are transferred to

the computer through an A/D transfer and, lastly, the data is processed using Mie Scattering theory. Mie theory describes scattering by homogeneous spheres of arbitrary size and is the most rigorous optical scattering model available. For non-spherical particles, Mie provides a volume-weighted equivalent spherical diameter and it has been applied with mixed success to the analysis of powders with diameters from several hundreds of micrometers down to about 100 nm. However, there are two assumptions made in this theory that are pertinent to the result obtained¹¹:

- *The particles are assumed to be spherical.* Laser diffraction is sensitive to the volume of the particle. For this reason, particle diameters are calculated from the measured volume of the particle, but assume a sphere of equivalent volume.
- *The suspension is dilute.* The particle concentration is assumed to be so low that scattered radiation is directly measured by the detector (i.e. single scattering) and not re-scattered by other particles before reaching the detector (i.e. multiple scattering).

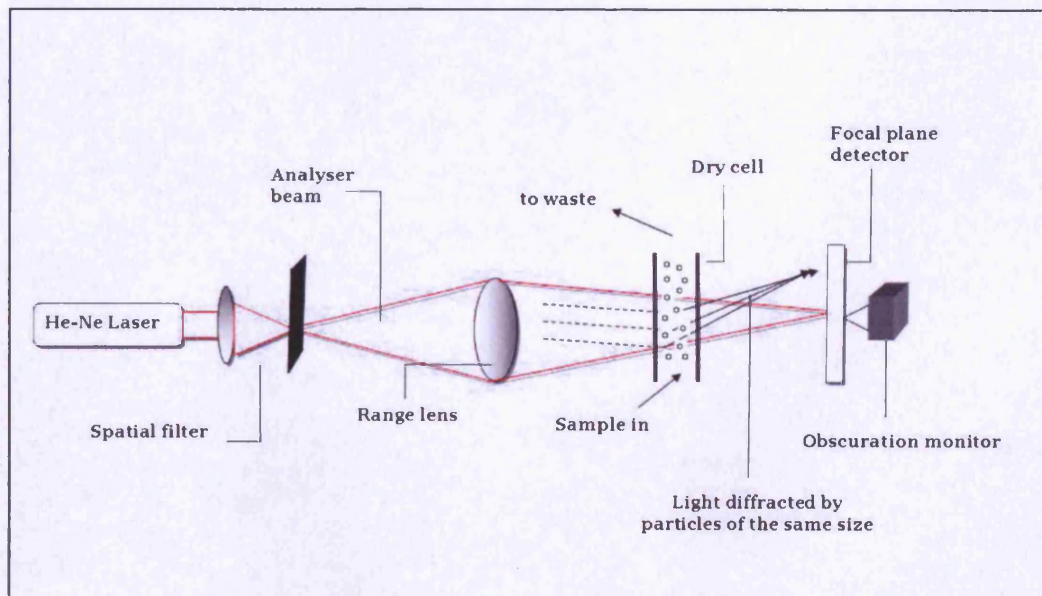


Figure 5.6: Fourier optics configuration used by the Mastersizer 2000.

5.2 MATERIALS AND METHODS

5.2.1 PREPARATION OF PHOSPHO SERINE IMPRINTED POLYMERS

Imprinted polymers were prepared for Boc-P-serine methyl ester using the following two protocols:

Protocol 1

Boc-phospho-L-serine methyl ester (0.19 g; 0.7 mmol) was dissolved in a mixture of EGDMA (3.4 mmol, 2.6ml), *N,N'*-diethyl-4 vinylbenzamidinium (0.54 g; 2.7 mmol) and 3.2 mL of DMF/DMSO (1:1). After addition of 1,1'-azobis cyclohexane-carbonitrile (BAZO) (0.039 g; 0.16 mmol) the solution was degassed by sonication under vacuum and purged with nitrogen for 10 minutes. The polymerization was conducted in a sealed glass vial and was left under UV (366 nm) for 24 hours.

Protocol 2

The functional monomer *N,N'*-diethyl-4 vinyl benzamidinium was used in the form of amidinium chloride salt. One equivalent of Boc-phospho-L-serine methyl ester (0.07 g; 0.25 mmol) was dissolved with two equivalents of the amidinium.HCl (0.100 g; 0.5 mmol) in dry methanol to form the 1:1 template-functional monomer pre-polymerisable complex. The remaining ammonium chloride precipitate was removed by membrane filtration. The solution was evaporated, and the dried complex dissolved in EGDMA (1.9 ml; 10 mmol) and methyl methacrylate (0.1 ml; 0.1 mmol) in 2 mL acetonitrile/toluene (1:1). The mixture was homogenized in an ultrasonic bath at a maximum temperature of 40°C for ~5 minutes. Finally, the initiator AIBN was added (0.02 g; 0.12 mol) and the monomer mixture was degassed. The polymerisation reaction was initiated by UV and was left for 72 hours¹².

Non-imprinted polymers (NIPs) were similarly prepared but in the absence of the template.

The resultant monolithic polymer was ground using a mortar and pestle and wet sieved in MeCN using stainless steel 250 μm and 45 μm sieves. Those particles passing through the 45 μm sieve were dried under vacuum and were subsequently sedimented to remove fine material.

5.2.2 SEDIMENTATION

Polymers were suspended in 200ml of acetonitrile contained in a 250ml measuring cylinder. The cylinder was shaken and, after ~ 6 hours, the solvent was carefully removed by vacuum so as not to disturb the sediment. This process was repeated until the sedimenting solvent appeared almost transparent. The yield of useful particles from this process was 35%. Therefore an alternative method was sought (section 5.2.3).

5.2.3 CENTRIFUGATION

Two centrifuge tubes were prepared, one containing the polymer in 40mL of MeOH and another filled with water to the same weight. Test tubes of polymer suspension were centrifuged so that the larger particles sedimented whilst the fine material remained in suspension. A range of centrifugation speeds and times were investigated. Particle size and distribution was monitored microscopically.

5.2.4 LASER DIFFRACTION

In our investigation, dry dispersion was achieved using the Scirocco 2000 dry powder feeder (Malvern Instruments, UK) equipped with a micro-volume powder feeder tray. A pressure titration was conducted in order to determine the correct dispersion pressure, and approximately

200-300 mg of polymer was found to provide enough material for a single measurement.

5.2.5 TEMPLATE REMOVAL

The template was removed by washing the polymer for 2-3 hours in presence of 1% of the competitor, di-sodium hydrogen orthophosphate. Subsequently, the particles were collected by filtration and the process repeated with a solution of HCl 1N. The recovered polymers were then washed 3 times in water before being recovered by filtration and dried overnight in a vacuum oven at 60°C. The effectiveness of template removal was assessed by a HPLC-UV system. To ensure template removal had been achieved, 5 mg of polymer were suspended in 1ml H₂O+0.001% acetic acid in a 2ml Eppendorf vial. The suspension was stirred magnetically at room temperature for 24 hours. The vials were subsequently centrifuged for 5 minutes at 13,000 rpm. 200 µl of the supernatant was analysed by HPLC [C₁₈ column (150mm x 4.6mm); mobile phase: acetonitrile:NaHCO₃/TBA-Cl (25/75); injection volume: 50µl; flow rate: 0.8 ml/minute; Boc-P-serine-OMe $\lambda_{\text{detection}} = 210\text{nm}$: (retention time= 3,8 minutes)].

5.2.6 DETECTION LIMIT OF BOC-P-SERINE METHYL ESTER

In order to evaluate the efficiency of the polymer cleaning, the limit of detection of Boc-P-serine methyl ester (LOD) was determined. LOD was defined as three times the highest base line noise value over the period of analysis. A series of template standard solutions were prepared and analysed (10⁻⁶ mol/l,-10⁻⁴ mol/l) and the peak heights recorded. Maximum values of baseline noise were also determined. This procedure was conducted before each experiment.

5.3 RESULTS AND DISCUSSION

5.3.1 CENTRIFUGATION

Initially, centrifugation was carried out at 500 revolutions per minute at room temperature and for 10 minutes. This resulted in a completely clear supernatant suggesting particle size separation had not been achieved between supernatant and pellet. Subsequently, centrifugation was repeated under different conditions (Table 5.2).

Experiment number	Time	Speed (rpm)	%MIP sedimented	Particle size in supernatant (μm)
1	5 min	300	10%	~35
2	10 min	500	2 %	~45
3	10 min	400	70 %	~12

Table 5.2: Centrifugation conditions.

Centrifugation had a number of advantages compared with 'measuring cylinder' sedimentation (Table 5.3):

1. An increase in the yield of the useful particle size polymer
2. More rapid
3. More efficient solvent usage

Method	Yield	Time	Solvent (ml)
Centrifugation	70%	10 min.	40 ml
Sedimentation	35%	6 hours x 3	600 ml

Table 5.3: Sedimentation and centrifugation process.

Therefore, centrifugation was identified as a better method to obtain particulate material with a mean diameter of 25-45 μm in high yield (70%).

5.3.2 POLYMER PREPARED WITH PROTOCOL 1

The polymer processing procedures resulted in a ~35% yield of usable polymer particles. These were analysed by laser diffraction and the particle size distributions identified two populations of particles of mean diameter 3-4 μm and ~25 μm (Figure 5.7).

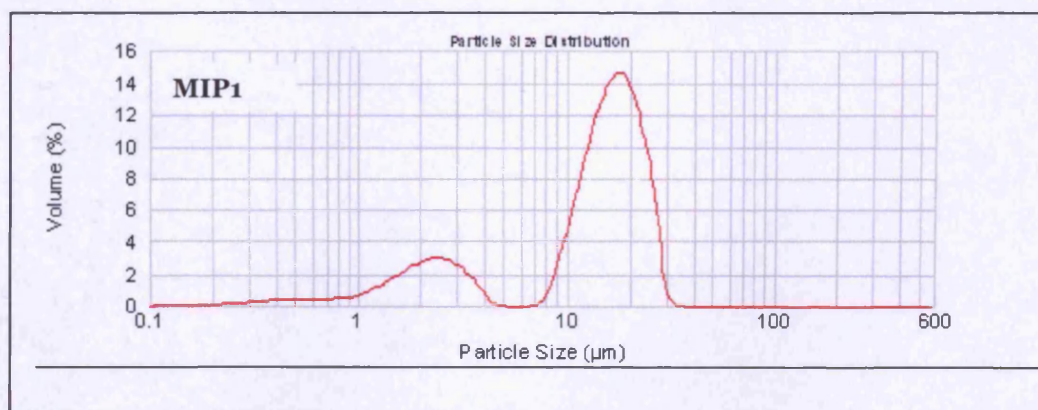


Figure 5.7: Particle size distribution for polymer prepared with protocol 1.

This suggested that sedimentation did not successfully remove the more fine material (< 5 μm). It was observed that when using acetonitrile, the

finer particles had a tendency to aggregate. Not only did this effect the grinding process, but it would also have resulted in particles sedimenting more slowly than predicted. Therefore, a proportion of this material carried over into the final product.

5.3.3 POLYMER PREPARED WITH PROTOCOL 2

MeCN/toluene was employed instead of DMSO/DMF. The latter solvents were initially used to overcome the issue of monomer-template solubility. However, as the template-monomer complex was based on hydrogen bond interactions, DMSO/DMF would have competed with the monomers and destabilized the complex.

After preparation, the polymer was ground and sieved (45 μ m) and sedimented by centrifugation in phosphate buffer/acetonitrile. The process yielded 70% of usable polymer particles. Analysis of the particle size suggested a single particle size population was present with a mean particle size of 30 μ m (Figure 5.8). In this case the aggregation problems described in section 5.3.2 were not observed.

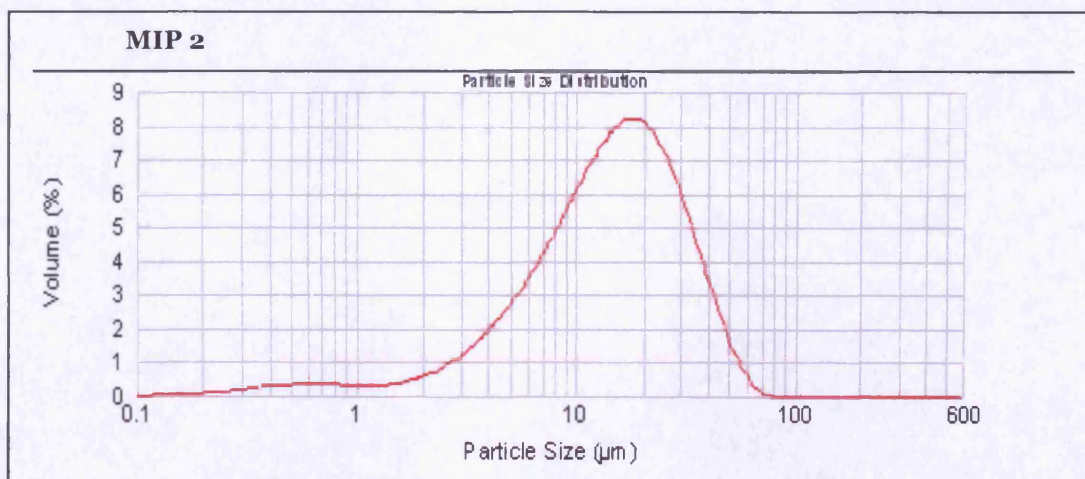


Figure 5.8: Particle size distribution for polymer prepared with protocol 2.

5.3.4 DETECTION LIMIT FOR BOC-PHOSPHO-L-SERINE METHYL ESTER

The detection limit for Boc-phospho-L-serine methyl ester occurred at concentrations between 10^{-5} - 10^{-4} mol/l. It was typically calculated by determining the maximum baseline noise and the peak height over a period of ~30 minutes, multiplying this value by 3 and then relating this to the standard curve.

Max baseline noise = 0.43 mV

Peak height = 3×0.43 mV = 1.29 mV

Detection Limit = $1.29\text{mV}/16.017\text{mV} \times 100\mu\text{M} = 8.05 \mu\text{M}$

5.3.5 WASHING STEP

Using the template removal procedure described in section 5.2.5, the amount of template present in the supernatant was below the limit of detection (LOD) for the HPLC method. This indicated successful removal or maximal reduction in template leaching.

5.4 CONCLUSION

Boc-phospho-L-serine methyl ester imprinted polymers were successfully synthesised. Protocol 1 yielded polymer particles comprising two population distributions (mean of 3-4 μm and 25 μm) whereas Protocol 2 yielded a single population distribution of particles (mean of 30 μm).

BIBLIOGRAPHY

1. Flory, P. (1953). Principles of Polymer Chemistry.
2. Stevens, M. P. (1999). Polymer Chemistry: An introduction.
3. Challa, G. (1993). Polymer chemistry: an introduction.
4. Peter A.G. Cormark and Amaia Z. Elorza (2004). "Molecularly imprinted polymers: synthesis and characterisation." Journal of Chromatography B **804**: 173-182.
5. Elias, Hans-Georg (2001). "An Introduction to Polymer Science."
6. Matsui J, et al (2000). "Atrazine-selective polymers prepared by molecular imprinting of trialkylmelamines as dummy template species of atrazine." Anal.Chem **72**: 1810-1813.
7. Theodoridis G, et al (2003). "Preparation of a molecularly imprinted polymer for the solid-phase extraction of scopolamine with hyoscyamine as a dummy template molecule." Journal of Chromatography A **987**: 103-109.
8. Ellwangner A, et al (2001). "Evaluation of methods aimed at complete removal of template from molecularly imprinted polymers." Analyst **126**: 784-792.
9. John D Stockham and Edward G. Fochtman (1977). Particle size analysis.
10. Bowen, P. (2002). "Particle size distribution measurement from millimeters to nanometers, and from Rods to Platelets." J.Disp.Sci.Tech. **23**(5): 631-662.
11. www.malvern.com
12. Emgenbroich, M. and Wulff, G. (2003). "A new enzyme model for enantioselective esterases based on molecularly imprinted polymers." Chem.Eur.J. **9**: 4106-4117.

Chapter 6

Optimisation of experimental conditions for the equilibrium evaluation of the imprinting effect

6.1 INTRODUCTION

In this study, equilibrium evaluation or batch rebinding analysis was used to investigate the affinity and selectivity of the molecular imprint for its template. Differential template binding to MIP/NIP is a useful indication of an imprinting effect but in most cases it is not conclusive. Confirmation that an imprinting effect is present can only be achieved by enantiomeric imprinting (Chapter 7) or through a careful and systematic study of cross-reactivity¹.

The aim of the studies described in this chapter was to maximise MIP/NIP differentiation by modification of the binding environment. Subsequently, an optimised set of conditions was used to study the cross-reactivity and enantio-selectivity of the MIP system (Chapter 7). Another key aim (Chapter 2) of this study was to develop a system that functioned in near physiological conditions.

Knowing the ionisation state of the template was also very important in understanding its binding behaviour under a range of conditions.

6.1.2 BATCH ANALYSIS

A common approach for evaluating an imprinting effect is an equilibrium batch rebinding (Figure 6.1). In this process, a known amount of polymer is incubated with a range of known template concentrations. When equilibrium is attained, the polymer is removed

by a combination of centrifugation and filtration and the concentration of the template remaining in the supernatant is determined to give the 'free' template concentration (C_f). Subtraction of C_f from the total substrate added gives the amount of substrate adsorbed to the MIP (C_b)².

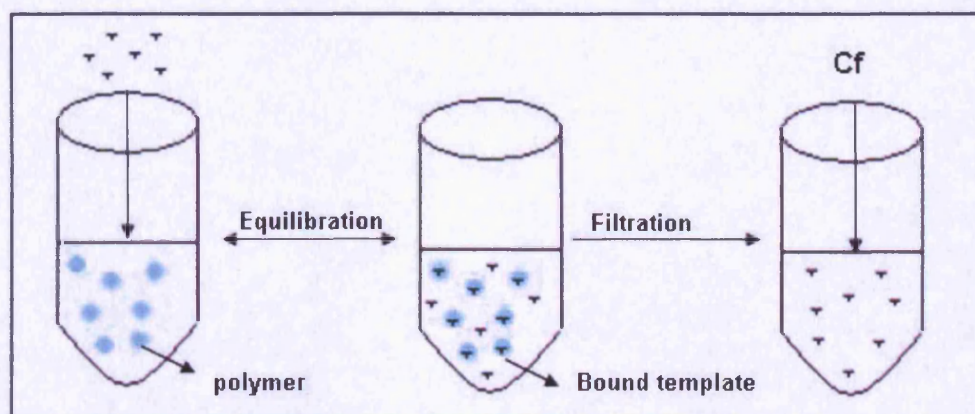


Figure 6.1: Batch analysis process.

To compare the polymer selectivity, the imprinting factor (I) (Equation 6.1) is determined. It is obtained from the ratio of distribution coefficients (DC) for the MIP and the NIP (Equation 6.1). Distribution coefficient, itself, is calculated by simply dividing the concentration of bound template (C_b) by the concentration of free template (C_f).

$$I = \frac{DC_{MIP}}{DC_{NIP}} \quad \text{Eq.6.1}$$

The imprinting factor represents how much better the substrate binds to its imprinted polymer compared to a non-imprinted control. It has been reasoned that this method takes account of non-specific binding leaving a value for binding that can be attributed only to imprinting effects³. This assumes that there are no additional differences, beyond the presence of imprint sites, between the two polymers. A better

confirmation of this assumption, based on enantiomeric discrimination, will be discussed in section 7.1 .

6.1.3 ANALYSIS OF BOC-PHOSPHO-L-SERINE METHYL ESTER

A novel reverse-phase ion-pair chromatography method was developed to effectively analyse the Boc-phospho-L-serine methyl ester since this was not achievable using conventional reverse phase chromatography.

In general terms, chromatography is a separation technique in which separation of the solute mixture results from differential solute distribution between a mobile phase and a stationary phase⁴. In liquid chromatography, solute molecules can interact strongly with either phase; those solutes that interact more strongly with the mobile phase elute through the chromatographic system more rapidly than those that interact more strongly with the stationary phase⁴. Thus, the solutes will elute in order of their increasing distribution coefficients with respect to the stationary phase⁴.

A reverse phase liquid chromatography mobile phase often consists of a mixture of water (containing a buffer or other additive) and an organic modifier such as acetonitrile (MeCN) and methanol (MeOH). If the target molecules are non-polar, separation can commonly be achieved using a mobile phase comprising a mixture of water and MeOH, a mixture of water and MeCN or a mixture of all three⁴. For more polar molecules, the aqueous component of the mobile phase should be buffered at a well-controlled pH based on the analyte's pKa value, so the analyte is more 'organic' and less 'ionic' at the pH of the buffer⁵. In general, if an analyte is charged at the pH of the mobile phase then it will elute rapidly because its solubility in the mobile phase is dominant⁵. Conversely, if an analyte is uncharged, i.e. more organic and less ionic,

then retention will be favoured since the solubility of the analyte in the stationary phase will be increased.

In some circumstances it is not possible to use a mobile phase that promotes analyte retention on the stationary phase. When this occurs, an ion-pairing reagent can be added to the mobile phase. These reagents are non UV- active, long-chain organic compounds containing acidic or basic functionalities. The ion-pairing reagent forms an ion-pair with the analyte, slowing the migration of the analyte through the column because the long alkyl chain of the ion pair reagent is highly attracted to the column packing⁵.

When selecting a suitable ion-pair reagent, alkyl chain lengths must be taken into consideration. The longer the chain, the more hydrophobic the counter-ion, and therefore, the greater the retention.

Although ion-exchange chromatography has become a popular mode of separation, it is not useful in all situations. The advantages of ion-pair chromatography over ion-exchange are:

- i. Simple preparation of buffers
- ii. Wide choice of carbon chain lengths for improved retention and separation
- iii. Significantly reduced separation time
- iv. Highly reproducible results
- v. Improved peak shape

In our study, Boc-phospho-L-serine methyl ester was strongly ionised under basic conditions and was ion-paired using tetrabutylammonium chloride (TBA-Cl) (Figure 6.2). Using this technique, rapid analysis of the target molecule was achieved without prior derivatisation of the

molecule and with avoidance of a very low pH that could have caused the cleavage of the Boc group.

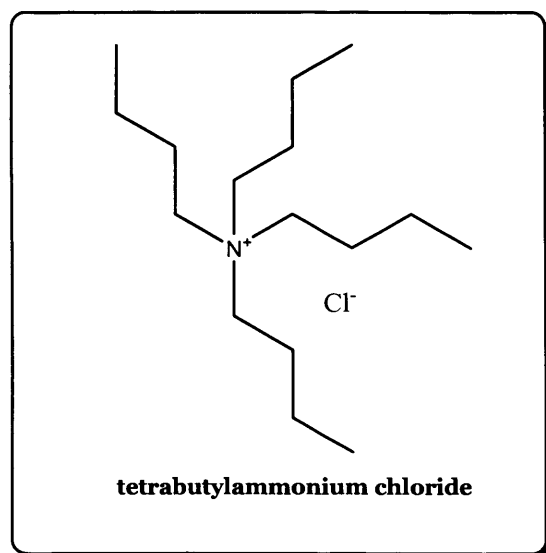


Figure 6.2: Molecular structure of the ion-pair reagent tetrabutylammonium chloride (TBA-Cl) used to combine the Boc-phospho-L-serine methyl ester.

6.2 MATERIALS AND METHODS

6.2.1 pKa CALCULATIONS

The equilibrium of a protonation/deprotonation reaction can be described by a dissociation constant (K_D). For the reaction⁶:



The dissociation constant K_D is defined as:

$$K_D = \frac{[\text{A}^-] \times [\text{H}^+]}{[\text{HA}]} \quad \text{Eq.6.3}$$

This can be rearranged to:

$$[\text{H}^+] = \frac{K_D \times [\text{HA}]}{[\text{A}^-]} \quad \text{Eq.6.4}$$

The dissociation constant corresponds to the equilibrium constant. Because the hydrogen ion concentration $[\text{H}^+]$ is expressed more conveniently as the pH value, Equation 6.4 can be described as the negative logarithm⁶:

$$\text{pH} = \text{pKa} - \log \frac{[\text{HA}]}{[\text{A}^-]} \quad \text{Eq.6.5}$$

$$= \text{pKa} + \log \frac{[\text{A}^-]}{[\text{HA}]} \quad \text{Eq.6.6}$$

The pKa value is defined as the negative logarithm of the dissociation constant. The pKa value is a property of an individual ionisable group.

Therefore, if a molecule has more than one ionisable group, it has more than one pKa value⁶. Equation 6.6 is called the Henderson-Hasselbach equation. It can be used to determine what proportion of an ionisable group is in the protonated or deprotonated state at a given pH. The pKa value corresponds to that pH value at which the ionisable group is half protonated⁶. The pKa value is a measure for the “strength” of an acidic or basic group. At pH values less than the pKa value (high [H⁺]), ionisable groups are mostly protonated; at pH values greater than the pKa (low H⁺), the groups are mostly deprotonated⁶.

6.2.2 BATCH REBINDING

Five mg of polymer, prepared with protocol 2 (section 5.2.1), were added to 0.5 mL of 100 μ M template solution into a 2mL Eppendorf vials. Five replicates were prepared for each experiment. The Eppendorfs were magnetically stirred until binding had reached equilibrium (approximately 24 hours). As controls, 0.5 mL of solvent (without template) was added to the Eppendorfs containing 5 mg of MIP/NIP and these vials were also stirred for 24 hours. The Eppendorfs were subsequently centrifuged (13,000 rpm/5 mins), the supernatant removed and a 500 μ l sample was filtered through a 0.22 μ m syringe filter prior to HPLC analysis.

6.2.3 HPLC ANALYSIS

HPLC analyses of Boc-phospho-L-serine methyl ester were carried out using a ‘SpectraSystem’ HPLC system (Hemel Hempstead, UK) consisting of a SCM1000 vacuum membrane degasser, a P4000 pump, an AS3000 auto-sampler and an UV3000 detector. The system was controlled by PC1000 software. The chromatographic conditions were: column: C18 (150mm x 4.6mm), mobile phase: 5mM of TBA-Cl + 50 mM of sodium bicarbonate and acetonitrile (75:25), detection: UV 210 nm and flow rate: 0.8 ml/min.

A stock standard solution of 100 μM of Boc-phospho-L-serine methyl ester was prepared. A range of standard solutions were prepared by dilution of the 100 μM stock solution (10 μM to 100 μM). Standard calibration solutions were prepared in a range of solvent conditions to correspond with each assay.

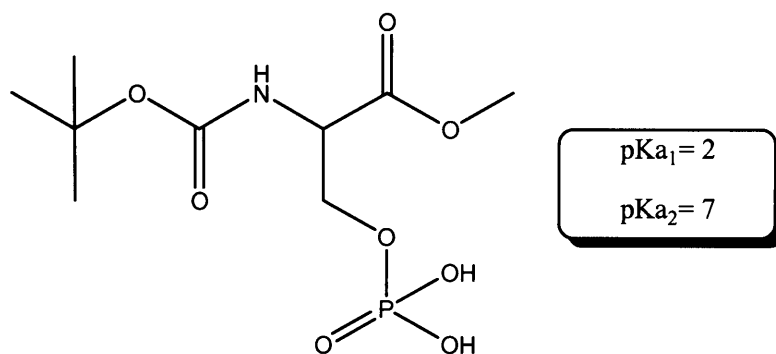
6.3 RESULTS AND DISCUSSION

6.3.1 INTRODUCTION

Binding studies were initially carried out in apolar and polar solvents. It was expected that higher specific binding would occur in non-polar solvents and higher non-specific binding in polar solvents such as water. Other experiments were carried out at different pHs and different ions in order to optimise the conditions for specific template rebinding.

6.3.2 PROTONATION STATE OF THE PHOSPHORYL GROUP OF THE SERINE AT DIFFERENT pH VALUES

The phosphate group of the serine presents two ionisable groups having $\text{pK}_a = \sim 2$ and $\text{pK}_a = \sim 7$.



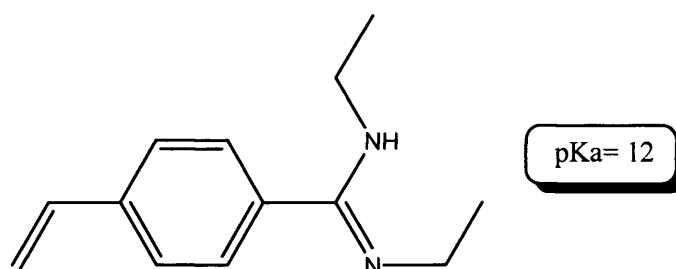
Since the pK_a of the ionisable groups are separated by more than two orders of magnitude, the ionisation of any one group should not affect

pH	% of group protonated [HA]	% of group deprotonated [A ⁻]
pKa +2	0.99	99.01
pKa +1	9.0	91
pH=pKa	50	50
pKa -1	91	9.0
pKa -2	99.01	0.99

Table 6.1: Ionisation states of the phosphorylated/acid group at different pH values.

6.3.3 PROTONATION STATE OF THE AMIDINE AT DIFFERENT pH VALUES

The amidine is a strong base with a pKa of ~ 12 in solution⁸.



Similarly to the phosphate group, the ionisation state of the amidine at different pHs can be calculated using the Henderson-Hasselbach

Equation 6.6 and a second Equation 6.10, where $[A^-]$ is replaced by $[B]$, for the deprotonated form of the base, and $[HA]$ by $[HB^+]$, for the protonated form of the base. Table 6.2 shows the degree of ionisation at various pHs.

pH	% of group protonated [HB ⁺]	% of group deprotonated [B]
pKa +2	0.99	99.01
pKa +1	9.0	91
pH=pKa	50	50
pKa -1	91	9.0
pKa -2	99.01	0.99

Table 6.2: Ionisation state of the amidine/basic group at different pH values.

Importantly, it has been reported⁸ that the pKa value of the amidine group in the polymer is lower (pKa= ~ 8.5) than in solution (pKa= ~ 12).

6.3.4 BATCH REBINDING: PARAMETERS AFFECTING HOST-GUEST INTERACTIONS

6.3.4.1 SOLVENT EFFECT

In order to achieve some basic understanding of how the template interacts with the MIP/NIP in different conditions, batch rebinding experiments were carried out in both polar solvents (water (H₂O) and methanol (MeOH)), and apolar solvents (chloroform (CHCl₃) and acetonitrile (MeCN)).

In all cases a significant degree of non-specific binding was observed (Figure 6.3).

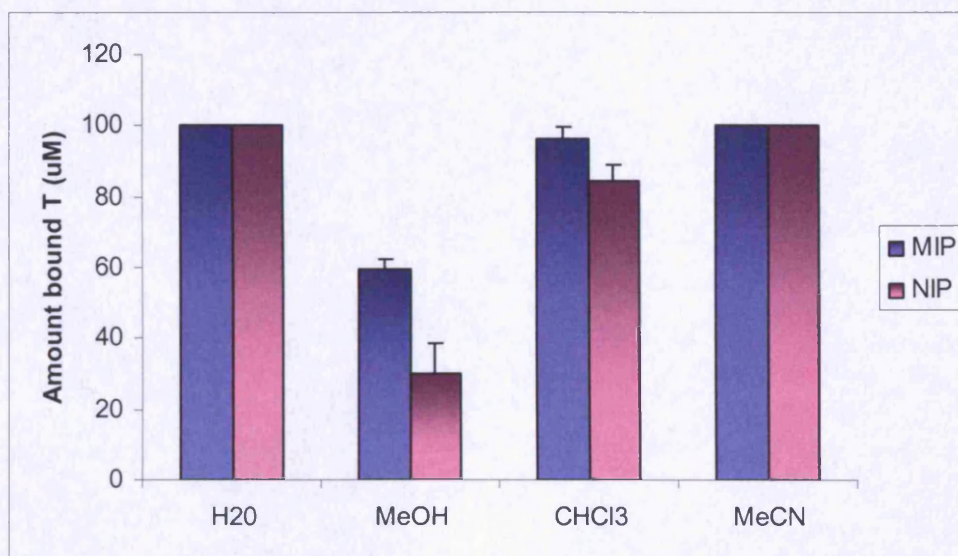


Figure 6.3: Binding for Boc-phospho-L-serine methyl ester imprinted in polar and apolar solvents; ($n=5 \pm SD$).

It is likely that the high degree of non-specific template binding observed in H₂O was due to a strong hydrophobic effect, as no difference was observed in the binding of the template to the MIP and the NIP. Similarly, a large amount of non-specific binding was also observed when rebinding experiments were carried out in MeCN and CHCl₃. Again binding to the MIP was similar to that of the NIP. The change from a very polar solvent to relatively non-polar solvents resulted in a reversal of the non-specific binding mechanism. In these cases it is likely, especially with chloroform, that binding was driven by polar effects such as hydrogen bonding and ionic interactions. The low solubility of the template in these solvents may also drive this effect. In addition, the degree of polymer swelling in different solvents would also have an effect and it would be expected that the larger surface areas available for binding in the swollen polymer i.e. in MeCN and CHCl₃ would promote template uptake.

Binding in MeOH gave the lowest non-specific binding and a noticeable difference in the amount bound to the MIP as compared to the NIP was observed (Figure 6.3). MeOH behaves as a 'middle polarity solvent', and neither apolar nor polar effects predominate.

Although the high degree of non-specific binding observed in water was not encouraging, the performance of the polymer in MeOH did suggest that the system could function in polar environments. However, since the aim of the project was to design a system that functions in water, it was reasonable to suggest that in subsequent optimisation experiments, water should be the focus and that, since both template and functional monomer were ionisable, the effects of pH in a range of aqueous systems were investigated.

6.3.4.2 pH-MODIFIED SYSTEMS

Binding studies were carried out in a range of buffered and pH-adjusted solutions over a range pH 2 to pH 11. Figure 6.4 shows the uptake of template by the NIP and MIP and Table 6.3 gives distribution coefficients (DC) and imprinting factors.

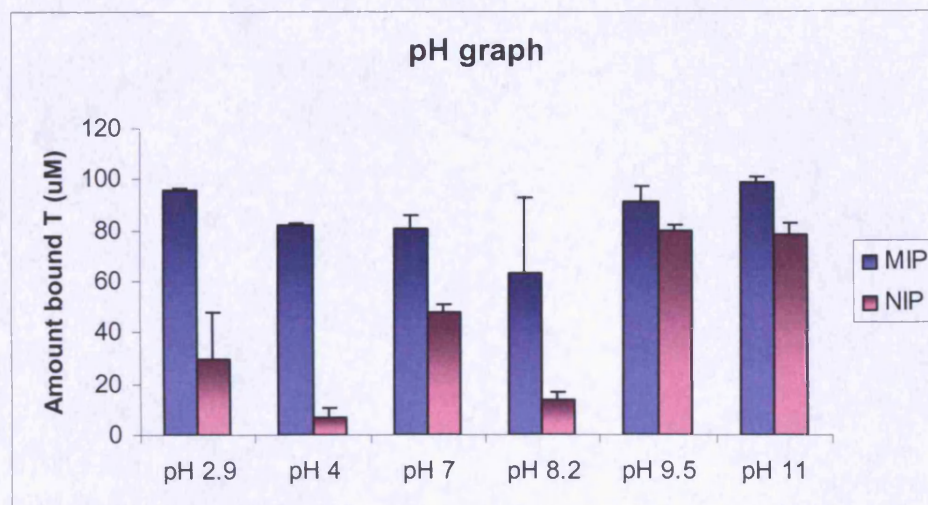


Figure 6.4: Binding for aqueous Boc-phospho-L-serine methyl ester at different pHs; pH=2.9 (0.001% trifluoroacetic acid); pH= 4 (0.01% Acetic acid); pH= 7 (0.01% trizma base HCl buffer 15 mM); pH= 8.2 (NaOH 2N)*; pH= 9.5 (0.01% borate); pH= 11 (NaOH 2N) *; (n=5 \pm SD).

* A solution of 2N NaOH was added dropwise to water to achieve the required pH.

pH	DC _{MIP}	DC _{NIP}	I _f
2.9	9.4 x 10 ⁻⁴	3.0 x 10 ⁻⁴	3.1
4.0	8.2 x 10 ⁻⁴	6.6 x 10 ⁻⁵	12.5
7.0	8.0 x 10 ⁻⁴	4.8 x 10 ⁻⁴	1.6
8.2	6.2 x 10 ⁻⁴	1.0 x 10 ⁻⁴	5.1
9.5	9.0 x 10 ⁻⁴	8.0 x 10 ⁻⁴	1.1
11.0	9.8 x 10 ⁻⁴	7.8 x 10 ⁻⁴	1.2

Table 6.3: Distribution coefficients (DC) and imprinting factors for MIP/NIP measured after 24 hours incubation with 100 μ M Boc-phospho-L-serine methyl ester.

The results were promising, as significant differences in template rebinding to the MIP and NIP, dependent on the type of buffer/pH modifier used and the pH, were observed.

At pH 7 (trizma base HCl buffer), a difference in template uptake was observed between the MIP and the NIP. Binding studies previously carried out in water (pH=6.8) (Figure 6.3) showed a higher degree of non-specific binding than was observed in this experiment. Therefore, it is reasonable to deduce that this result was not directly attributable to the small change in pH, but was due to the addition of the trizma base HCl to the system. It is likely that addition of this base reduced the hydrophobic effect by limiting non-specific interactions with the polymeric surface.

At pH 2.9 (0.001% TFA solution) and pH 4 (0.01% acetic acid solution), noticeable variation in the distribution coefficient was observed for MIP and NIP ($I_f = 3.13$ and 12.5). For the template, at both of these pHs, one P-OH group was mainly deprotonated (pH 2.9 = 90% at pH 4 = 99%) whilst the amidine was protonated. Under these conditions interaction between the template and the functional monomer was favoured. The data suggests that either a small variation in the degree of ionisation of the template has an important effect on differential MIP/NIP binding or that the pH adjusting anionic species has some other effect. In both of the cases the pH adjustment was made using a carboxylic acid. The anionic, deprotonated forms of both of these acids are capable of interacting with the polymeric amidine residue and therefore of reducing template polymer association. In particular, at pH 4, non-specific binding to the NIP was significantly reduced resulting in a high I_f (Table 6.3).

Although the imprinting factors for the template at pH 7 (trizma base HCl) and at pH 4 (0.001% acetic acid solution) are very different ($I_f = 1.6$ and 12.5 respectively), the distribution coefficients of template to the

MIP are similar ($DC=8.0 \times 10^{-4}$ and 8.2×10^{-4}). The difference in I_f arises due to changes in distribution coefficients of the template to the NIP. At pH 4, the phosphate exists in the mono-deprotonated form whilst at pH 7 the second P-OH group is 50% deprotonated. At both of these pH values the amidine is fully protonated. In addition, at pH 4 acetic acid is still partially protonated and therefore, it is possible that it reduces non-specific binding to the NIP. Alternatively, or in combination, the additional negative charge resulting from the partial deprotonation of the non-complexing P-OH group at pH 7, results in greater non-specific interaction with the polymer matrix. However, surprisingly, this effect results in no overall change to the amount of template binding to the MIP. A further interesting observation comes from molecular modelling (section 4.2.3) that suggests the existence of an intermolecular hydrogen bond between the non-complexed P-OH and NH of the template. If the assumption is made that this form of the template was the predominant template species during the polymerisation step, at pH 7 the partial loss of the non-complexed P-OH would change the conformation of the template and would reduce MIP binding between pH 7 and pH 4. However, this change was not demonstrated experimentally and suggests that perhaps the logic of extrapolating from observations made *in vacuo* to complex solvated systems is questionable.

An important observation regarding the pKa of polymerised amidine monomers was made by Strikovskiy *et al*⁸. In this study the measured pKa of the same polymerised amidine species was 8.5. If a similar value is assumed for this study, then at pH 8.2 the amidine residue is partially deprotonated (~50%) whilst the phosphate group is primarily deprotonated (90%) and possesses two negative charges. Therefore the reduction in distribution coefficients for template binding to the NIP at pH 8.2 compared to the NIP at pH 7 resulted from the change in the amidine protonation state. Again, it was surprising that a much lesser reduction was observed for the MIPs.

At pH 9.5 and pH 11, the phosphate and the amidine group are fully deprotonated and the distribution constants for MIP and NIP at both pHs are similar. The key to explaining this result is the increase in non-specific apolar template–polymer interactions due to the loss of surface charge resulting from the deprotonation of the amidine. It is likely that the hydrophobic Boc group (or other apolar areas of the template molecule) adheres hydrophobically to the polymer surface, whilst the charged phosphate group protrudes into the aqueous solution in an arrangement analogous to surfactants at a water–oil interface.

The degree of template binding to MIP and NIP is a product of the balance between the hydrophilicity and hydrophobicity of the polymer surface and the charge on the template. This results in a complex pattern of varying template–polymer interactions for the pH systems described. Significantly, despite great variation being observed for the NIP, the template–MIP binding is ‘relatively’ constant over the range of conditions. It seems that pH and solution composition readily affects NIP template interactions whilst template-MIP interactions are in some way ‘buffered’ from external effects.

Further analyses were performed in order to optimise conditions that favour the template rebinding and to more fully understand the relationship between binding/selectivity and pH/competitor ion.

6.3.4.3 COMPETITOR ION TYPE EFFECT

The affinity of the amidine imprinted polymer for the original template ligand, when challenged with competitors, was investigated in a series of competitive binding experiments. Three different competitor ions were used and the results were compared to those obtained by measuring the uptake of the template at the same pH, but in absence of competitive ligands. The results are shown in Figure 6.5 (a,b,c).

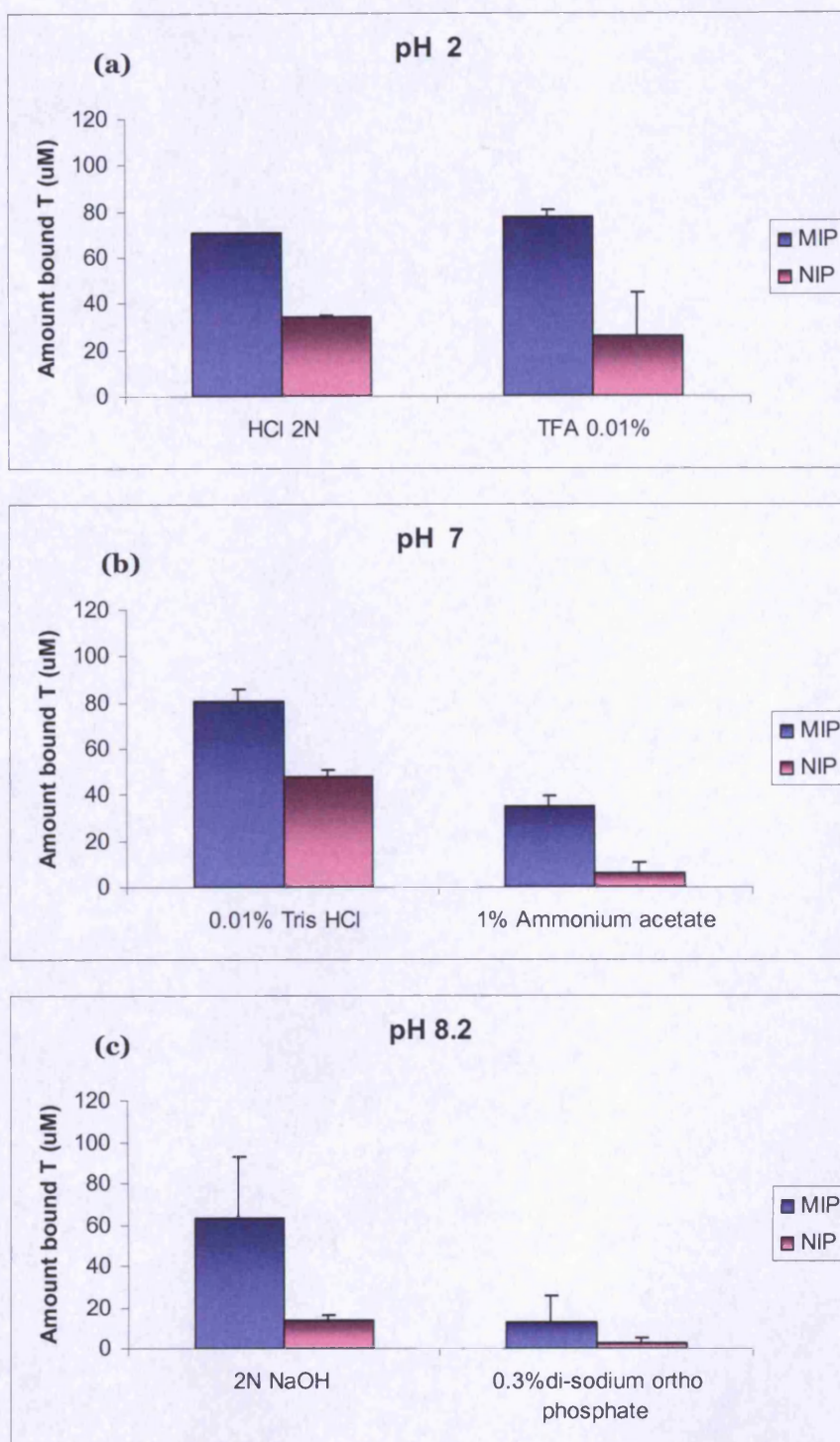


Figure 6.5: Binding for aqueous Boc-phospho-L-serine methyl ester at: (a) pH= 2 in HCl 2N and TFA 0.01%; (b) pH= 7 in 0.01% tris HCl and ammonium acetate 1%; (c) pH= 8.2 in NaOH 2N solution and 0.3% w/v di-sodium orthophosphate; (n=5 ± SD).

Ionic specie	pH	DC _{MIP}	DC _{NIP}	I _f
HCl 2N	2.0	7.0 x 10 ⁻⁴	3.3 x 10 ⁻⁴	2.1
TFA 0.01%	2.0	7.7 x 10 ⁻⁴	2.6 x 10 ⁻⁴	2.9
Tris 0.01%	7	8.0 x 10 ⁻⁴	4.8 x 10 ⁻⁴	1.6
AA 1%	7	3.5 x 10 ⁻⁴	5.8 x 10 ⁻⁵	6.2
NaOH 2N	8.2	6.2 x 10 ⁻⁴	1.3 x 10 ⁻⁵	4.5
Ortho 0.3%	8.2	1.2 x 10 ⁻⁴	2.2 x 10 ⁻⁵	5.4

Table 6.4: Distribution constants and imprinting factors for MIP/NIP measured after 24 hours incubation with 100µM Boc-phospho-L-serine methyl ester in different solutions.

At pH 2, the I_{fs} for MIP and NIP in the presence of HCl and trifluoroacetic acid (TFA) were similar (Figure 6.5 (a)). This result suggests that TFA did not act as a competitor for the template either specifically or non-specifically. TFA is almost completely dissociated in water and therefore is a strong acid. Its acidity is also attributed to the electronegativity of the fluorine atoms that pulls electron density away from the carboxylate anion. Being a strong acid, its conjugate base (CF₃COO⁻) is weak and it is likely that, under this form, it exhibits only weak interactions in solution with cations.

At pH 7, the distribution constants of the template binding to the MIP and NIP in the presence of ammonium acetate were lower than observed for a Tris HCl pH 7 adjusted system (Figure 6.5 (b)). In this case, the ammonium acetate appears to reduce non-specific and specific binding.

The displacement effect was most apparent when di-sodium orthophosphate was used as competitor. Compared to a pH-matched

control, binding of the template to both MIP and NIP was greatly reduced by addition of the orthophosphate (Figure 6.5 (c)).

6.3.4.4 CONCENTRATION EFFECT

The effect of competitor concentration on template binding was investigated for TFA, ammonium acetate and di-sodium orthophosphate. The results of the equilibrium batch rebinding tests are shown in (Figure 6.6 (a,b,c)) and distribution constants and imprinting factors are listed in tables 6.5.

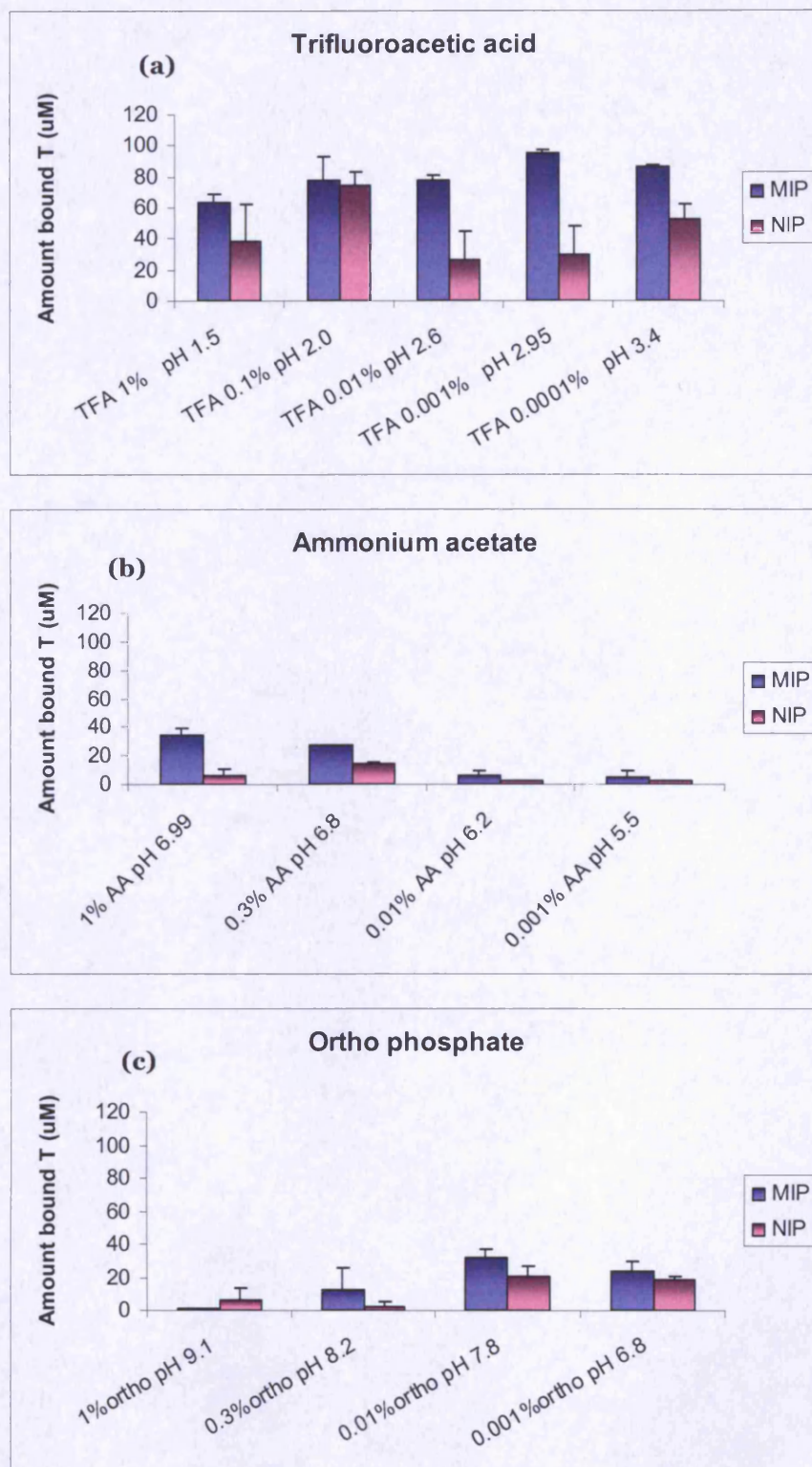


Figure 6.6: Binding for aqueous Boc-phospho-L-serine methyl ester at: (a) different concentrations of trifluoacetic acid (TFA); (b) different concentrations of ammonium acetate (AA); (c) different concentrations of di-sodium ortho phosphate; (n=5 ± SD).

Concentration (%) TFA	pH	DC _{MIP}	DC _{NIP}	I _f
1%	1.5	6.3 x 10 ⁻⁴	3.8 x 10 ⁻⁴	1.6
0.1 %	2.0	7.7 x 10 ⁻⁴	7.4 x 10 ⁻⁴	1.0
0.01 %	2.6	7.7 x 10 ⁻⁴	2.6 x 10 ⁻⁴	2.9
0.001%	2.95	9.5 x 10 ⁻⁴	2.9 x 10 ⁻⁴	3.3
0.0001%	3.4	8.6 x 10 ⁻⁴	5.1 x 10 ⁻⁴	1.7

Concentration Ammonium acetate (%)	pH	DC _{MIP}	DC _{NIP}	I _f
1%	6.9	3.5 x 10 ⁻⁴	5.8 x 10 ⁻⁵	6.2
0.3 %	6.8	2.6 x 10 ⁻⁴	1.4 x 10 ⁻⁴	1.8
0.01 %	6.2	5.8 x 10 ⁻⁵	2.0 x 10 ⁻⁵	2.9
0.001%	5.5	5.0 x 10 ⁻⁵	3.9 x 10 ⁻⁵	2.6

Concentration di-sodium orthophosphate (%)	pH	DC _{MIP}	DC _{NIP}	I _f
1%	9.1	1.0 x 10 ⁻⁵	6.3 x 10 ⁻⁵	0.2
0.3 %	8.2	1.2 x 10 ⁻⁴	2.2 x 10 ⁻⁵	5.4
0.01 %	7.8	3.2 x 10 ⁻⁴	2.0 x 10 ⁻⁴	1.6
0.001%	6.8	2.3 x 10 ⁻⁴	1.8 x 10 ⁻⁴	1.2

Table 6.5: Distribution constants and imprinting factors for MIP/NIP measured after 24 hours incubation with 100µM Boc-phospho-L-serine methyl ester.

When TFA was used in the analyses, the distribution coefficient of template binding to the MIP was similar for all concentrations over a pH range of pH 1.5–pH 3.2, whilst the distribution coefficients for the NIP were variable. As observed in section 6.3.4.3, TFA is a weak competitor and only has a marginal effect on non-specific (NIP) template interactions even at high concentration (1%).

Ammonium acetate, on the other hand, demonstrated a surprising, almost inverse concentration effect on binding affinity. It is likely that the competitive effect of the acetate ion is complicated by changes in pH that result from changes in the concentration of the ammonium acetate solutions (pH 5.5 – pH 6.9).

Additional binding studies were carried out using di-sodium orthophosphate. In these experiments, over a pH range of 6.8–9.1, an increase in orthophosphate concentration resulted in a reduction in the amount of template that bound to both MIP and NIP. In 0.001% w/v orthophosphate (pH 6.8), the distribution coefficient of the template binding to MIP is lower than that in 0.01% w/v orthophosphate and, therefore, this result did not demonstrate an inverse proportionality of binding to the concentration used. This suggests that concentration was not the only parameter to affect binding. Interestingly, at pH 6.8, the distribution coefficients of the template binding to MIP in 1% w/v ammonium acetate was similar to the distribution coefficients of the template bound to MIP in 0.001% w/v ortho phosphate. It is likely that ortho phosphate possesses a more similar geometry to the phosphate template than ammonium acetate and therefore a lower amount of di-sodium orthophosphate was necessary to displace the template from binding the amidine.

For TFA, little effect on template binding was observed, whilst for ammonium acetate and di-sodium orthophosphate, the degree of template binding was shown to be affected by competitor concentration.

However, an underlying and unavoidable associated change in pH complicates the interpretation of this data.

6.4 CONCLUSION

Rebinding of Boc-phospho-L-serine methyl ester to the *N,N'*-4-vinyl-diethyl-benzamidine containing MIP and NIP was shown to be dependent on four effects: solvent, pH, ionic composition and concentration. In general, the greatest I_{fs} were observed between pH 3 and pH4 at 0.001% TFA and 0.01% acetic acid.

BIBLIOGRAPHY

1. Ramstrom, O., Yan, M (2005). Molecular Imprinting-an introduction. Molecularly Imprinted Materials: Science and Technology. M. Yan, Ramstrom,O. New York.
2. Spivak, D. (2005). "Optimisation, evaluation, and characterisation of molecularly imprinted polymers." Advanced Drug Delivery Reviews.
3. Spivak, D. (2005). Selectivity in molecularly imprinted matrices. Molecularly imprinted materials: Science and Technology. M. Yan, Ramstrom,O. New York: 395-418.
4. Scott, R. (1995). Principles and Practice of Chromatography.
5. Kirkland, J., Snyder, LR (1979). Introduction to Modern Liquid Chromatography. New York.
6. Meisenberg, G., Simmons, W (1998). Principles of Medical Biochemistry.
7. De Levie, R. (2003). "The Henderson-Hasselbach equation: its history and limitations." J.Chem.Educ. **80**: 146.
8. Strikovskiy, A., et al (2003). "Catalytically active, molecularly imprinted polymers in bead form." Reactive & Functional Polymers **54**: 49-61.

Chapter 7

Confirmation of an imprinting effect

7.1 INTRODUCTION

Despite reporting, in Chapter 6, large differences between the amount of template binding to the MIP compared to the NIP, confirmation of an imprinting effect can only be assumed when either enantiomeric selectivity or a logical pattern of selectivity is demonstrated, following a comprehensive evaluation of cross-reactivity. Commonly, a non-imprinted polymer (NIP), prepared in the same way as the MIP, but in absence of the template, is employed as the control. However, differential MIP/NIP template binding can be misleading, since it can arise either due to an imprinting phenomenon or as a result of differences in the morphology or chemical structure of the MIP and the NIP. For example, the surface area and porosity of a templated polymer (MIP) can be very different from that of a non-templated control polymer (NIP), and this can significantly influence template binding.

Initially, the cross-reactivity was investigated by studying MIP and NIP affinity for two physiologically occurring triphosphates: adenosine 5'-triphosphate (ATP) and uridine 5'-triphosphate (UTP).

ATP is a multifunctional nucleotide primarily known as the “molecular currency” of intracellular energy transfer¹. In this role, ATP transports chemical energy within the cells. Furthermore, in signal transduction pathways, ATP is used to provide the phosphate for protein kinase reactions¹. The structure of this molecule consists of adenine bonded to a sugar, ribose, which is connected to a chain of three phosphates² (Figure 7.1).

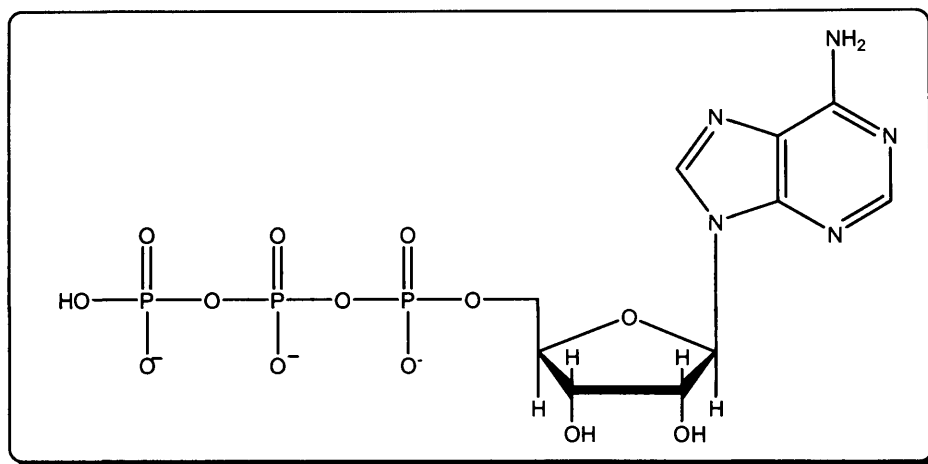


Figure 7.1: Molecular structure of adenosine 5'-triphosphate (ATP).

UTP is an activated precursor in the synthesis of RNA³. It also acts as the chief transferring coenzyme in carbohydrate metabolism to produce sucrose in plants, lactose and glycogen in mammals, and chitin in insects⁴. UTP is involved in the formation of ATP as a donor of phosphate groups to adenosine diphosphate (ADP)⁴. The UTP molecule consists of the nitrogenous base uracil linked to the sugar, ribose, and has a chain of three phosphate groups attached to the ribose⁵ (Figure 7.2).

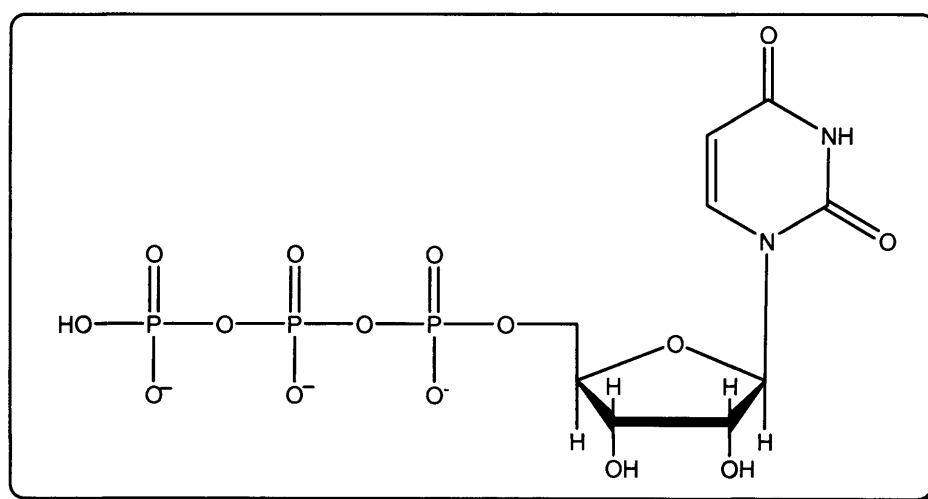


Figure 7.2: Molecular structure of uridine 5'-triphosphate (UTP).

To investigate MIP enantioselectivity, the previously synthesised D-enantiomer (section 3.2.5.1) of the Boc-phospho-serine methyl ester (Figure 7.3), was also studied.

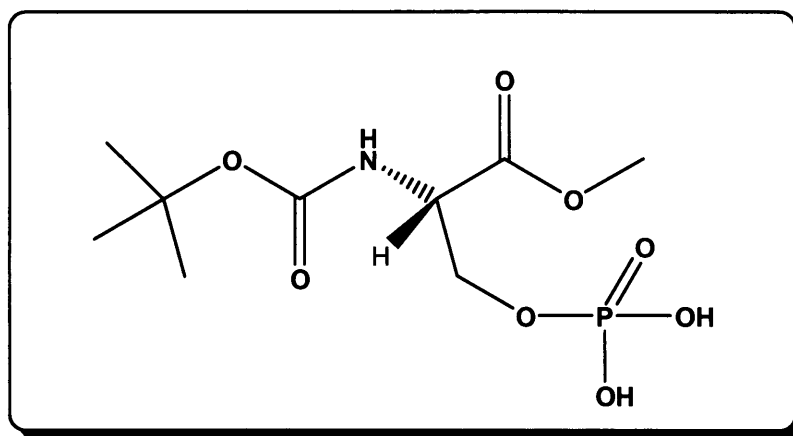


Figure 7.3: Molecular structure of Boc-phospho-D-serine methyl ester.

7.2 MATERIALS AND METHODS

7.2.1 REAGENTS

Adenosine 5'-triphosphate disodium salt hydrate and uridine 5'-triphosphate trisodium salt dihydrate were purchased from Sigma-Aldrich (Dorset, UK).

Boc-phospho-D-serine methyl ester was synthesised as described in section 3.2.5.1.

7.2.2 BATCH REBINDING

Batch rebinding studies were carried out as previously reported in section 6.2.2., using 100 μ M of ATP, UTP and Boc-phospho-D-serine methyl ester. These binding studies were performed for ATP and UTP in conditions (0.001% TFA/H₂O) that were previously shown to favour MIP/NIP differential template binding (section 6.3.3.2), whilst binding of the D-template were carried out at TFA concentrations of 0.001% and 0.01%.

7.2.3 HPLC ANALYSIS

HPLC analyses of Boc-phospho-D-serine methyl ester were conducted using the method described in section 6.2.3.

UTP was analysed by isocratic HPLC using, as mobile phase, a buffer solution of ammonium dihydrogen orthophosphate (0.05 mol) and tetrabutylammonium hydrogen sulphate (0,05 mol) (pH 5 adjusted with pellets of NaOH) 85%; methanol 15%. Analyses were run at flow rate of 1mL/min, using a C18 column (150mm x 4.6mm), an injection volume of 20 μ l/minute and UV detection at λ = 256 nm .

A similar approach was used to analyse ATP, but in this case the mobile phase was (75% : 25%) in order to decrease the retention time.

7.3 RESULTS AND DISCUSSION

7.3.1. HPLC PERFORMANCE

Standard curves were prepared for ATP and UTP and were found to be linear in the range 0 μM to 100 μM (Figure 7.4 (A-B)). These systems were later used to analyse UTP and ATP concentration in equilibrium batch evaluation assays.

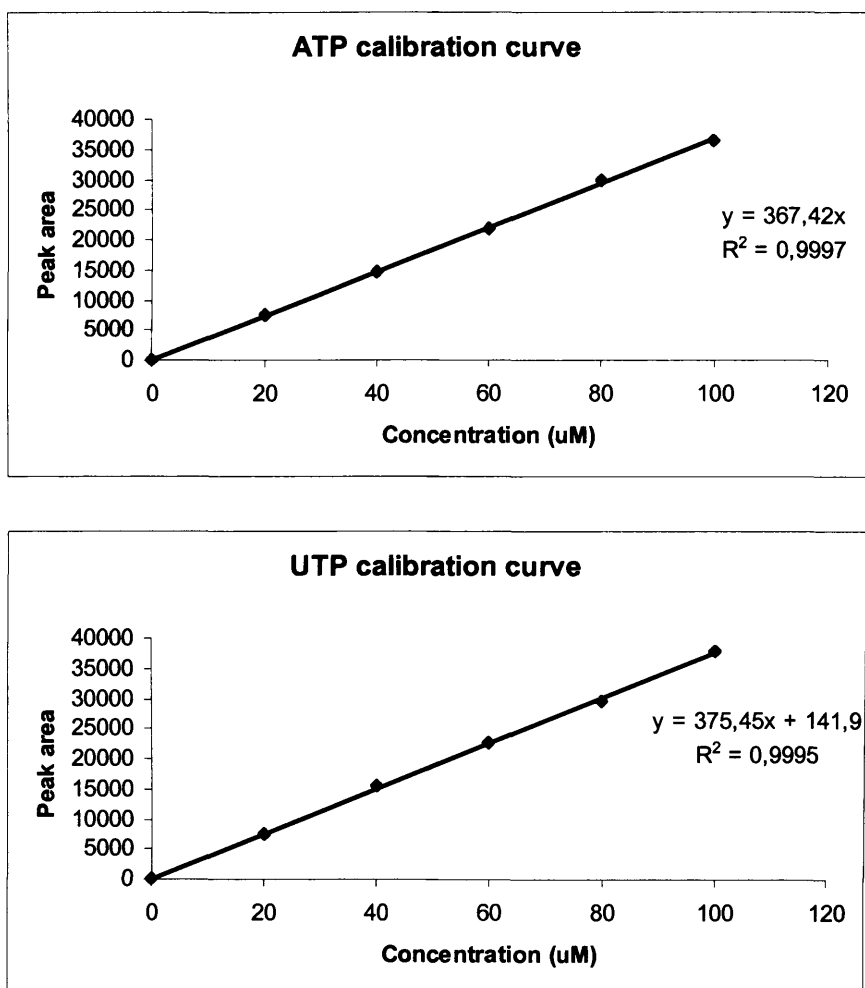


Figure 7.4: Standard curve obtained from plotting a series of ATP and UTP standards ($\text{H}_2\text{O}/0.001\%\text{TFA}$) against peak area, analysed using HPLC. Five standards were used ranging from 20 to 100 μM .

7.3.2 CROSS-REACTIVITY STUDIES

7.3.2.1 BATCH RESULTS

Distribution constants and imprinting factors (section 6.1) for ATP and UTP are given in table 7.1. It was observed that for both ATP and UTP, rebinding was generally lower for all polymers when compared to the template (Figure 7.5). In addition, it was also observed, for both ATP and UTP, that binding to the NIP was greater than to the MIP (Figure 7.5). This effect was assumed to arise due to the extra size of the triphosphates, making it impossible for them to fit into the template imprinted cavity. The induced rigidity of the MIP arose due to the homogeneous distribution of functional monomer in the MIP, which made access to the imprinted cavities impossible for the big molecules.

Compound	DC _{MIP}	DC _{NIP}	I _f
Boc-phospho-L-serine methyl ester	4.7 x 10 ⁻⁴	1.4 x 10 ⁻⁴	3.3
ATP	3.9 x 10 ⁻⁵	6.34 x 10 ⁻⁵	0.6
UTP	1.19 x 10 ⁻⁵	2.16 x 10 ⁻⁴	0.55

Table 7.1: Distribution coefficients and imprinting factors for the cross-reactants (ATP/UTP) and Boc-phospho-L-serine methyl ester in an aqueous solution of 0.001% TFA.

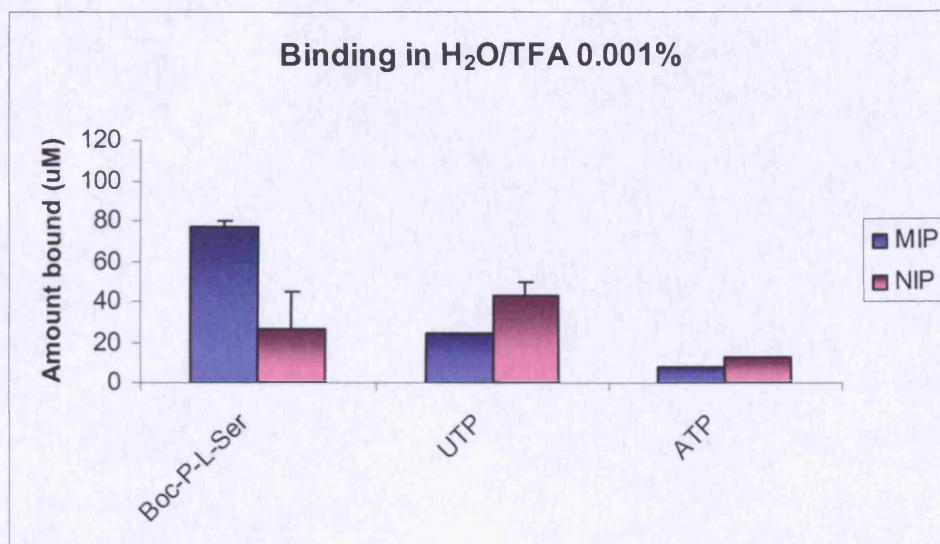


Figure 7.5: Comparison of binding data between the template and the cross-reactants in an aqueous solution of 0.001% TFA; (n=5 ± SD).

7.3.3 ENANTIOMERIC EFFECT

7.3.3.1 BATCH RESULTS

Binding of the D-template enantiomer (Figure 7.6) was compared to that of L-template enantiomer obtained under the same conditions. The results in Figure 7.6 combined with the data of the imprinting factors for both enantiomers in Table 7.2, clearly demonstrate enantioselectivity. The ability of the MIP to discriminate between two configurations of the serine molecule is extremely strong evidence for template induced selectivity of an imprinting effect.

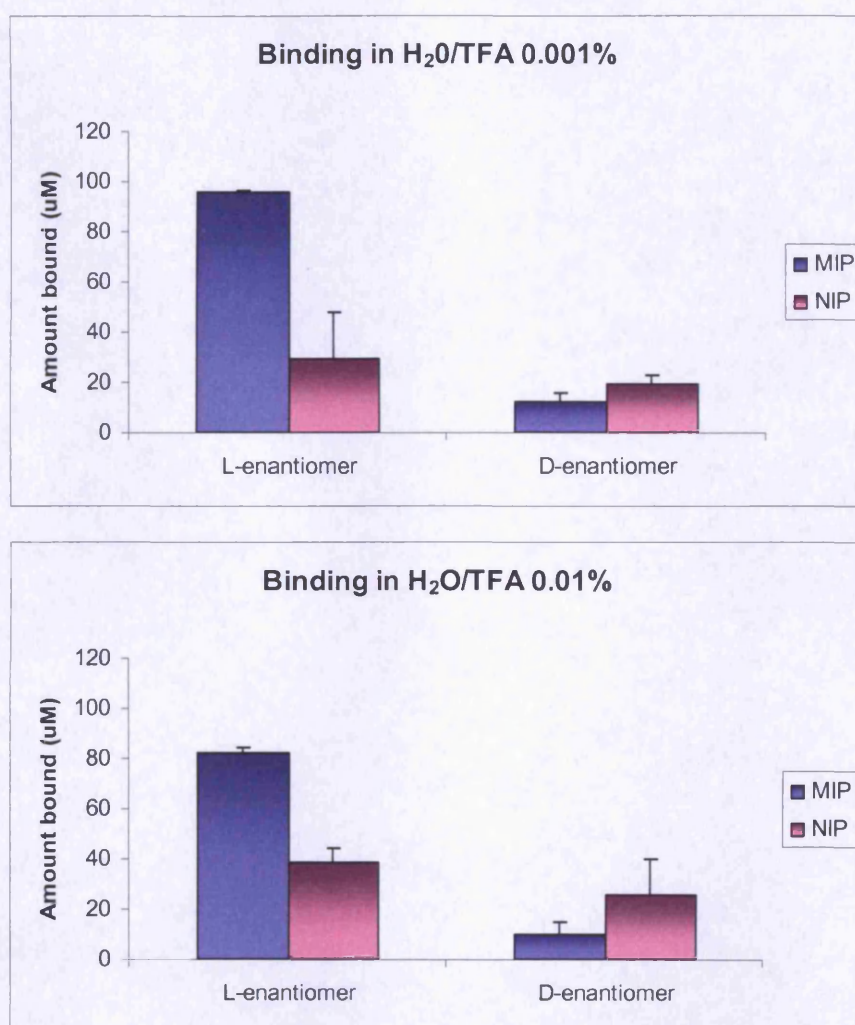


Figure 7.6: Binding for L/D templates in H₂O/ TFA 0.001% and H₂O/ TFA 0.01%; (n=5 ± SD).

Compound	Aqueous solution	DC _{MIP}	DC _{NIP}	I _f
L-enantiomer	0.001% TFA	4.7 x 10 ⁻⁴	1.4 x 10 ⁻⁴	3.3
D-enantiomer	0.001% TFA	6.2 x 10 ⁻⁵	9.7 x 10 ⁻⁵	0.6
L-enantiomer	0.01% TFA	3.8 x 10 ⁻⁴	1.3 x 10 ⁻⁴	2.9
D-enantiomer	0.01% TFA	4.8 x 10 ⁻⁵	1.2 x 10 ⁻⁴	0.3

Table 7.2: Binding data for L and D enantiomers of Boc-phospho-serine methyl ester.

7.4 CONCLUSION

The enantioselective behaviour of the Boc-phospho-L-serine methyl ester-MIP for the L-template, clearly demonstrates a molecular imprinting effect. The cross-reactivity data also demonstrates some further selective behaviour.

BIBLIOGRAPHY

1. Harold, F. M. (2003). The way of the cell: Molecules, Organisms, and the order of life. Oxford University Press.
2. Dubyak, G. (1991). Biological actions of extracellular ATP, New York Academy of Science.
3. Loewenstein, W. (1999). The touchstone of life: Molecular information, cell communication, and the foundations of life, Oxford University Press.
4. Schops, W. (2002). Life's origin: the beginnings of biological evolution, University of California Press.
5. Seyed-Morteza, Monir-Vaghefi (2005). Nucleoside triphosphates and their analogs: chemistry, biotechnology and biological applications., Dekker Marcel Inc.

Chapter 8

Study of the imprinting effect for phospho-serine containing peptides

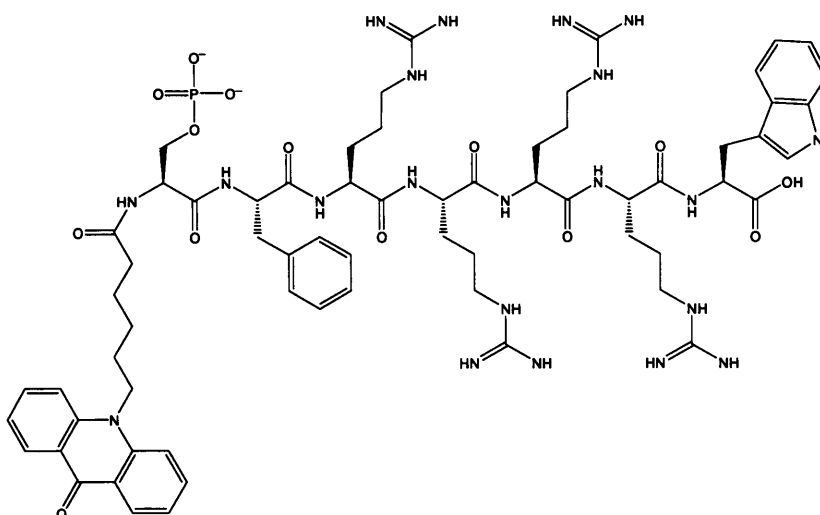
8.1 INTRODUCTION

The aim of the project was to design a molecularly imprinted synthetic receptor that would differentiate a peptide containing serine from a peptide containing phospho-serine. Therefore, the affinity and the selectivity of the Boc-phospho-L-serine methyl ester imprinted polymer for the phosphorylated and unphosphorylated serine containing peptide was investigated.

The names and the structures of the two pairs of peptide are given in Figure 8.1 and Figure 8.2. Peptide pair A was fluorescently labelled with 10-(6-oxoheptyl) acridin-9(10H)-one whilst peptide pair B was labelled with a propriety GE Healthcare fluorescent probe, Cy3B.

PEPTIDE PAIR A

Acridone-pSFRRRRW-OH



Acridone-SFRRRRW-OH

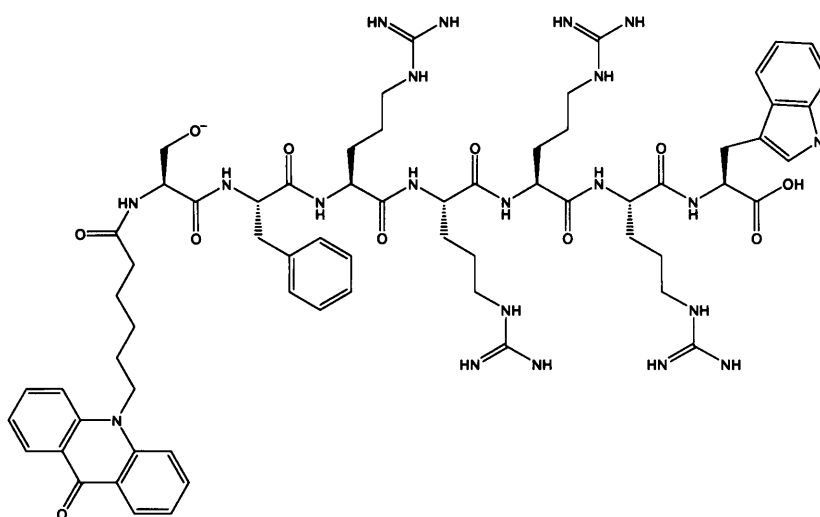
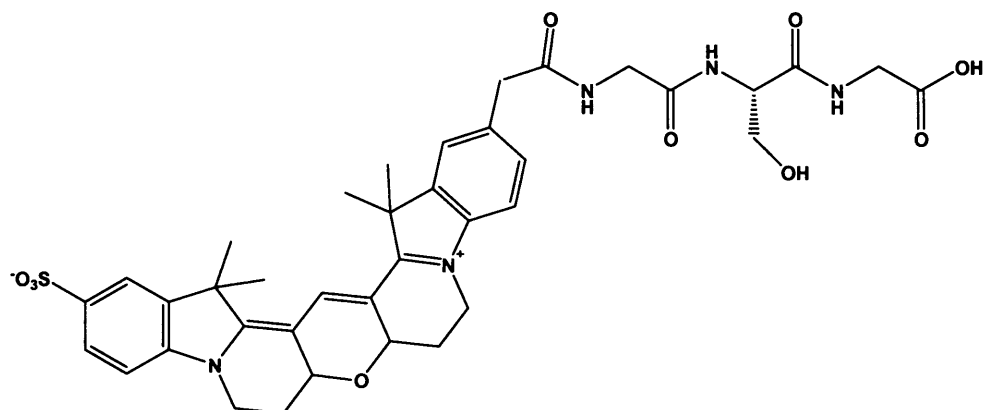


Figure 8.1: Molecular structure of acridone-pSFRRRRW-OH containing a fluorescent label, a phospho-serine, a phenylalanine, four arginines and a tryptophan and acridone-SFRRRRW-OH containing a fluorescent label, a serine, a phenylalanine, four arginines and a tryptophan.

PEPTIDE PAIR B

Glycine-serine-glycine (GSG)



Glycine-phosphoserine-glycine (GpSG)

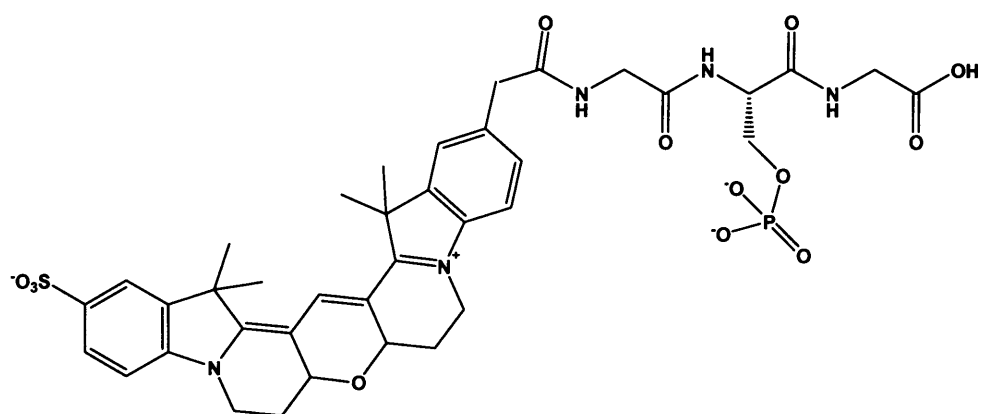


Figure 8.2: Molecular structure of GSG consisting of a fluorescent label, a glycine, a serine and a glycine and GpSG consisting of a fluorescent label, a glycine, a phosphoserine and a glycine.

8.2 MATERIALS AND METHODS

8.2.1 REAGENTS

Peptide pairs A and B were provided by GE Healthcare (Cardiff,UK).

8.2.2 BINDING STUDIES-PEPTIDE PAIR A

Binding assays were performed as described in section 6.2.2, using the Boc-phospho-L-serine methyl ester imprinted polymer as reported in section 5.2.1.

Solutions of 1 μ M of each peptide of pair A were prepared using different binding solvents: water + 0.01%wt. Acetic acid, water + disodium orthophosphate (1%wt. and 10%wt.) and a buffer solution of ammonium acetate 10mM + acetic acid to achieve a pH= 4.

8.2.3 BINDING STUDIES - PEPTIDE PAIR B

Binding studies for peptide pair B were performed as described in section 8.2.2.

Binding experiments were carried out in a number of aqueous systems, of varying pH, in order to try to evaluate the non-specific interactions of peptide pair B to the NIP. In addition further experiments were performed in a number of different aqueous mixtures of methanol systems (table 8.2)

Binding experiment	Solvent	pH
4	HCl 2N*	2.7/5.2
5	1% wt. CH ₃ COO-NH ₄ ⁺	6.99
6	H ₂ O	7.00
7	0.3% wt CH ₃ COO-Na ⁺	7.1
8	NaOH 2N*	8.00
9	0.3% wt Na ₂ HPO ₄	8.2
10	1% Na ₂ HPO ₄	9.1
11	NaOH 2N*	11.0

Table 8.1: Aqueous systems used for the batch analyses of peptide pair B. (* NaOH 2N and HCl 2N were added dropwise to water to reach the desired pHs).

Binding experiment	Solvent	TFA
1	MeOH/H ₂ O (8:2)	0.001%
2	MeOH/H ₂ O (8:2)	0%
3	MeOH/H ₂ O (4:6)	0.001%

Table 8.2: MeOH/H₂O systems used for the batch analyses of peptide pair B.

8.2.4 FLUORESCENCE DETERMINATION FOR PEPTIDE PAIR A AND B

Free peptide concentrations were determined by fluorescence using a Fluostar OPTIMA plate reader (BMG, Germany). Fluorescence was measured at 440 nm of emission and 390 nm of excitation for peptide pair A and at 570 nm of emission and 550 nm of excitation for peptide pair B. A calibration curve was constructed for each peptide pair in the range of 0.2-1 $\mu\text{g/ml}$.

8.3 RESULTS AND DISCUSSION

8.3.1 BINDING STUDIES

8.3.1.1 PEPTIDE PAIR A

The results of the rebinding experiment for peptide pair A are illustrated in Figure 8.3.

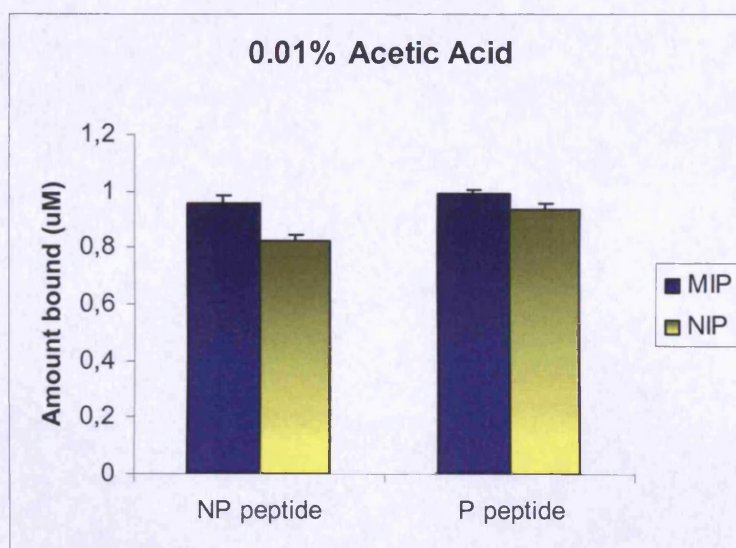


Figure 8.3: Binding for non-phospho (NP) and phospho (P) peptide pair A in an aqueous solution of 0.01% Acetic acid (pH4).

The graph showed a high percentage of non-specific interactions on the MIP and NIP for both peptide species. It was likely that this resulted as consequence of the presence of multiple arginine residues on the backbone of the peptide. The guanidine group of the arginine amino acid has a pKa of ~11, very similar to the pka of the amidine group. Therefore, at pH=4 all the four arginine residues are positively charged. It is rather surprising that, since the polymer surface will also be positively charged at this pH, such a high degree of polymer-peptide interaction occurs. It was significant that there was little difference between the binding of the phosphorylated peptide compared to the non-phosphorylated peptide. This suggests that the phosphate group was not involved in binding. In order to investigate the role of the polymeric amidine groups, similar experiments were carried out using orthophosphate and ammonium acetate as a 'competitors' for the amidine (Figure 8.4 (a,b) and Figure 8.5).

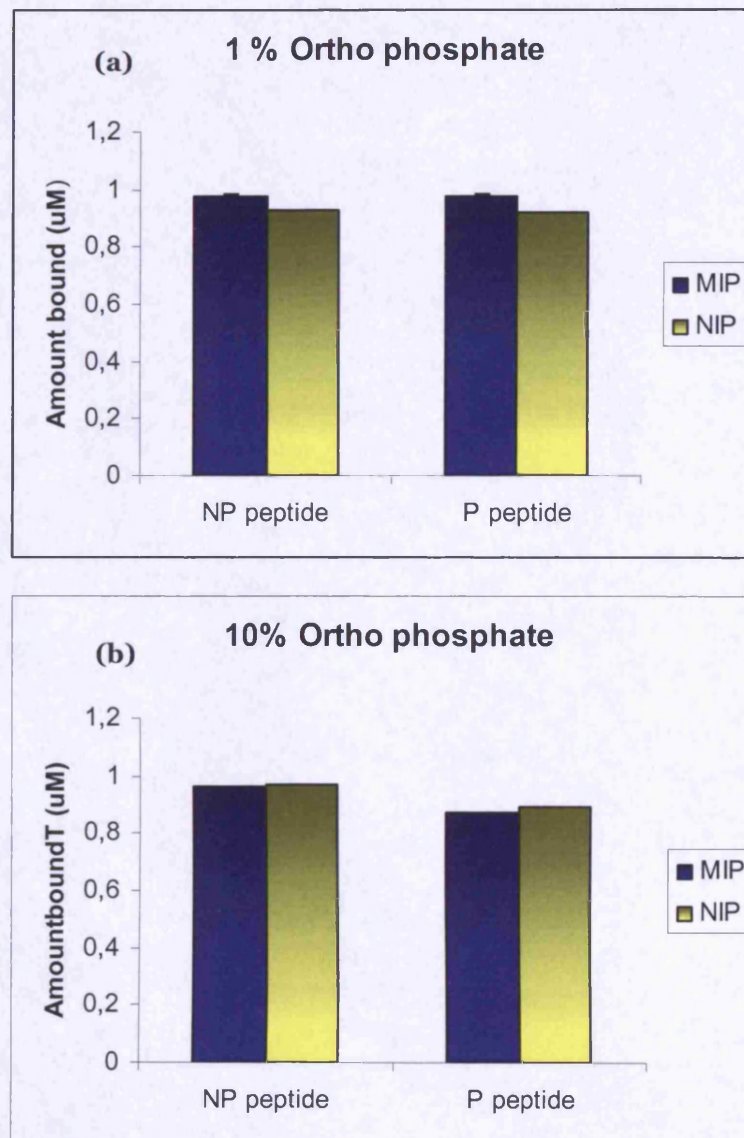


Figure 8.4: Binding of peptide pair A in aqueous solution of (a) 1% ortho phosphate and (b) 10% ortho phosphate.

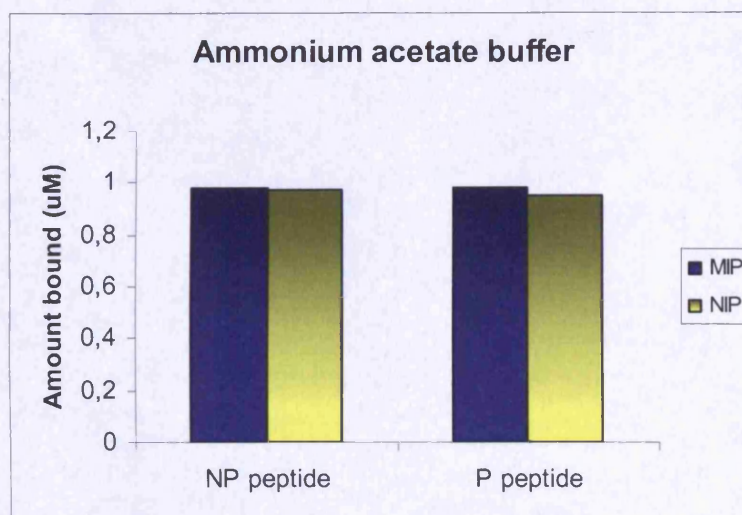


Figure 8.5: Binding for non-phospho peptide A (NP peptide) and phospho peptide A (P peptide) in a buffer solution of ammonium acetate 10 mM.

Again the results showed that the competitor ions had little effect on binding suggesting that the amidine was not playing a significant role in the binding process. Therefore, it seems probable that the high degree of non-specific binding to both MIP and NIP was brought about due to a hydrophobic effect. In particular, it is likely that the acridone group plays a role in this process and it is possible that the peptide behaves like a surfactant in that the charged arginine domain would be repelled from the charged polymer surface whilst the non-polar acridone 'head' group remain firmly bound.

A further anticipated problem with peptide A was that the basic arginine groups could compete with the polymeric amidine groups for the serine phosphate. This would result in *inter* or even *intra* peptide-peptide interaction. In order to avoid this situation a second peptide, peptide B, was employed in the analyses.

8.3.1.2 PEPTIDE PAIR B

The results of the binding analyses for peptide B to the NIP, under a range of conditions, are shown in Figure 8.6.

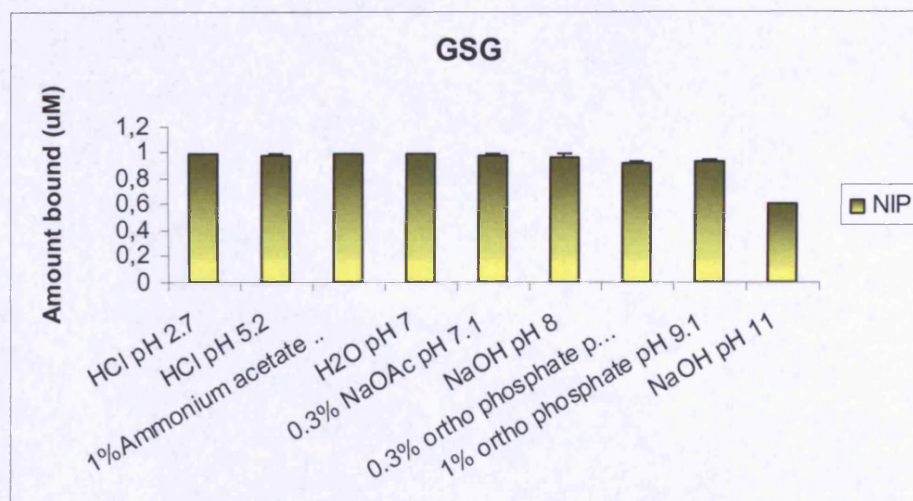


Figure 8.6: Binding of the non phosphorylated peptide B for NIP in different aqueous systems of varying pHs (Table 8.1).

A high degree of non-specific binding was observed at all pHs. This result further supported the hypothesis that non-specific binding was due to the hydrophobic effect. Therefore, additional studies were carried out, using a less polar co-solvent i.e. MeOH. Initially, batch tests were performed using MeOH/H₂O (8:2, pH=6.8). An additional experiment was carried out using MeOH/H₂O (8:2) +0.001% TFA (pH= 2.3).

The rebinding graph (Figure 8.7 (a)) showed that by adding a less polar solvent non specific interactions were suppressed. No binding was observed to either the MIP or the NIP for the phosphorylated form, whilst for the non-phosphorylated form more peptide bound to the MIP than to the NIP. However, when TFA was added to the system, and the pH reduced to 2.3, the phosphorylated form (GpSG) bound to the MIP and the NIP to a similar degree. Whilst for the non-phosphorylated form

(GSG), binding was observed to the NIP but not to the MIP (Figure 8.7 (b)).

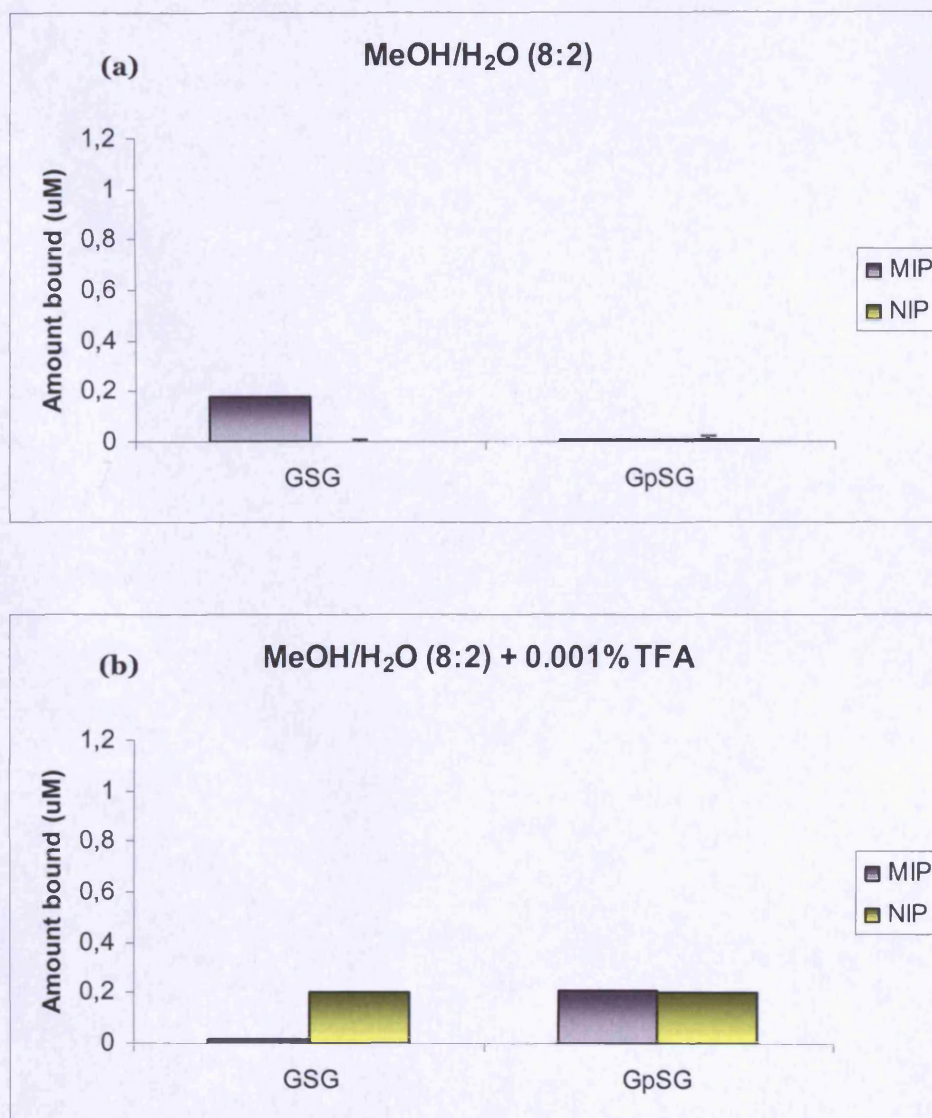


Figure 8.7: Binding of peptide pair B using (a) MeOH/H₂O (8:2) and (b) MeOH/H₂O (8:2) + 0.001% TFA (pH= 2.3).

In order to increase the amount of peptide binding, a further experiment was performed using a reduced amount of MeOH (MeOH/H₂O 4:6 +.001% TFA) (Figure 8.8).

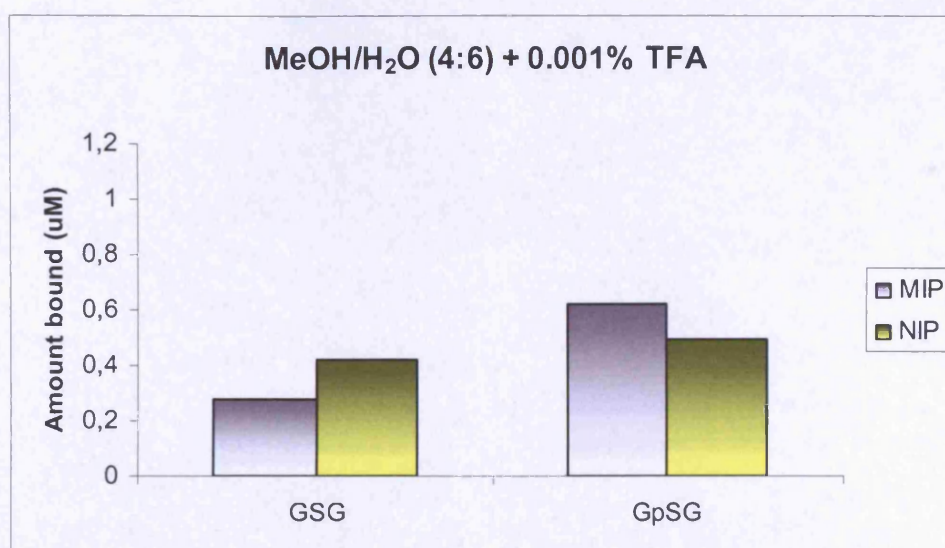


Figure 8.8: Binding of peptide pair B using MeOH/H₂O (4:6) + 0.001% TFA to achieve a pH= 2.3.

In this case the binding generally increased but it was not possible to confirm differences between the binding of the phosphorylated and non-phosphorylated peptides to the MIP and NIP. However, despite this interpretation, the binding data illustrated in Figures 8.7 (b) and Figure 8.8 were in some ways quite encouraging.

8.4 CONCLUSIONS

The MIP amidine-based was able to discriminate between the phosphorylated and the non-phosphorylated form of the two peptide pairs (Figure 8.7 (b)). However, since the NIP bound the same amount for both peptide pairs A and B, a conventional molecular imprinting interpretation of the data is not appropriate.

Chapter 9

General discussion and future outlook

9.1 DISCUSSION

The principle aim of this study was to develop an artificial molecularly imprinted receptor capable of recognising and binding to phosphorylated serine residue, present on a peptide. Prior to commencement of these studies, this aim was recognised as a significant scientific challenge within the field of MIPs and numerous hurdles were anticipated.

However, a molecularly imprinted receptor system, capable of selective interaction with the phosphate group of the Boc-L-serine methyl ester was successfully prepared, and therefore, upon consideration of the project objectives, a number of comments can be made.

The first stage in the process was to synthesise the template and since Boc-phospho-L-serine methyl ester was not commercially available, it was synthesised from the Boc-L-serine methyl ester in a complex reaction scheme that produced a 77% yield (Chapter 3). The second stage was to identify a suitable monomer system with which to molecularly imprint Boc-phospho-L-serine methyl ester. A range of different monomers were evaluated and polymerisable amidines were identified as suitable candidate based on their strong interaction with the phosphate group. Again the suitable monomer was not available commercially and N,N'-diethyl-4-vinylbenzamidinium was successfully synthesised in a four step reaction starting from 4-vinyl benzoic acid (Chapter 3). In addition, molecular modelling of the monomer-template was employed in order to determine which isomer (E,E or E,Z) interacted more favourable with the template. These conformational

studies, combined with NMR experiments, suggested that the E,E isomer of the amidine-containing monomer interacted more strongly with the template than other conformations (Chapter 4).

Following preparation of the artificial molecularly imprinted receptor by a stoichiometric non-covalent approach (Chapter 5), equilibrium evaluation was used to assess the affinity and selectivity of the MIP (Chapter 6). The binding studies for the phospho-template were analysed under different conditions: pH, type of solvents, type of counter-ion and concentration.

In H₂O/0.01% acetic acid (pH=4), the amidine-based MIP showed excellent binding affinity and extremely high specificity for Boc-phospho-L-serine methyl ester. The low cross-reactivity of ATP and UTP were particularly impressive, indicating useful specificity. Furthermore, binding studies showed that the L-isomer was retained by the MIP to a much greater degree than the D-isomer. These findings confirmed a 'real' imprinting effect and also demonstrated that the chirality of the Boc-phospho-L-serine methyl ester was 'memorised' by the MIP binding site.

A selective molecularly imprinted receptor has been created, and, most importantly, the highest degree of specific template binding was achieved in water and 0.001% TFA (pH=2.9) mixture or water and 0.01% acetic acid (pH= 4).

This was a promising result, as one of the objectives of the project was to extend the MIP system to study imprint binding in aqueous systems. Water molecules strongly interfere with polar interactions, including hydrogen bonding, and hydrophobic effects predominate in water. Therefore, the observation that Boc-phospho-L-serine methyl ester-imprinted polymers showed high binding affinity and specificity in aqueous buffers was significant since the rebinding could be performed under conditions compatible with biological systems. This could also lead to the use of MIPs for isolation/purification of peptides containing phosphorylated serine residues.

The use of the MIPs to recognise a phosphorylated serine residue in a peptide chain was one of the most challenging objectives of this project. Since the position of the serine motif within the peptide is random, MIP affinity could not rely on the presence of specific neighbouring amino acid residues.

Some promising results were obtained using the MIP system to target phospho-serine residues in a tri-peptide.

Binding studies in MeOH/H₂O demonstrated a variation in phospho-serine tripeptide bound to the MIP when compared to the unphosphorylated form of the serine tripeptide (Chapter 7). These results were obviously not conclusive of a real and selective discrimination between the two forms of the tripeptide. However, the amidine-based MIP demonstrated great potential for producing selective MIPs that can recognise non-terminal motifs.

9.2 FUTURE OUTLOOK

The ability to perform phosphorylation assays without specific antibodies was also an important aim of this study.

Once the artificial receptor had been produced, the purpose of the project was to evaluate and compare the efficiency of the MIP technology with the antibodies and/or fluorescent assay methodologies (Chapter 1).

Molecularly imprinted polymers were thought to be a more favourable alternative to fluorescent assays as they minimise reagents and reduce the time necessary for assay development. A further advantage of the MIP would be to quantify protein kinases activity directly from complex cellular mixtures, with high resolution and sensitivity.

Some promising experiments were conducted using the MIP as an alternative to IMAP technology for assaying serine/threonine kinases and phosphatases¹. These experiments are not described in the bulk of this thesis yet but they are worthy of mention.

The IMAP technology is based on the high affinity binding of phosphate by immobilised metal (M^{III}) coordination complexes on nanoparticles². This IMAP “binding reagent” complexes with phosphate groups on phosphopeptides and causes a change in the rate of the molecular motion of the peptide. This results in an increase in the fluorescence polarization (FP) value observed for the fluorescein label that is attached to the end of the peptide (Figure 9.1). Because the IMAP binding reagent interacts directly with phosphate through metal-ligand coordinate covalent bonds, detection of kinases that phosphorylate Ser, Thr or Tyr residues is equally enabled³. Furthermore, there is no influence on binding exerted by amino acids that flank the phosphoacceptor residue⁴.

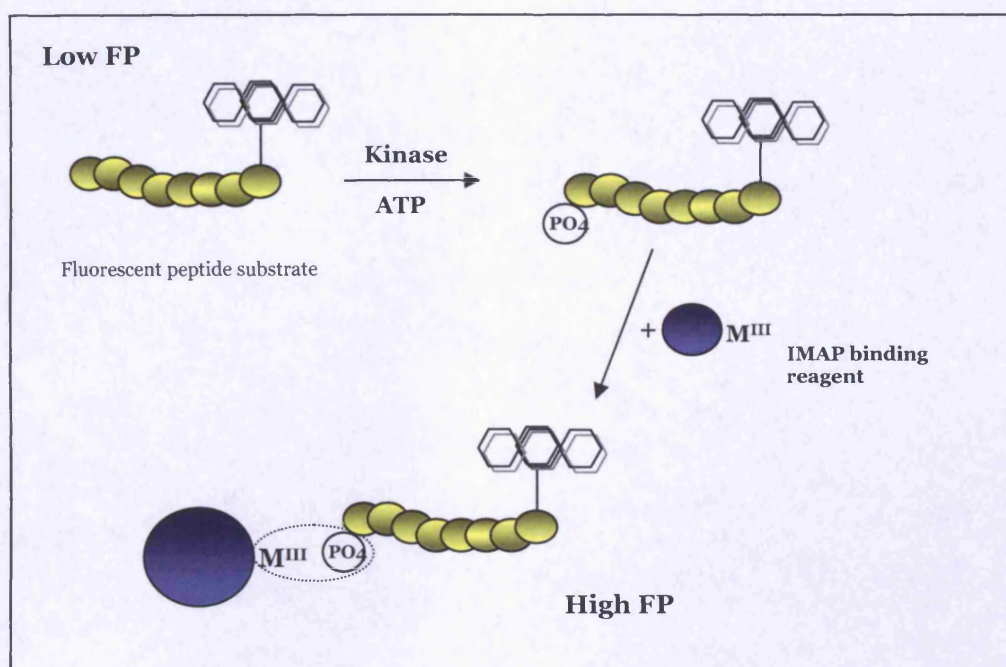


Figure 9.1: Principle of IMAP assay, (Adapted from ref. 1).

In this assay, the amidine-based MIP would act like the IMAF binding reagent, binding the products of protein kinase reactions (i.e. phosphorylated peptides or proteins) but not the unphosphorylated substrates. This would result in an increase in FP value measured.

When a preliminary experiment was carried out using the MIP in place of the IMAF binding reagent a small but significant change in FP was observed.

Unfortunately, this latter work represents only a beginning as it was carried out at the end of the project, and, despite its obvious promise, an inadequate number of experiments were performed. Therefore, any firm conclusions would be premature and subsequent studies need to be carried out for the development of this new and exciting application of MIPs.

BIBLIOGRAPHY

1. Gaudet, E., et al (2003). "A homogeneous fluorescence polarization assay adaptable for a range of protein serine/threonine and tyrosine kinases." Journal of Biomolecular Screening **8**(2): 164-175.
2. Beasley, J., et al (2003). "Evaluation of compound interference in immobilized metal ion affinity-based fluorescence polarization detection with a four million member compound collection." Assay and drug Development Technologies **1**(3): 455-459.
3. Sportsman, J. R., et al (2003). "Fluorescence polarization assays in signal transduction discovery." Combinatorial chemistry and High throughput Screening **6**: 195-200.
4. Huang, W., et al (2002). "A fluorescence polarization assay for cyclic nucleotide phosphodiesterases." Journal of Biomolecular Screening **7**: 215-222.

Appendix I

Experimental Procedures

GENERAL METHODS

Thin Layer Chromatography

Thin Layer Chromatography (TLC) was performed on commercially available Merck Kieselgel plates and separated components were visualized using ultra violet light (245 and 366nm).

Chromatography

Column chromatography procedures were carried out using silica gel 60, particle size 35-70 μm as stationary phase. Glass columns were slurry packed using the appropriate eluent under gravity and samples were applied in the same eluent.

Fractions containing the product were identified by TLC and the solvent removed *in vacuo*.

NMR Spectroscopy

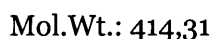
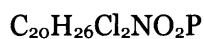
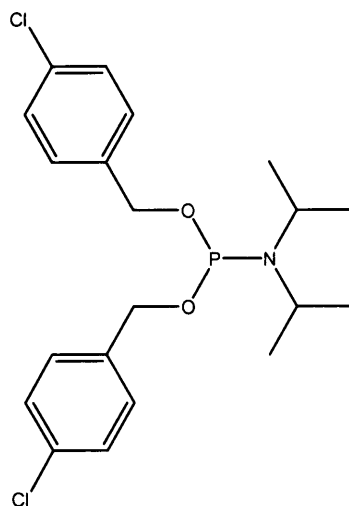
Proton (^1H), Carbon (^{13}C) and Phosphorus (^{31}P) nuclear magnetic resonance (NMR) spectra were recorded at 500 Mhz, on the Bruker Avance instrument. Spectra were auto-calibrated to the deuterated solvent peak and all ^{31}P spectra were proton-decoupled. Chemical shifts are quoted in parts per million (ppm) and the following abbreviations are used in the assignment of NMR signals: s (singlet), d (doublet), t (triplet), q (quartet), m (multiplet), dd (doublet of doublets).

Mass Spectroscopy

Low resolution mass spectra were run on a Bruker, MicroTOF instrument (electrospray mass spectroscopy) in either positive or negative mode.

Reagent and Solvents

Anhydrous solvents were purchased from Sigma-Aldrich (Poole, Dorset UK) and Fluka (part of Sigma-Aldrich Laborchemikalien GmbH).

***N,N'*-DIISOPROPYLAMINO-BIS-(4-CHLOROBENZYL)-
PHOSPHORAMIDATE (26)**

To a solution of phosphorus trichloride (0.025 mol, 2.135 mL) and dry pyridine (2.02 mL) in 15 mL of dry ethyl ether was added 4-chlorobenzylalcohol (3.56g) in 15 mL of dry ethyl ether within 90 minutes at -78° under argon. The solution was used directly for the preparation of benzyloxybis-(diisopropylamino)-phosphine, adding diisopropylamine (22 mL) to the benzyloxy-dichlorophosphine within 1 hour at -10° and leaving the reaction stirring for 2-3 hours. After coevaporation of diethyl ether the product was used directly for the preparation of phosphoramidite.

N,N-diisopropylamino-bis-(4-chlorobenzyl)-phosphoramidite was synthesized by addition of 4-chlorobenzyl alcohol (2.13g) in dry dichloromethane (15 mL) and triethylamine (2.3 mL) to a solution of benzyloxybis-(diisopropylamino)-phosphine in dry dichloromethane (15 mL). After complete addition, stirring was continued for another 2 hours. The mixture was poured into 250 mL of saturated sodium bicarbonate solution which was then extracted 3 times with 25 mL of

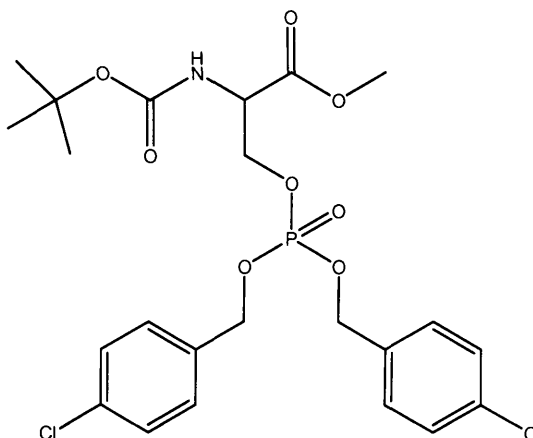
dichloromethane. The combined organic layers were dried on magnesium sulfate and evaporated. The resulting crude oily material was purified by short-column chromatography with $\text{CH}_2\text{Cl}_2/\text{EtOAc}/\text{Et}_3\text{N}$ (80:15:5).

Yield 44%

δ_{H} (CDCl_3): 1.00-1.15 (12H, m, 4x CH_3), 3.35-3.60 (2H, m, 2x NCH), 4.48-4.67 (4H, d, 2x CH_2Ar), 7.10-7.28 (8H, m, 2xAr).

δ_{P} (CDCl_3): 14.634

BOC-PHOSPHO-4-CHLORO-(DIBENZYL)-L-SERINE METHYL ESTER (28)



$\text{C}_{23}\text{H}_{28}\text{Cl}_2\text{NO}_8\text{P}$

Mol.Wt.: 548,35

After coevaporation of the N-Boc-D/L-Ser-OMe (1g, 0.0045 mol) with dioxane (2x5 mL), the reaction flask was charged with Argon and N,N-diisopropylaminobis-(4-chlorobenzyl)-phosphoramidite (2.85 g) was introduced, followed by addition of solution of 1H-tetrazole in acetonitrile (8 mL) to the reaction components. The reaction was monitored by TLC (Hexane/ CH_2Cl_2 1:1) and left overnight at room temperature.

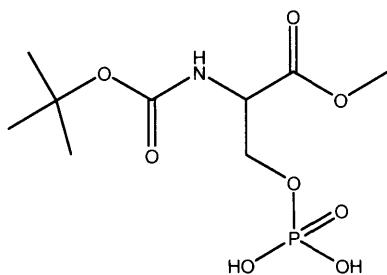
After cooling the reaction mixture to 0°C, 3-chloroperoxybenzoic acid (1.55g) was added and stirring continued at room temperature for 2 hours. Subsequently, excess oxidizing agent was destroyed with 10% aq. sodium sulfite (10 mL) and the mixture was transferred to a separator funnel. Ethyl acetate (70 mL) was added and the organic layer was washed with 10% aq. sodium sulfite (10 mL), saturated aqueous sodium bicarbonate (10 mL), water (10 mL), brine (10 mL) and dried (Na₂SO₄). After evaporation the crude was purified by crystallization from MeOH/H₂O to give a white powder.

Yield 60%

δ_{H} (CDCl₃): 1.37 (9H, s, 3xCH₃), 3.65 (3H, s, OCH₃), 4.15-4.21 (1H, m, CH₂OP), 4.29-4.36 (1H, m, CH₂OP), 4.40-4.46 (1H, m, CH), 4.89 (2H, d J= 7.2 Hz, CH₂Ar), 4.91 (2H, d J= 7.2 Hz, CH₂Ar), 5.32 (1H, d J= 7.7 Hz, NH), 7.16-7.20 (4H, m, Ar), 7.24-7.28 (4H, m, Ar).

δ_{C} (CDCl₃): 170.066 (CO₂CH₃), 156.30 (CO-BOC), 135.38 (CHAr), 135.13 (C-Cl), 80.6 (C[CH₃]₃), 69.244 (CH₂-Ar), 54.388 (CH), 53.22 (OCH₃), 28.70 (3xCH₃).

δ_{P} (CDCl₃): 0.1625

HYDROGENATION METHODS**BOC-PHOSPHO-L-SERINE METHYL ESTER (29)** $C_9H_{18}NO_8P$

Mol.Wt.: 299,21

METHOD 1

Boc-phospho-L-4-chloro-benzyl-serine methyl ester (200 mg, 0.35 mmol) was added to a solution of 25mL H₂O/t-BuOH (1:2) in presence of Pd 10% (50 mg) in a hydrogen atmosphere. TLC (EtOAc) showed the reaction to be complete after 24 hours. The palladium was filtered off and the crude concentrated in vacuum. ¹H-NMR and mass spectrum confirmed the formation of the desired product.

Yield 60%

δ_H (D₂O): 1.39 (9H, s, 3xCH₃), 3.75 (3H, s, OCH₃), 3.98-4.06 (1H, m, CH₂OP), 4.10-4.17 (1H, m, CH₂OP), 4.32-4.39 (1H, m, CH).

δ_P (D₂O): 2.479

MS (ES⁻): m/z 298.1

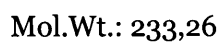
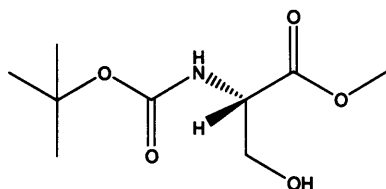
METHOD 2

Dibenzyl-phospho-Boc-serine methyl ester (350mg; 0.62 mmol) was added to a solution of 40 mL H₂O/tBuOH (1:2) and ammonium acetate buffer (47 mg; 0.62 mmol). Palladium 10% (50 mg) was then added and the flask treated with hydrogen gas (2 atm). After 2-3 hours, the catalyst was filtered off over celite, the solvent removed and the product analysed by ¹H and ³¹P-NMR and mass spectrometry, which confirmed the complete deprotection of the Boc-phospho-L-serine methyl ester with a yield of 77%.

δ_{H} (D₂O): 1.55 (9H, s, 3xCH₃), 3.91 (3H, s, OCH₃), 4.05-4.10 (1H, m, CH₂OP), 4.12-4.17 (1H, m, CH₂OP), 4.18-4.23 (1H, m, CH).

δ_{P} (D₂O): 3.83

MS (ES⁻): m/z 298.1

BOC-D-SERINE METHYL ESTER (30)

A cold solution of N-Boc-D-Serine (2g, 0.01 mol) and sodium potassium carbonate (0.01 mol) were dissolved in dimethylformamide (20 mL). After stirring for 10 minutes in an ice water bath, methyl iodide (0.025 mol) was added to the white suspension and stirring continued at 0°C for 30 minutes whereupon the mixture solidified. The reaction was warmed to room temperature and stirred for an additional hour or so at which point TLC analysis indicated complete formation of the methyl ester. The reaction mixture was filtered by suction and the filtrate partitioned between ethyl acetate (80 mL) and water. The organic phase was washed with brine, dried on magnesium sulfate, filtered and concentrated to give the N-Boc-D-serine methyl ester as a pale amber oil which was used without further purification.

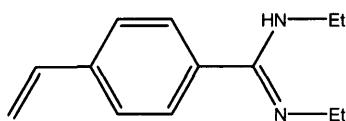
TLC analysis on silica gel plates eluting with (1:1) ethyl acetate-hexanes showed the clean formation of ester, R_f 0.64 (visualized with 0.5% phosphomolybdic acid in 95% ethanol), at the expense of starting material at the origin. Yield: 83%.

δ_{H} (CDCl_3): 1.46 (9H, s, 3x CH_3), 3.79 (3H, s, OCH_3), 3.88-3.93 (1H, ddd $J = 11.1$ Hz, $J = 5.93$ Hz, $J = 3.59$ Hz, $\underline{\text{CH}_2\text{OP}}$), 3.94-3.99 (1H, ddd $J = 11.1$

Hz, $J = 5.93$ Hz, $J = 3.59$ Hz, $\underline{\text{CH}_2\text{OP}}$), 4.37-4.41 (1H, m, CH), 5.45 (1H, bs, NH).

MS_(MeOH) ES⁺: 243 (220+23Na⁺).

***N,N'*-DIETHYL-4-VINYL BENZAMIDINE (35)**



$\text{C}_{13}\text{H}_{18}\text{N}_2$

Mol.Wt.:202,30

The compound above was obtained in four steps from 4-vinyl benzoic acid:

(I) 4-VINYL BENZOYL CHLORIDE (32): 4-vinyl benzoyl chloride was prepared by the addition of triethylamine (0.0067 mol) and thionyl chloride (0.25 mL) to an ice-cold solution of 4-vinyl benzoic acid (0.0037 mol) in THF anhydrous (10 mL). The reaction was stirred for 30 minutes at room temperature under Argon and was followed by TLC. After that time, the reaction was filtrated and the solution was evaporated.

(II) N-ETHYL-4-VINYL BENZAMIDE (33): N-ethyl-4-vinyl-benzamide was prepared by the addition of aqueous ethylamine (70%, 0.090 mol) to an ice-cold solution of 4-vinyl benzoyl chloride (0.006 mol) in ether (5 mL), followed by stirring at room temperature for 24 hours. Water was added, and the mixture stirred for another 2 hours. The resulting precipitate was collected by suction filtration and purified by column chromatography (Hexane:EtOAc/8:2).

δ_{H} (CDCl_3): 1.15 (3H, t $J= 7.2$ Hz, CH_2CH_3), 3.38 (2H, q $J= 7.2$ Hz, CH_2CH_3), 5.27 (1H, d $J= 11.03$ Hz, $\text{CH}_2=\text{CH}$), 5.74 (1H, d $J= 17.3$ Hz, $\text{CH}_2=\text{CH}$), 6.64 (1H, dd $J= 11.03$ Hz, $J= 17.3$ Hz, $\text{CH}_2=\text{CH}$), 7.35-7.40 (2H, m, Ar), 7.62-7.67 (2H, m, Ar).

(III) N,O-DIETHYL-4-VINYL BENZIMIDATE (34): N-ethyl-4-vinylbenzamide was dissolved in a 1.0M solution of triethyl oxonium tetrafluoroborate in dichloromethane. After stirring at room temperature under argon for 24 hours, the solvent was removed in vacuo. The residue was treated with ice-cold sodium carbonate solution (2.5 ml) and extracted with ice-cold ether (12 ml). The organic extract was dried over sodium sulfate and concentrated. Crude was distilled once (Kugelrohr, $160^\circ/0.02$ mbar) and used without further purification.

δ_{H} (CDCl_3): 1.00 (3H, t $J= 7.3$ Hz, NCH_2CH_3), 1.25 (3H, t $J= 7.1$ Hz, OCH_2CH_3), 3.22 (2H, q $J= 7.3$ Hz, NCH_2CH_3), 4.15 (2H, q $J= 7.1$, OCH_2CH_3), 5.23 (1H, d $J= 10.8$ Hz, $\text{CH}_2=\text{CH}$), 5.71 (1H, d $J= 17.5$ Hz, $\text{CH}_2=\text{CH}$), 6.65 (1H, dd $J= 10.8$ Hz, $J= 17.5$ Hz, $\text{CH}_2=\text{CH}$), 7.22-7.24 (2H, m, Ar), 7.37-7.39 (2H, m, Ar).

(IV) N,N'-DIETHYL-4-VINYL BENZAMIDINE (35): A solution of N,O-diethyl-4-vinylbenzimidate and ethylamine hydrochloride in dry ethanol was stirred at room temperature under argon for 5 days. The solvent was removed in vacuo and the residue suspended in ice-cold ethyl acetate. The mixture was then washed with ice-cold aqueous sodium hydroxide 2M. The organic phase was collected, dried over sodium sulfate and concentrated. The crude was purified once by distillation to give a pale powder that was kept in dry condition.

δ_{H} (CDCl_3): 1.10 (6H, bs, 2 x CH_2CH_3), 3.23 (4H, bs, 2 x CH_2CH_3), 5.32 (1H, d $J= 10.8$ Hz, $\text{CH}_2=\text{CH}$), 5.81 (1H, d $J= 17.7$ Hz, $\text{CH}_2=\text{CH}$), 6.74 (1H, dd $J= 10.8$ Hz, $J= 17.7$, $\text{CH}_2=\text{CH}$), 7.21-7.27 (2H, m, Ar), 7.41-7.48 (2H, m, Ar).

